AD-A132 470 AN EXPERIMENTAL STUDY OF A METHOD TO ATTENUATE SURFACE WAVES USING ARTIFI..(U) STEVENS INST OF TECH HOBOKEN NJ DAVIDSON LAB R I HIRES APR 83 SIT-DL-82-2302 1/2

UNCLASSIFIED N00014-78-C-0740 F/G 8/3 NL

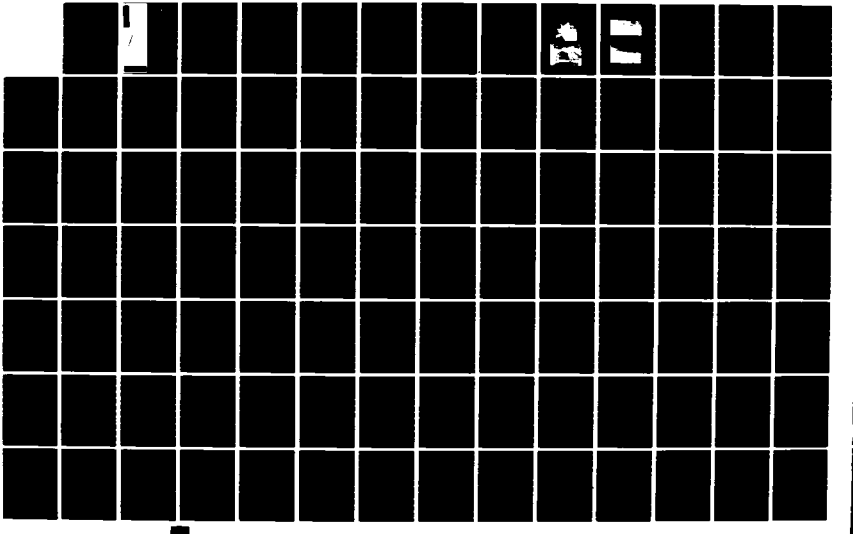

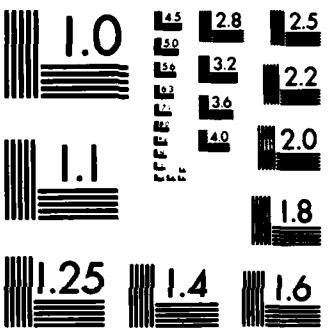

(12)

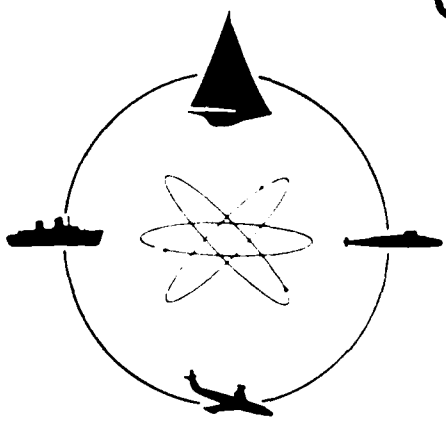

DAVIDSON LABORATORY

Report SIT-DL-82-2302

April 1983

AN EXPERIMENTAL STUDY OF A METHOD TO ATTENUATE SURFACE WAVES USING ARTIFICIALLY GENERATED SURFACE CURRENTS

by

Richard I. Hires

Prepared for

Technology Assessment and Research Program
Minerals Management Service

under

Office of Naval Research Contract
N00014-78-C-0740
DL Project 4628/045

STEVENS INSTITUTE
OF TECHNOLOGY

CASTLE POINT STATION
HOBOKEN, NEW JERSEY 07030

R-2302

UNCLASSIFIED

SECURITY CLASSIFICATION OF THIS PAGE (When Data Entered)

REPORT DOCUMENTATION PAGE		READ INSTRUCTIONS BEFORE COMPLETING FORM
1. REPORT NUMBER: SIT-DL-82-9-2302 ✓	2. GOVT ACCESSION NO.: AD-A132470	3. RECIPIENT'S CATALOG NUMBER
4. TITLE (and Subtitle): AN EXPERIMENTAL STUDY OF A METHOD TO ATTENUATE SURFACE WAVES USING ARTIFICIALLY GENERATED SURFACE CURRENTS.		5. TYPE OF REPORT & PERIOD COVERED: FINAL AUGUST 1978 -APRIL 1983 6. PERFORMING ORG. REPORT NUMBER: SIT-DL-82-9-2302
7. AUTHOR(s): Richard I. Hires		8. CONTRACT OR GRANT NUMBER(s): N00014-78-C-0740.
9. PERFORMING ORGANIZATION NAME AND ADDRESS: Davidson Laboratory STEVENS INSTITUTE OF TECHNOLOGY Castle Point Station, Hoboken, NJ 07030		10. PROGRAM ELEMENT, PROJECT, TASK AREA & WORK UNIT NUMBERS
11. CONTROLLING OFFICE NAME AND ADDRESS: OFFICE OF NAVAL RESEARCH 800 North Quincy Street Arlington, VA 22217		12. REPORT DATE: APRIL 1983 13. NUMBER OF PAGES: xii+35 pp + 63 pp. of figs.
14. MONITORING AGENCY NAME & ADDRESS(if different from Controlling Office): Technology Assessment & Research Program Minerals Management Service 647 National Center Reston, VA 22091		15. SECURITY CLASS. (of this report): UNCLASSIFIED 15a. DECLASSIFICATION/DOWNGRADING SCHEDULE

16. DISTRIBUTION STATEMENT (of this Report)

APPROVED FOR PUBLIC RELEASE; DISTRIBUTION UNLIMITED.

17. DISTRIBUTION STATEMENT (of the abstract entered in Block 20, if different from Report)

18. SUPPLEMENTARY NOTES

19. KEY WORDS (Continue on reverse side if necessary and identify by block number)

Surface Waves
Wave/Current/Interaction

20. ABSTRACT (Continue on reverse side if necessary and identify by block number)

Earlier model studies have shown the effectiveness of laterally-sheared wakes of towed rigid grids in achieving substantial attenuation of following regular wave trains by refraction. Significant attenuation could be obtained in wakes with widths comparable to the incident wave length, with depths of the order of 10% of the incident wave length and with grid tow speeds about 10% of the incident wave celerity. In the present study,

[Cont'd]

DD FORM 1 JAN 73 1473 EDITION OF 1 NOV 65 IS OBSOLETE
S/N 0102-014-6601

UNCLASSIFIED

SECURITY CLASSIFICATION OF THIS PAGE (When Data Entered)

20. ABSTRACT (Cont'd)

model-scale experiments were conducted to extend the earlier results to the cases of random waves and of oblique waves, to determine attenuation for two possible operational scenarios for the prototype application of this method, and to test the effectiveness of a towed net to replace the towed rigid grid for full-scale use. The test results for random following seas were consistent with the earlier tests with regular following waves. For oblique seas, the region of attenuation in the wake of the grid was shifted laterally towards the downwave side of the wake. In addition, peak attenuation was less than that expected from a simple extrapolation of the semi-empirical prediction formula developed for following seas to the case of oblique waves. Model tests with a towed flexible net held open with attached paravanes revealed that similar levels of attenuation could be obtained with this apparatus as that achieved with the towed rigid grids.

Field tests of this wave attenuation method were conducted at intermediate scale in New York Harbor and at full-scale in the ocean off Miami, Florida. The intermediate-scale tests primarily served to develop at-sea procedures for deployment and towing of the net and paravanes and for obtaining wave measurements within and outside the wake region. Data from the full-scale experiments showed significant attenuation behind the towed net, however the extent of the attenuated region was substantially less than that found in model studies.

STEVENS INSTITUTE OF TECHNOLOGY
DAVIDSON LABORATORY
Castle Point Station, Hoboken, New Jersey 07030

Report SIT-DL-82-2302

April 1983

AN EXPERIMENTAL STUDY OF A METHOD TO ATTENUATE SURFACE WAVES USING ARTIFICIALLY GENERATED SURFACE CURRENTS

by

Richard I. Hires

Prepared for

Technology Assessment and Research Program
Minerals Mangement Service

under

Office of Naval Research Contract

N00014-78-C-0740

DL Project 4628/045

ABSTRACT

Earlier model studies have shown the effectiveness of laterally-sheared wakes of towed rigid grids in achieving substantial attenuation of following regular wave trains by refraction. Significant attenutation could be obtained in wakes with widths comparable to the incident wave length, with depths of the order of 10% of the incident wave length and with grid tow speeds about 10% of the incident wave celerity. In the present study, model-scale experiments were conducted to extend the earlier results to the cases of random waves and of oblique waves, to determine attenuation for two possible operational scenarios for the prototype application of this method, and to test the effectiveness of a towed net to replace the towed rigid grid for full-scale use. The test results for random following seas were consistent with the earlier tests with regular following waves. For oblique seas, the region of attenuation in the wake of the grid was shifted laterally towards the downwave side of the wake. In addition, peak attenuation was less than that expected from a simple extrapolation of the semi-empirical prediction formula developed for following seas to the case of oblique waves. Model tests with a towed flexible net held open with attached paravanes revealed that similar levels of attenuation could be obtained with this apparatus as that achieved with the towed rigid grids.

Field tests of this wave attenuation method were conducted at intermediate scale in New York Harbor and at full-scale in the ocean off Miami, Florida. The intermediate-scale tests primarily served to develop at-sea procedures for deployment and towing of the net and paravanes and for obtaining wave measurements within and outside the wake region. Data from the full-scale experi-

ments showed significant attenuation behind the towed net, however the extent of the attenuated region was substantially less than that found in model studies.

TABLE OF CONTENTS

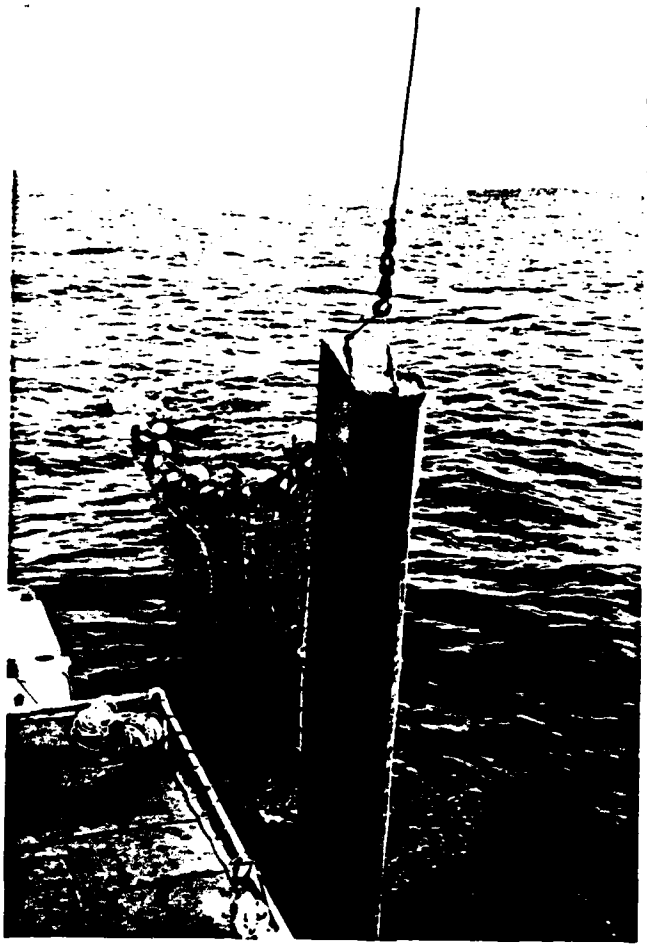

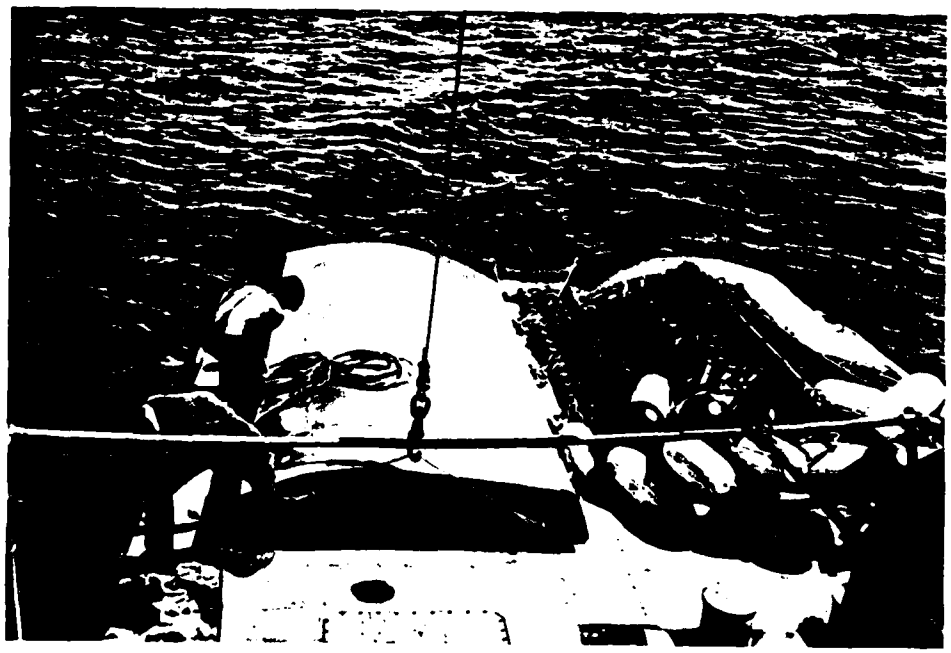

PHOTOGRAPHS OF DEPLOYMENT

OF NET AND BOARDS

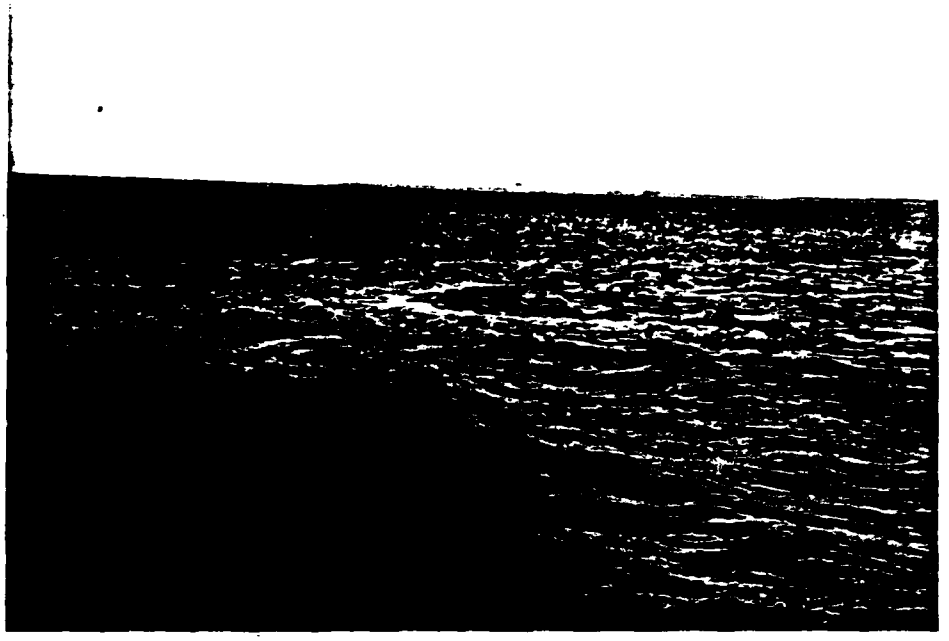

PHOTOGRAPHS OF FULL SCALE

NET AND BOARDS UNDER TOW

1. INTRODUCTION

A preliminary study of wave attenuation in the laterally sheared wake of towed rigid grids, Reference 1, revealed that relatively narrow (of the order of a wave length), shallow surface currents could be employed to refract following wave trains away from the wake region. The subsequent attenuation of the waves in the wake was substantial. In this initial study a finite width, finite depth surface current was generated in a 75-foot square wave tank by towing rigid grids (width, W_g, and draft, d_g) through the water at a constant speed, U_g. The velocity distributions in the wake of the grids were determined using hot-film anemometers. Regular long-crested wave trains with still-water wave celerity, C_o, and wave length, λ_o, were generated in the tank with their initial direction of propagation the same as that of the towed grid. Upon encountering the grid wake, the waves were refracted by the laterally sheared velocity distribution in the wake with a subsequent attenuation, γ, (where $\gamma = \frac{H_o - H}{H_o}$ and H_o is the initial wave height and H the wave height after refraction) of the waves in the wake.

The first result of this initial study was the determination of the dependence of γ on the characteristic parameters of the initial wave train and of the wake produced by the grid. Since the wake characteristics were determined by the grid width, draft, and tow speed, the experimental results for γ were reported as a function of three dimensionless parameters W_g/λ_o, d_g/λ_o and U_g/C_o. An empirical functional dependence of γ on these parameters was derived with

the aid of a two-dimensional theoretical analysis (Reference 2) of the interaction of waves with a finite depth surface current. This relationship,

$$\gamma = 4.7 \tanh (1.65\ W_g/\lambda_o)\ (C_B/C_o - 1), \qquad (1)$$

where $C_B/C_o = f(U_g/\lambda_o, d_g/\lambda_o)$ and the functional dependence of C_B/C_o on U_g/λ_o and d_g/λ_o is obtained from the two-dimensional theory presented in Reference 2, provided for a satisfactory collapse of all of the experimental results.

A second result of the first experimental study was the determination of the combination of parameters W_g/λ_o, d_g/λ_o, and U_g/C_o which would achieve a specified attenuation of the initial wave train with the minimum expenditure of power to tow the grid. The results of this analysis suggest that for initial wave lengths of up to 300 feet, significant attenuation could be obtained with reasonable expenditures of power. Table 11 in Reference 1 summarizes the power required as a function of initial wave conditions and specified levels of attenuation. Finally, the values of the dimensionless parameters which minimize the required power for attenuations ranging from 50 to 70% were found to be

$0.1 \leq U_g/C_o \leq 0.2$, $0.14 \leq d_g/\lambda_o \leq 0.17$, and $W_g/\lambda_o = 0.85$.

The presently reported experimental study of wave attenuation by refraction in laterally sheared currents represents an extension of the earlier fundamental studies reported in Reference 1 with an overall objective of a practical demonstration of the method's utility in the open ocean. This present

research included additional model studies in the wave tank, meso-scale field testing in New York Harbor and full-scale field work in the ocean off Miami, Florida. In the following paragraphs the objectives of the model-scale, meso-scale and full-scale experiments are presented.

The specific objectives of the model scale tests were as follows:

(1) To determine the effectiveness of a grid-generated wake on attenuation of random waves.

(2) To determine the effect on the attenuation in the grid wake when the waves are incident to the wake at oblique angles.

(3) To investigate the grid design in terms of solidity ratio and shape such that the required power to tow the grid is reduced to a minimum.

(4) To determine the operational procedures for attaining the wave attenuation required in the specific missions which we have labeled Scenarios 1 and 11.

(5) To determine the arrangement of tow lines and paravanes required to tow a floating non-rigid grid which would simulate the type of grid to be employed in practical, at-sea applications.

The previous experimental work, Reference 1, was limited to a study of the attenuation of <u>regular</u> wave

trains propagating in the same direction as the grid induced velocity field. The first two objectives of the proposed model-scale experiments were to extend this initial work to include a determination of the attenuation of random following seas and a determination of the attenuation of both regular and random waves at oblique angles of incidence to the wake.

The third objective of the model experiments was to investigate two methods to reduce the power required to generate a suitable wake to achieve a specified level of attenuation. Our previous work was limited to rectangular grids with one solidity ratio. In the present study we tested a modified grid with a higher solidity ratio. The rationale behind this approach was as follows: The drag coefficient, C_D, for a grid is expected to increase with increasing solidity ratio but it is also expected that an increase in solidity ratio should lead to an increase of the velocity in the wake. It would appear then that an increase in solidity could reduce the required grid towing speed, U_g. Since the required power $P = \frac{1}{2} \rho C_D W_g d_g U_g^3$ a reduction in U_g with increased grid solidity, could offset the expected increase in the drag coefficient. Our specific objective was to test the validity of this argument. A second approach was to reduce the projected area of the grid. The results of wake surveys (Reference 1) conducted behind the rectangular grids suggest that the submerged corners of the rectangular grid could be removed without seriously altering the near surface current field. Consequently, we

investigated the effectiveness of grids with a trapezoidal shape in producing a suitable wake to achieve a specified level of attenuation.

While the objectives of the experiments outlined above served to extend the results obtained previously to conditions more closely approximating the ocean and to extend our previous efforts towards reducing the power required to generate an effective current, the remaining two objectives of the proposed model scale tests were: (1) to demonstrate the applicability of this wave attenuation method for two possible missions (Scenarios 1 and 11) and (2) to determine the design of a floating, non-rigid, towed grid which would be employed in the full-scale tests.

The two operational scenarios for the application of this wave attenuation procedure were developed from a consideration of two possible missions: The first was to facilitate floating object recovery such as an unmanned submersible by a single ship; the second, to use two ships to provide local wave damping at a fixed site in the ocean. The first scenario requires wave attenuation in the vicinity of a surface vessel during the recovery of a submersible. To be practical the recovery vessel would also serve as the tow ship for the wake-producing grid. One approach to this mission would be for the recovery vessel to approach the submersible from upwind towing the grid in the same direction as the prevailing direction of propagation of the wind generated waves. As the vessel comes alongside the submersible, it would quickly release the grid. The wake produced by the grid would evenutally overtake the vessel and

persist for a sufficient period of time to allow the submersible to be retrieved with markedly attenuated wave conditions. This scenario was simulated in the model experiments by simply stopping the towed grid, allowing the wake to pass through the stopped grid and measuring the wave attenuation in front of the grid. The second scenario required significant wave attenuation over a fixed local region of the ocean. Although there are several approaches to achieving this effect, one that appeared promising would be to employ two vessels each towing a floating flexible grid. The vessels would tow their grids on either side of the region in which local attenuation is required and in an opposite direction to the prevailing wind-generated waves. Under these conditions wave energy would be focused towards the centerline of each wake and we expect there would be a divergence of wave rays in the region between the wakes. Consequently, there should be significant wave attenuation in this region. We evaluated this approach in the wave tank for a systematic variation of grid separations and for a range of incident wave conditions.

The final series of experiments in the wave tank employed a floating, non-rigid grid which simulated the actual application of this method in the ocean. The characteristics of this grid, i.e., length, draft and solidity, were determined from the results obtained from the tests with rigid grids. The rigid grid was replaced with a net with buoyant elements along the top and weights at the bottom. The net was held open while under tow by paravanes at each end

of the net. An initial series of tests were conducted to determine the proper arrangement of tow lines and paravane orientation to achieve satisfactory performance. A subsequent series of tests were made to compare the capability of the wake induced by the net to attenuate waves with the previous results obtained with the rigid grids.

Following the completion of the experimental studies in the tank, we conducted meso-scale experiments to demonstrate the practical applicability of the method. These tests were undertaken in the waters of New York Harbor using the Ocean Engineering Department's 26-foot research vessel as the tow ship. Our objectives in this initial series of field experiments, which would be at an intermediate scale between the wave tank and the open ocean, were:

(1) to determine the capability of the grid design and operational procedures developed from the model-scale test results,

(2) to develop and test alternative designs of these experiments including tests of the field wave measurement system as we gained experience in what could and could not be reasonably accomplished in the field, and

(3) to use the results of these intermediate scale experiments in the design of the open ocean, full-scale demonstration. These initial series of field observations provided us with the opportunity to test and refine our design of the

full-scale, at-sea experiments at a relatively low cost.

Two series of full-scale tests of the method were conducted in the ocean off Miami, Florida. The objective of these tests were to demonstrate that the procedures devised in the wave tank experiments and refined in the meso-scale studies would be applicable at full-scale in the ocean.

It should be clear from the foregoing that the test plan to achieve the final objective of an at-sea demonstration was based on an orderly transfer of results from model tests in the towing tank to the tests at an intermediate scale and that the combination of these initial test results led to the final detailed plans for the full-scale trials. We shall follow a similar pathway in presenting the results of our multi-scale experiments by reporting first on the wave tank tests, next the meso-scale experiments in New York Harbor, and then conclude with a description of the full-scale tests and results.

2. WAVE TANK STUDIES

2.1 Test Procedure

As in Reference 1, towing tests of grid models were conducted in Davidson Laboratory Tank 2 which is 75 ft x 75 ft x 4.5 ft deep (22.86m x 1.37m). A plunger-type wave generator extends along one side of the tank with a wave absorbing beach on the opposite side. A towing carriage runs at a preset uniform speed on a monorail suspended from a movable bridge which spans the tank.

Figure (1) shows sketches of the facility and the placement of the bridge for head (180°) following (0°) and oblique (30°) towing directions with respect to the direction of wave advance.

Wave heights were measured by impedance-type probes, the placement of the probes varying with the type of experiment, as shown in Figure (2). A stationary probe #7 (not shown in Figure 2) was positioned 10 ft from the wave-maker to monitor the generated waves. In general, moving probes located in the wake of the moving grid, were used to obtain time-averaged heights of attenuated waves. After the grid was halted, both stationary and moving probes located ahead of the grid were used to measure variation in wave attenuation as the grid wake travelled past them. The latter procedure was used primarily to document Scenario 1 tests which are described in section 2.2.4.

To measure drag force in smooth water and in waves, grids were attached to a drag balance suspended from the towing carriage.

Electrical outputs from the wave probes and drag balance transducers were transmitted by cables to signal conditioners on shore. Conditioned signals were displayed as amplitude time histories on chart paper; the signals also were digitized and processed on-line by a PDP-8e digital computer. Standard computer programs were used to obtain mean drag force, average

amplitudes of attenuated regular waves, and energy spectra of attenuated random waves.

Although the term "random" is used to describe test waves which varied in height and length, the same sequence of waves could be repeated in successive test runs. This reproducibility was obtained by varying the frequency of each cycle of the wave generator automatically according to a preset program.

2.1.1. Model Grid Configurations and Test Program

Figure (3) shows schematic elevation views of the grid configurations; Figure (4) shows construction details of the rigid and flexible grids. These configurations were tested to achieve the objective outlined in the Introduction, as follows:

1. Attenuation of random waves
   a. 4 ft rigid grid, 0° and 30° headings.
   b. Flexible grid, 0° heading.
   c. Two 2-ft grids spaced 4 ft, 180° heading.

2. Attenuation of regular and random waves at a 30 degree angle of incidence to the track of a 4 ft rigid grid.

3. Comparison of regular wave attenuation and drag measurements for rectangular grids of differing solidity; and for rectangular and trapezoidal grids of equal solidity in smooth water and regular waves at 0° heading.

4. Using rigid grids in regular waves for ease of testing, studying the potential for wave

attenuation by the following techniques:

a. Scenario 1 where a grid, towed at 0° heading, is stopped and its wake drifts past the motionless grid to cause wave attenuation over an area downwave of the grid.

b. Scenario 11 where two grids are towed at 180° heading to produce wave attenuation in the area between the grids.

5. Develop a suitable technique for towing a floating, flexible grid, and evaluate its drag and wave attenuation performance in regular and random waves at 0° heading.

Portions of representative test runs for Scenarios 1 and 11 were recorded on 16mm color movie film. A scale model of an offshore drilling crew boat was anchored in the areas of expected wave attenuation so that film viewers would see the calming effect on boat motions.

2.1.2. Data Reduction Procedures

Wave attenuation in random waves was evaluated by comparing rms wave heights obtained as a by-product of spectrum analysis of wave records. Incident wave records were taken at a fixed location without a grid in the water; a moving probe was used to obtain records of attenuated waves. Several runs were made in different sections of the reproducible wave sequence to obtain an adequate sample size, and rms values of these runs were averaged.

Spectra of incident waves and attenuated waves were compared to examine how attenuation varied with wave frequency. Since attenuated wave records were obtained with a probe moving at V ft/sec, computer analysis produced wave spectra based on frequency of encounter, ω_e. For purposes of the comparison, it was necessary to transform the zero speed, unattenuated wave spectra based on wave frequency, ω, to frequency of encounter:

$$\omega_e = \omega - (\omega^2 V \cos\mu)/g,$$

where μ is the angle of incidence. Also, the total energy in a spectrum cannot change when frequencies are transformed, i.e., the sepctrum areas $\int s(\omega)d\omega = \int s(\omega_e)d\omega_e$ where s stands for spectral ordinate. Therefore, a transformation of s must be made as follows:

$$s(\omega_e) = s(\omega)/\sqrt{1 - (4\omega_e V\cos\mu)/g}$$

In regular waves, attenuated wave heights were averaged over the run interval by a "peak-trough" program in the tankside digital computer. The program also computed the theoretical attenuation for the test wave length and the velocity, draft and width of the grid.

2.2. Test Results

2.2.1. Random Waves, 0^o Heading

The random wave program selected for these tests had a "control time" of 110 sec and the crank on the Tank No. 2 wave maker was set so as

to produce a significant wave height between 2.5 and 3 inches. The control time is the time set for the random wave program to generate 100 waves. Thus, the average "wave period" for the waves was preset to be 1.1 seconds. The incident wave power spectrum for the random waves was obtained from measurements at a fixed probe at the center of the line along which the grid would be subsequently towed. This spectrum was transformed to one based on encounter frequency for a 1 ft/sec tow speed using the procedure outlined in the previous section. This transformed incident wave spectrum is shown in Figure 5. The peak spectral density of 0.195 in^2-sec occurs at an encounter wave frequency of 4.7 radians/sec which corresponds to a wavelength of about 6.0 feet. The significant wave height, $H_{1/3}$, was found to be 2.75 inches.

The four-foot wide grid was set at a draft of 7 inches and towed at a nominal 1 foot/sec in order to provide for an attenuation of the peak in the incident wave spectrum to 25% of its original value, which corresponds to a 50% reduction in wave height at the peak frequency. The choice of tow speed and grid draft was determined from the regular wave results reported in Reference 1. Four runs were made with the grid with the starting time of each successive run delayed 20 waves in the random wave program to allow for most of the 100 waves in the random wave sequence to be incident on the grid wake. Spectra for each of the four tows were

obtained from measurements obtained with the towed wave wire (labelled No. 1 in Figure 2a) located 61 inches behind the grid. The average of these four individual spectra is shown in Figure 5. As predicted the peak spectral value was attenuated to 25% of its value in the incident wave spectrum. At encounter frequencies lower than 4 rad/sec the components were not significantly attenuated, while at frequencies higher than 5.5 rad/sec the spectral values were attenuated to 10-15% of their incident initial values.

We have also shown in Figure 5, a calculated attenuated spectrum derived from the predicted attenuation of wave components using equation (1) which was developed from attenuation measurements in regular waves. The agreement between the observed and predicted attenuated spectra is excellent for frequencies less than 5 rad/sec. At higher frequencies the predicted attenuation is greater than that which was observed. This discrepancy is not unexpected since the predictive formula for attenuation was based on observation of regular wave attenuation restricted to a range of wave height attenuation from 0-80%. Since the predicted values for wave height attenuation at encounter frequencies greater than 5 rad/sec exceed 80% we recognize that the range of validity of the predictive formula has been exceeded. Further clarification of this point can be had by reviewing the development of this formula in Ref. 1.

2.2.2. Regular Waves, 30° Heading

An initial series of tests with the 4 ft. wide grid towed at 30° heading revealed that the attenuated region was no longer symmetric about the centerline of the grid as was the case with following waves. After some preliminary work in attempting to map out the region of wave attenuation it was determined that the arrangement of wave probes behind the grid shown in Figure 2b would insure coverage of the region of highest attenuation. In fact, we concluded that the peak attenuation would be found in the vicinity of wave wire No. 1, 22.5 inches to the left of the grid centerline. With this wave wire configuration a series of tests were undertaken with regular waves of 4, 6 and 8-foot lengths, with tow speeds ranging from 1.4 to 2.5 ft/sec and with grid drafts of 4 and 10 inches.

The results of the oblique waves tests are summarized in Figure 6 where the experimentally determined values of wave attenuation are plotted against the calculated values of C_B/C_o-1. We recall from Reference 1, that C_B is the phase speed that the wave train would attain when encountering a finite depth current and C_o is the phase speed in still water. Results of measurements in the grid wake reported in Reference 1 suggested that the wake speed a short distance behind the grid could be taken as one-half the tow speed and that the depth of the current was approximately equal to the grid draft. For our

present case of oblique incident waves we calculate C_B/C_o using 1/2 $U_g \cos 30^o$ as the appropriate velocity in the wake current.

Two results are immediately apparent from Figure 6 which are in sharp contrast with the results obtained with following waves. First, there is no apparent dependence of wave attenuation on the ratio of grid width to wave length whereas for following waves there was a clearly discernable dependence on this ratio. Secondly, the attenuation for a given value of C_B/C_o is about 50% less for the oblique waves than that found for following waves. A least squares fit of the experimental data suggests that for the 30^o wave heading the wave attenuation $\gamma=2.6$ $(C_B/C_o - 1)$. For following seas (with a very wide grid) we have found that $\gamma=4.7(C_B/C_o - 1)$.

2.2.3. Random Waves, 30^o Heading

The random wave test for oblique waves was conducted in an analogous manner to that for the following sea case except that the probe arrangement shown in Figure 2c was employed. The random wave program employed in this test was the same as for the following random waves. The incident wave spectrum was determined from wave measurements mid-way along the oblique line of tow. This spectrum was transformed to one based on encounter frequency using the nominal speed of tow, which we selected to be U_g = 1.50ft/s, multiplied by the cosine of the heading angle. This transformed spectrum is

shown in Figure 7. The significant height, $H_{1/3}$, was 2.47 inches. Four runs were made with the four-foot wide grid set at a draft of 4 inches. The average of the four spectra found from the wave measurements at Wave Wire No. 1 is also shown in Figure 7. Again we obtain an attenuation of the incident spectral peak to about 25% of its incident value. Thus, the results of random wave test at a 30° heading are similar to those for the following sea case except that the tow speed was 50% greater and that the attenuated region was not on the grid centerline.

2.2.4. Scenario 1

In this simulation of a possible operational scenario the four-foot wide grid was towed at 0° heading about 2/3 of the available length of tow and then stopped. The wave wires were arranged as shown in Figure 2d. Incident waves with lengths of 4, 6, and 8 feet were employed. The tow speed was varied from 0.5 to 1.5 feet/sec and grid drafts of 4, 7 and 10 inches were tested. For each test condition, the predicted wave attenuation was determined from Equation 1, which was based on measurements in the wake while the grid was moving. The maximum attenuation at each wave wire location except for Wave Wire No. 2 was determined after the grid was stopped. For Wave Wire No. 2 the maximum attenuation was determined during the tow period. All attenuations were calculated relative to the wave height measured at each wire just prior to each run.

An initial analysis of the Scenario 1 test results was obtained by comparing the measured attenuation values at each wave wire location with the predicted attenuation for every experimental run. The result of this comparison for Wave Wire No. 2, located 31 inches behind the grid on the centerline, is shown in Figure 8a. If we assume that the experimental attenuation values are linearly proportional to the predicted attenuation values we can use a least squares curve fitting approach to determine the constant of proportionality. For Wave Wire No. 2 we find $\gamma_{EXP} = 1.1\gamma_{PRED}$ which implies that 10% higher attenuation was found in this series of tests than in the earlier experiments from which the empirical formula for attenuation was derived. In view of the scatter exhibited in Figure 8a this discrepancy was not judged highly significant.

In Figure 8b the comparison of experimental attenuations determined from Wave Wire No. 3 (31" in <u>front</u> of the grid) after the grid had stopped with the predicted values is presented. For this case the least squares fit shows $\gamma_{EXP} = 1.05\ \gamma_{PRED}$ which implies that nearly equal attenuation can be expected ahead of the grid after stopping the tow as that found in the grid wake during the tow. Similar results are shown in Figure 9a for Wave Wire No. 4 (62" in front of the grid) and for Wave Wire No. 6 (120" in front of the grid). The least squares fit for the correlation of the experimental

attenuation values with the predicted values gives $\gamma_{EXP} = 0.93\ \gamma_{PRED}$ for Wave Wire No. 4 and $\gamma_{EXP} = 0.96\ \gamma_{PRED}$ for No. 6. We can conclude that the attenuation region extends at least 1½ to 2 wave lengths in front of the stopped grid.

The results for Wave Wires No. 1 and No. 5 (located 31 inches ahead of the grid and at lateral positions 12 and 24 inches respectively, from the centerline of the grid) are presented in Figures 10a and 10b. The least squares fit shows that $\gamma_{EXP} = 0.86\ \gamma_{PRED}$ for Wave Wire No. 1 and $\gamma_{EXP} = 0.83\ \gamma_{PRED}$ for No. 5. As expected, the greatest attenuation was found at the grid centerline (Wave Wire No. 3) but the results for Wave Wires No. 1 and No. 5 demonstrate that the attenuation does not decrease substantially over the lateral extent of the grid.

The duration of wave attenuation after the grid is stopped is an essential feature to be evaluated for this scenario. The time interval for which the waves exhibited maximum attenuation was determined for each wave wire for each of the Scenario 1 Tests. This determination from oscillograph records was most readily accomplished for cases where the attenuation exceeded 40%. For these cases the beginning and end of the time interval of quasi-steady minimal wave height could be most clearly identified.

It proved difficult to establish any clear correlation of the duration of attenuation with

the test parameters nor did any pattern emerge for duration as a function of location. For tests where the attenuation exceeded 40% the duration ranged from 3 to 41 wave periods with most values lying between 6 and 12 wave periods. The failure to find a consistent pattern in the duration measurements for the Scenario 1 Tests makes the full scale application of this procedure a speculative proposition.

2.2.5. Scenario 11: Regular Waves

In the first series of tests of this operational scenario two-two-foot wide rectangular grids separated by a gap of four-foot (shown in Figure 3c) were towed at 180° heading (head seas). The wave probe arrangement for these tests is shown in Figure 2e. Wave Wires 1-4 were towed with the grids while Wires 5 and 6 were stationary at the mid point of the tow. The basic premise underlying this scenario was that wave heights would be amplified behind such grid due to refraction while in the gap between the grids there would be an attenuation. Wave Wire No. 1 was placed behind the grid simply to verify wave amplification at this location. Such amplification was, in fact, observed during the test runs, thus serving to confirm in part the underlying phenomenological understanding of the wave behavior under these test conditions.

The wave measurements at Wave Wires No. 3 and No. 4, (both moving with the grid) revealed significant wave attenuation. An extremely

interesting characteristic of the attenuation at these wave wire locations was that the attenuation for a particular wave length reached a clearly defined maximum at a particular tow speed and at lower and, most surprisingly, at higher tow speeds the attenuation was significantly reduced. In contrast, for the following seas test with a single grid, attenuation invariably increased with increasing tow speed or, at worst, it remained at nearly maximum values (80 to 90%) as the speed was increased. Our conclusion was that attenuation at a fixed point relative to the grid exhibited the properties of a tuned system and that the position of the attenuated region changed with differing wave lengths and tow speeds. Rather than attempt to map out this variation in location by rearrangement of the towed wave wires, we relied on the fixed wave wires (No.5 and No.6) to establish the maximum attenuation.

Figure 11 presents a summary of test results for regular waves (4-foot wavelength) in which we have plotted the maximum attenuation for wave wires 5 and 6 as a function of the quantity C_B/C_o-1. The nearly linear dependence of attenuation on C_B/C_o is similar to results found in the wake of a single grid in following seas.

Results of a similar nature to those shown in Figure 11 were found for incident wavelengths of 3 feet and 2.5 feet. These test results are presented in Figures 12 and 13. An interesting aspect of these results is that the particular grid configuration employed in the initial

Scenario 11 tests is most efficient for 3-foot wavelengths. We find that to obtain an attenuation of 50% the required values of C_B/C_o-1 are approximately 0.18 for both 2.5 and 4-foot waves but it is about 0.15 for the 3-foot wavelengths.

For wavelengths greater than the space between the grids the wave attenuation becomes markedly less. Results for incident wavelengths of 6 and 8 feet are presented in Figures 14a and 14b. For these test conditions the attenuation obtained at Wave Wires 5 and 6 did not exceed 35%. It should be noted that for these tests the length of the waves were 3 and 4 times greater than the individual grid widths and thus we should expect significantly reduced effectiveness.

In order to further investigate Scenario 11 under a wider range of test conditions we employed the grid configuration shown in Figure 3d. The use of 4-foot wide grids eliminated the large ratios of wavelength to grid widths encountered in the first series of Scenario 11 Tests. In Figure 15 we present attenuation result for 8-foot wavelengths and for 4, 6 and 8-foot spacing between the grids. These results clearly show that attenuation is enhanced with increased spacing between the grids. The results for 6-foot wavelengths are presented in Figure 16. For values of C_B/C_o-1 less than 0.16 it is again apparent that increased spacing increases attenuation. For larger values of C_B/C_o-1 the attenuation for first the 8-foot and then the 6-foot

spacing is observed to decrease. This result is similar to that discussed previously for the wave wires towed with the grid but are here found for the fixed wave wires as well. No clear explanation of this phenomenon has as yet been found. The rather surprising behavior depicted in Figure 16 is further reinforced in Figure 17 in which test results for 4-foot waves are presented. For an 8-foot space between the grids the attenuation exceeds 80% at C_B/C_o-1 = 0.10, 0.22, and at 0.33. But at an intervening value of C_B/C_o-1 = 0.14 the attenuation drops to 53% and at C_B/C_o-1 = 0.28 it is only 43%. For a 4-foot space the attenuation increases with increasing C_B/C_o for values of C_B/C -1 less than 0.2 but then decreases at larger values of C_B/C_o. For a 6-foot space between the grids the attenuation reaches a minimum at C_B/C_o-1 = 0.2 and then increases with increasing values of C_B/C_o.

Just as wave attenuations in the Scenario 11 tests (second series with 4-foot grids) exhibit maxima at particular values of C_B/C_o-1 the duration of attenuation also reaches maximum values. For example, for 4-foot wavelengths and an 8-foot space between the grids the duration is 5 wave periods at C_B/C_o-1=0.09; it is 16 wave periods at C_B/C_o-1=0.14 (where, incidently, that attenuation is at a relative minimum); at larger values of C_B/C_o-1 the duration decreases reaching just 2 wave periods at

C_B/C_o-1 = 0.33. As with the behavior of attenuation the pattern of duration of attenuation for Scenario 11 proved difficult to rationalize.

2.2.6. Scenario 11: Random Waves

A series of tests to determine the effectiveness of the Scenario 11 configuration in random sea was conducted with the two 2-foot wide grids. The grid draft was 4 inches and the two speed was 1.1 ft/s. The attenuated spectrum for Wave Wire No. 4 (see Figure 2e, for location) was obtained and compared with the incident wave spectrum suitably transformed for frequency of encounter in head seas. The results are shown in Figure 18. Interestingly there was significant attenuation for incident wavelengths from 3 to 6 feet but virtually no attenuation at either longer wavelengths or shorter wavelengths. This behavior is consistant with the results obtained in regular waves in which it was noted that at a fixed location, relative to the grids, measured wave attenuation exhibited a maximum value for a particular values of the ratio of tow speed to incident wave celerity. At either higher or lower values of this ratio the attenuation decreased. For a fixed tow speed this implies that attenuation will be maximum for a particular incident wavelength and decrease for both longer and shorter wavelengths.

2.2.7. Increased Grid Solidity

The solidity of the 4-foot wide grid was increased from 0.34 to 0.53 by modifying the grid construction as shown in Figure 4. A series of tests were made with the modified grid in regular following seas. A comparison of the observed attenuation at Wave Wire No. 1 (5 feet behind the grid) and at Wave Wire No. 2 (2½ feet behind the grid) for these tests with the predicted attenuation for grid solidity of 0.34 is shown in Figure 19. For Wave Wire No. 2 it is readily apparent that the increased solidity yields consistently higher attenuation values than would be found with the lower solidity grid. A least squares fit of the data reveals that γ(0.53 solidity) = 1.27γ(0.34 solidity) for Wave Wire No. 2. For Wave Wire No. 1 the effect of the increased solidity is less apparent. A least squares fit of these data yields γ(0.53 solidity) = 1.08 γ(0.34 solidity).

The cost of obtaining improved performance with the increased solidity is a substantially increased drag coefficient C_D. For the 0.34 solidity grid the average drag coefficient was found to be 0.65. For the 0.53 grid the average drag coefficient increased to 1.03. The effect of this increased drag coefficient on the tow force required to achieve a given level of wave attenuation is offset to some extent by the reduction in tow speed. An example best illustrates this point. We begin by specifying a desired attenuation of 50%. From the procedures

outlined in Reference 1 we find that for the 0.34 solidity grid the requirements to achieve this attenuation are $W_g/\lambda_o = 0.85$, $d_g/\lambda_o = 0.15$ and, most importantly, $U_g/C_o = 0.15$. For the grid with increased solidity we can follow the same procedure in Reference 1 but note that the predicted attenuation for this grid is (for Wave Wire No. 2) 27% greater than for the lower solidity grid. The required parameters are, under this condition, $W_g/\lambda_o = 0.85$, $d_g/\lambda_o = 0.15$, and $U_g/C_o = 0.12$, i.e., there is a 20% reduction in the required tow speed. Since the total drag will be proportional to the product of C_D and U_g^2 we find for this case that the required towing force for the high solidity grid will be about 1% greater than that for the normal solidity grid. The power required (= Drag x U_g) would be 19% less for the higher solidity grid.

These results are in general agreement with the initial premise underlying the use of increased solidity grids. Two factors, however, mitigate against adopting a higher solidity grid for practical application. First, the real limiting factor in towing a grid is the bollard pull avaiable from the towing vessel. For a work boat this does not exceed a value of about 20 lbs. per installed horsepower. Thus a vessel with a 500 hp power plant could develop a maximum tow force of 10,000 lbs. If we were to continue with our example, we can show the limitation imposed by the bollard pull constraint in the following manner. Suppose we seek to obtain

50% attenuation of waves with an incident period of 6 seconds for which λ_o = 184 ft and C_o = 30.7 ft/s. For the 0.34 solidity grid we would require W_g = .85(184 ft) = 156.4 ft., d_g = 0.15 (184 ft) = 27.6 ft and U_g =0.15(30.7 ft/s) = 4.6 ft/sec. The total drag (or required towing pull) would be $1/2 C_D \rho W_g d_g U_g^2$ = 59,371 lbs. The required power calculated as simply drag times tow speed is 496 horesepower. But, to obtain the required pulling force of nearly 60,000 lbs. we would need a ship with at least 3,000 hp! In view of this type of constraint it is far more essential to reduce drag significantly than to effect a saving in the calculated power requirements. Since the increased solidity grid did not lead to a reduction in drag it does not offer a practical advantage over the lower solidity grid. A second reason for discounting the use of a higher solidity grid is that the region of enhanced wave attenuation did not extend far behind the grid as can be readily seen by comparing Figures 19a and 19b.

2.2.8. Trapezoidal Grid

A series of tests were conducted with the trapezoidal grid shown in Figure 3b. The trapezoidal grid had a projected area equal to 75% of the 4-foot wide grid with both grids at a draft of 8 inches. This decrease in area produced an equivalent decrease in the measured drag. There was, however, a marked decrease in the wave attenuation obtained behind the trapezoidal grid compared to that obtained

behind the rectangular grid. This comparison is shown in Figure 20. The 10-15% decrease in performance with the trapezoidal grid serves to neutralize the advantage of reduced drag since higher tow speeds will be required to obtain the same attenuation as that found for the rectangular grid.

2.2.9. Flexible Grid

The development of a flexible grid; one which could, at full scale, be stowed aboard a work boat, be readily deployed and retrieved, and would perform in an analogous manner to the model rigid grids tested previously, proved to be a lengthy process of trial and error. After consideration of various candidate designs, it was determined that for the full scale application a cargo net might prove to be an adequate replacement for the rigid grid. A preliminary series of tests with a grid, 4 feet wide and with a draft of 6 inches, consisting of sewn strips of ribbon held in a rigid frame were performed to determine its effectiveness in achieving wave attenuation in the wake. The results for regular waves at 0° heading are shown in Figure 21 and for random following seas in Figure 22. It is apparent that the ribbon proved as effective as the rigid wooden grid in achieving wave attenuation.

Having demonstrated that a ribbon grid could be used as a replacement for the rigid wooden grid, the next step was to find a suit-

able method to spread the net aft of a tow boat. The use of rigid framework, while sensible for model scale tests, appeared inappropriate for prototype applications. Fortunately, a wealth of information on maintenance of a spread net towed behind a vessel was available from commercial fishing technology, Reference 3. In fishing applications trawl nets are kept open via the use of vane-like structures variously called doors, otter boards or paravanes, attached to the ends of the net. The hydrodynamic side force or lift developed on the otter boards serves to keep the net spread open. These devices come in a variety of configurations ranging from flat plates to cambered wing sections. A review of otter board performance summarized in Reference 3 revealed that the "suberkrub type" cambered board would be most suitable for our application. This type of board had the highest lift/drag ratio of all types reviewed and was judged to be the best type available for midwater trawling above the sea bed. (Several other boards were judged superior to the suberkrub type for trawling on the sea bed; since we are concerned with towing at the sea surface it was decided that the suberkrub board would provide the best chance of achieving satisfactory results for our intended use).

The basic design of the suberkrub board is shown in Figure 23. Its towing configuration is shown schematically in Figure 24 (plan view) and Figure 25 (profile view). Model scale ver-

sions of the suberkrub boards were fabricated from aluminum. The board length on model scale was 10 inches and the chord was 5 inches, which was in accord with the 2:1 aspect ratio recommended in Reference 3. A new ribbon grid was sewn which had a length of 32 inches and a draft of 10 inches its solidity was 0.31 as compared to 0.34 for the rigid grids. Fishing line was used as the tow lines for deployment of the ribbon grid with attached boards. Further construction details for this net are shown in Figure 4. The dimensions for the tow line arrangement are shown in Figures 24 and 25.

The ribbon grid with attached boards was tested in regular following waves to determine its effectiveness for wave attenuation and to determine its drag characteristics. Visual inspection of the apparatus under tow revealed that the effective width of the net and boards was about 80% of its total net length, i.e., the 32-inch wide net had a projected width of about 24-28 inches. It was also apparent that the effective depth of the net was about 80% of the total net draft. Thus, for comparison of the attenuation results for the ribbon grid with the rigid grids it was assumed that the ribbon grid width was 25.6 inches and the draft was 8 inches. The attenuation results with the ribbon grid are shown in Figure 26 plotted against the predicted results (from equation 1) for a rigid grid. A least squares fit suggests

that the attenuation for the ribbon grid is 86% of that which would be found for an equaivalent rigid grid. This could readily be attributed to the decreased solidity of the ribbon grid relative to that for the rigid grids.

The drag coefficient for the combination of net and boards was calculated on the basis of a constant projected area of 25.6 inches width by an 8-inch draft. With this constant projected area the drag coefficient decreased from 1.12 at a tow speed of 1 foot per second to 0.98 at 2 feet per second. This decreasing trend suggests that the effective projected area decreases slightly with increasing tow speed.

It is useful to attempt to rationalize the drag coefficient derived from measurements with available data on the lift and drag of the suberkrub boards and reasonable assumptions concerning the effective drag of the net. The drag coefficient for the boards is 0.25 while the lift coefficient is 1.52 (Reference 3). These values are for an angle of attack of 15° which was approximately the angle obtained in the tests. The lift on the boards is absorbed by the net. The lift at 90° to the line of tow does not affect the drag. Thus, the total tow force accounted for by the two boards is $0.25 \times (\frac{1}{2}\rho V^2) \times 2A_B = 0.5A_B(\frac{1}{2}\rho V^2)$ where ρ is the water density, V is the tow speed, and A_B is the area of one board (equal to the chord times the span). The drag coefficient for a rigid grid with sol-

idity of 0.34 was found to be 0.65. The ribbon grid with a solidity of 0.31 could be expected to have a drag coefficient of 0.59 (.31/.34 x .65). Since the ribbon grid deforms when under tow its projected area is somewhat uncertain. Earlier we assumed that its width and depth were both reduced to 80% of its original dimensions which yields a projected area equal to 64% of the nominal net area. If we assume a drag coefficient of 0.59 and a projected area of 64% of the total net area A_n we obtain for the drag due to the net $D_n = 0.38A_n$ x $(\frac{1}{2}\rho V^2)$. The combined drag of the net and boards is then found to be

$$D_{TOTAL} = \frac{1}{2}\rho V^2(0.50A_B+0.38A_n). \qquad (2)$$

If we substitute into equation (2) the appropriate values for A_B and A_n then

$$D_{TOTAL} = 1.02\ (\frac{1}{2}\rho V^2) \qquad (3)$$

For a tow speed of 1 ft/sec with ρ = 1.95 slug/ft^3 we obtain a predicted drag of 0.99 lbs which is 38% less than the measured drag of 1.6 lbs for this tow speed.

The discrepancy between the predicted drag values and measured values may be attributed to three factors: (1) the lift and drag coefficients of the boards were obtained from published data and for a particular angle of attack of 15°. We did not measure the angle of attack experimentally but simply estimated it by eye. Thus, our estimate of the tow force absored by

the boards could be substantially in error if the true angle of attack differs from 15°. (2) The effective projected area of the net was also a visual estimate and (3) the drag coefficient for the net was determined from a simple solidity ratio.

3. MESO-SCALE TESTS IN NEW YORK HARBOR

3.1 Test Apparatus

Following the completion of the model scale tests in the towing tank, the design of the intermediate scale net and boards was undertaken. Our original intent was to scale up from model size to meso-scale by a factor of 12 e.g. The boards for the meso-scale tests would have had a span of 10-feet and chord of 5-feet as opposed to the model scale dimension of 10-inch span and 5-inch chord. However, early in the design process we determined that the boards should be constructed of fiberglass-covered marine plywood and, as a very practical consquence - it is simply very difficult and expensive to obtain 5 x 10-foot sheets of marine plywood - we reduced the board dimensions to an 8-foot span and a 4-foot chord.

There were primarily two choices for building material in the construction of the boards, wood/fiberglass and steel/aluminum. Even though metal construction would be more durable than the wooden counterpart, we have chosen to use a wood core - fiberglass reinforced type of construction for two reasons: (1) Due to the density difference

in the construction material, the wooden board (when weighted to neutral buoyancy by weights on the bottom) will have a lower center of gravity which will help the board maintain the designed tow attitude in waves. The inherent stability of the wooden boards with ballast weights at the bottom would also make deployment simpler since the boards would float vertically. (2) It proved far easier with the facilities at hand to work with wood than with metal. The boards were constructed using 4' x 8' sheets of 3/8" marine grade plywood, bent around crossribs to maintain camber. The crossribs and end panels were cut out of 1/2" marine grade plywood. The two sheets of plywood were first cut lengthwise 2/3 of the way through (1/4") every 4" along the width (11 cuts total) to facilitate bending. Once bent the plywood sheets were glued and bolted to the 4 crossribs (1 on each end and 2 equally spaced in between) and the end panels (tow attachements) were glued and bolted on. Then the boards were covered with fiberglass cloth and resin (10 yards of 42" cloth and 2 gallons of polyester resin per board) and the board ends, cross ribs, and leading edges were reinforced with 6" fiberglass tape and resin and the warp and net attachments (4 per board) were reinforced with metal plates.

The net was purchased from Atlantic Industrial Supply Co. It was constructed of 1-3/4" nylon webbing on 9" centers. This provided a solidity ratio of 0.36. Nylon ropes were used

for the towlines. The towline dimensions are given in Figures 24 and 25.

The towing vessel was the Ocean Engineering Department's 26-foot catamarran, R/V DOUBLET, equipped with two 50 hp outboard motors. The maximum bollard pull available with the DOUBLET was 1350 lbs at 4300 RPM. The ample fore deck space on the DOUBLET (10 feet by 12 feet) provided adequate space to stow the boards and net.

3.2 Initial Towing Test Results

The deployment procedure which evolved from an appraisal of various methods tried in the initial mesoscale tests was to launch one board off the side of the DOUBLET, play out the net around the bow and finally launch the second board. The DOUBLET was then backed slowly away from the net and boards while the towlines were played out by hand from the fore deck. It was found that just a small amount of tension in the lines was sufficient to keep the boards separated and to prevent entaglements. Upon reaching the end of the tow warp the towing hawser was walked to the stern of the DOUBLET at the same time as the DOUBLET executed a 180° turn. The tow vessel and net and boards were then ready to commence towing of the net.

The first series of mesoscale tests were undertaken with the ends of the tow warp attached to the DOUBLET, i.e., there was no towing hawser. The following difficulties were

encountered during these initial tests:

(1) The approximate 100 foot distance between the DOUBLET and the net was clearly insufficient for the propeller wash to be dissipated: thus, there was substantial interaction between the net and the flow field from the propellers.

(2) The top of the net because submerged as the pulling force was increased. This behavior persisted despite the addition of several inflatable boat fenders to increase buoyancy along the top of the net.

(3) After a short duration of tow one of the suberkrub boards would begin to rise out of the water and then collapse inward toward the centerline of the tow.

The first of these problems was elminated by the simple expedient of adding a tow hawser at the end of the tow warp. Moving the net an additional 2-300 feet aft of the catammaran proved sufficient to eliminate interaction of the propeller wash with the net. The second problem was not overcome until we added six vertical stiffeners equally spaced along the net to prevent the top of the net from being pulled below the water surface. These stiffeners were 2" by 2" wooden braces, 8 feet in length, which were tied to the webbing of the net. The third

problem proved more troublesome to analize and overcome. It finally became apparent that the instability in the boards could be controlled by slight (of the order of 3-6 inches) changes in the length of the bridle line attached to the bottom of the board. The rising up out of the water of the board could be eliminated by shortening the length of this line. In light of subsequent difficulties with the full-scale tests it should be noted that throughout the mesoscale tests the nature of the board instability was consistently for it to rise out of the water and collapse inward towards the opposite board.

Although foregoing solutions to the problems encountered in the initial mesoscale tests can be readily described, the actual working out of these remedies involved a rather lengthy process of trial and error. This repeated cycle of testing-modification-and retesting was accomplished at very low expense. The only cost for the catamarran was for fuel. The crew aboard DOUBLET for most of this work consisted of one graduate student assistant and one undergraduate. Finally, there was no travel costs since DOUBLET was berthed at Stevens and the testing was conducted in the Hudson immediately adjacent to the Stevens campus. The cost of finding solutions to the initial problems encountered in field testing of the apparatus at full-scale would, by contrast, be prohibitive.

3.3. Developement of Field Instrumentation

3.3.1 Wave Measurements

Clearly, the most important measurements to be obtained in the experiments were simultaneous observations of waves both within and outside the wake of the towed net. The wave probe in the wake would have to be towed with the net while the probe outside of the wake could be either towed alongside the net or maintained at a fixed location. It was determined that towing the second probe at the same speed and direction as the net but clearly outside the influence of the net wake would eliminate uncertainty in the comparison of the two spectra.

After careful consideration of a variety of options for the wave measurement system it was decided that a vertical accelerometer mounted in a 4-foot model boat would be used. Two existing 4-foot models of outboard runabouts were selected from the inventory stored in the Davidson Laboratory. The choice was dictated largely by the relatively small length/beam ratio of these boats (of the order of 3:1). The next design decision in the development of the wave measurement system was whether the accelerometer should either be mounted in the tow vessel in gimbals or, alternatively, fixed rigidly within the vessel. For the latter case, the accelerometer will respond to the pitch and roll attitude of the vessel as well as the vertical accelerations. In a well-designed gimbal

mounting the accelerometer will maintain its vertical orientation despite the pitch and roll of the vessel. In this case, however, any horizontal acceleration, in particular surge motions in following seas, will change the orientation of the suspended accelerometer and, thus, provides a source of error. An analysis of the error induced by the pitch and roll on the fixed accelerometer and of the error induced by horizontal accelerations on the gimbal-suspended accelerometer revealed no substantial difference in measurement errors between the two configurations. In view of this result, it was decided to fix the accelerometer in the model and avoid the added complexity of the gimbal mounting.

The accelerometers were Gulton Type LA 820233±2g servo accelerometers. These were mounted in the models such that their sensitive axes were aligned vertically with the model floating in still water. A careful static calibration of each accelerometer was performed by inclining it at known angles. The response was proportional to the cosine of the angle from vertically upright to upside down. Thus, it was determined that a two-point field calibration (upright and upside down) would be sufficient. The dynamic response of the combined accelerometer-boat model system was checked in the towing tank in a series of regular wave tests. The model was lightly constrained with flexible cord to remain in a nearly stationary

following sea orientation. Wave height records obtained with a wave wire just upwave from the model were compared with the accelerometer records. Double integration of the acceleration record revealed elevation amplitudes in excellent agreement with the measured wave heights for wave periods greater than about 1.0 seconds.

For application in the field, water tight decks were added to the models with a gasketed access hatch to the accelerometer. A 4-conductor cable, through which the excitation voltage to the accelerometer and the output signal were transmitted, was suspended in the water between the model and the tow vessel by small inflated boat fenders. The remainder of the system consisted of a signal conditioner, which provided 28V D.C. excitation and provided for calibrated gain adjustment of the output signal, and a 4-channel TEAC analog tape recorder. In view of the 0-2g field calibration and the expected 0.1 to 0.3g amplitude of the accelerations during tests it was essential to be able to change the signal gain by an order of magnitude in order to maintain an adequate signal to noise ratio on the tape recorder. During tests the input to the tape recorder was monitored on an oscilloscope to insure that signal levels were fluctuating within the ±1V range specified for the tape recorder.

Initial field testing of the towed wave measurement system were accomplished in the

Hudson River. Unfortunately, the system was not completed until the Fall of 1979 whereas the towing tests of the mesoscale net and boards were conducted during the Summer of 1979. Thus, the field test of the wave system were not conducted simultaneously with the towing tests but sequentially. The initial tests were concerned chiefly with the towing behavior of the models in waves. It was found that the addition of small canvas sea anchors to the models reduced surge motions in following seas to an acceptable level. In subsequent tests wave records were obtained for test of the data reduction procedures.

The analysis of the analog wave records consisted of the following six steps:

(1) The analog record was written on a visicorder to allow for visual inspection of the record. In addition to looking for obvious errors in the record, we also were concerned with the identification of the highest frequencies in the signal.

(2) The analog record was digitized at a scan rate at least twice that of the highest frequencies contained in the wave record. The resulting digital file was stored on tape for further processing.

(3) Each digital record was corrected to zero sample mean, and a 10% Tukey cosine taper was applied. This has

the effect of distorting the first 10% of the record and the last 10% of the record.

(4) The power spectrum of the acceleration was obtained by a fast Fourier transform algorithm. From this spectrum we determined a low frequency cutoff, below which the energy content of the spectrum could be neglected.

(5) Double integration of the acceleration to obtain displacement was accomplished in the frequency domain by dividing the raw fast Fourier transform above the low frequency cutoff by the square of the frequency. The squared modulus of the modified transform is the spectrum of the wave elevations. Smoothing of the wave elevation spectrum was accomplished by frequency averaging.

(6) The time history of the wave elevations was obtained by an inverse transform of the modified direct fast Fourier transform. The first 10% and final 10% of this time history show attenuated elevations due to the application of the cosine taper to the original acceleration record.

The application of this procedure to the wave records obtained in the Hudson River provided highly satisfactory results. All subsequent wave records obtained in the full-scale

tests were analyzed in the same manner.

3.3.2 Tow Speed Measurements

The determination of the speed of tow of the net and boards through the water was made using a Hydro Products Model 451 savonius rotor current meter suspended from the tow vessel. The average water speed past the current meter was determined by counting the output pulses (10 pulses for each complete rotation of the rotor) over a known time interval.

The current meter was employed on several occasions during the field testing of the meso-scale net and boards. The maximum measured speed of tow achieved with the catamarran was 2.5 ft/sec at full throttle on the engines. At reduced engine RPM the measured speeds of tow were less, falling to 1.5 ft/s at 2,000 RPM.

With a measure of tow speed available it is useful to consider the maximum drag due to the towed net and boards and compare this with the bollard pull available with the DOUBLET. Two estimates of the total drag force on the meso-scale net and boards are available: First, the experimental value for the drag coefficient found in the model scale tests of 1.0 based on the reduction of net width and net draft to 80% of their nominal dimensions could be used. Second, equation (2) developed in section 2.2.9 could be applied. For a tow speed of 2.5 ft/s and water density of 2.0 slug/ft^3 (appropriate

for the brackish water in the Lower Hudson River), the first estimate of total drag is 1280 lbs. while equation (2) yields a total drag of 860 lbs. Both estimates are less than the bollard pull and appears consistent with the results obtained in the towing tank tests.

3.4. Summary of Mesoscale Test Results

The chief results of the testing in New York Harbor of the intermediate scale net and boards are as follows:

(1) Various problems associated with the field deployment and towing of the net and boards were identified and practical solutions were found.

(2) A wave measurement system was designed, built and field tested. A procedure for analysis of the wave measurements was established.

(3) Tow speed of the apparatus was adequately measured by use of a current meter suspended from the towing vessel.

(4) For the mesoscale net and boards towed at full throttle the total drag estimated from model test results was consistent with the total bollard pull available from the catamarran.

4. FULL SCALE STUDIES

4.1. Test Apparatus

The full scale tests were conducted in the

waters off Miami Beach, Florida. The choice of this site was dictated by several facotrs including: (1) A reasonable expectation of favorable wave conditions, (2) a relatively short distance of travel from the harbor area to open water, (3) the availability of suitable charter vessels with shoreside facilities for assembly of the apparatus and (4) the presence of a USGS field station on Fisher Island to provide back-up support if needed. The vessels used in the full scale tests were chartered from Offshore Scientific Services Inc. in Miami Beach. In the first full scale trials in January the 121-foot RV VENTURE was used to deploy the boards and net and the tug boat, MICHAEL HOLMES was used for most of the towing tests. The VENTURE has a large foredeck with a winch and boom for lifting the boards in and out of the water. The MICHAEL HOLMES at full power could develop a measured towing pull in excess of 13,000 lbs. During the second trials off Miami the 80-foot MOBY 11 with a large afterdeck and boom was used in place of the VENTURE.

On the basis of results obtained in the mesoscale tests it was determined that the full scale tests should be conducted with the dimensions of the net and boards scaled up by a factor of 1.75. Thus, the span of the full scale boards was 14 feet, the chord was 7 feet, and the net was 70 feet long with a 14 foot draft. The webbing and mesh size of the net were the same as for the mesoscale net. The

net was again obtained from Atlantic Industrial Supply Company. The plans for the construction of the full scale boards were completed by the Design Department of the Davidson Laboratory. Competitive bids for their construction were obtained from Offshore Scientific Services Inc. and Marine Safety Equipment Corporation in Farmingdale, New Jersey. Offshore Scientific Services was the low bidder (by $3,200). In addition, construction of the boards in Miami eliminated the cost of shipping the boards from New Jersey. Construction plans for the full-scale boards are shown in Figures 27 and 28.

The rationale for the choice of the dimensions of the full scale net and boards was based on the following reasoning: We expected to encounter waves with significant periods of 4-5 seconds. The wave length for a 5-second wave period is 125 feet and the phase speed is 25 ft/s. For an effective full-scale grid width of 56 feet (80% of 70 feet) and a draft of 14 feet (based on the assumption that vertical stiffeners are effective in maintaining the net draft), the ratio of width to wavelength is 0.45 and the ratio of draft to wavelength is 0.11. While these ratios are both less than the optimal value for minimum power requirements (see Section 1) we can still expect to achieve 50% attenuation for $U_g/C_o \sim 0.2$. Since the meso-scale tests appeared to confirm the model scale drag measurements, a scaling up of the model results to the proposed full scale dimensions

appeared reasonable and resulted in a calculated total drag of about 10,000 lbs at a tow speed of 5 ft/s (20% of C_o which is 25 ft/s for a wave period of 5 seconds). Based on the installed power in the MICHAEL HOLMES this required pulling force was judged to be readily obtainable. In fact, it was considered possible that the VENTURE could be used for towing as well as for deploying the nets and boards. Based on this possibility an alternative test plan was developed in which a single vessel would be used. The salient feature of this alternative plan was to obtain wave measurements inside and outside the wake of the net sequentially rather than simultaneously.

Once the dimensions of the full scale boards and net were established and the expected maximum tow force estimated, the towline dimensions could be determined. The lengths of the full-scale bridle and tow warp are listed on Figures 24 and 25. The bridle lines were 3/8" wire rope while the single lines were 1/2" wire rope. Turnbuckles were installed in the bridle lines to the bottoms of each board to facilitate adjustment, if required, for stable towing of the boards. A 600 ft length of 2" diameter polypropylene rope was purchased to serve as a towing hawser.

Wave and tow speed measurements for the full scale tests were to be obtained in the same manner as that described in Section 3.3.

In addition to these measured parameters it was determined that direct measurement of the total drag force would be useful. A 100,000 lb. capacity strain gage type load cell was used for this purpose. The load cell was installed between the end of the tow line and the towing bit on the tow vessel. The load cell was calibrated at Stevens for loads up to 20,000 lbs. Field calibration was accomplished by using an equivalent resistor for the measured electrical resistance of the load cell at a 10,000 lb. load.

4.2. Full-Scale Tests: First Series, January 1980.

The field program off Miami was scheduled for the week of 20 January 1980. All of the equipment required for the field tests was transported by van to Miami.

The first task was to determine the amount of lead ballast required for the boards. One board was lowered into the water at dockside and weights were added until it floated with about 1 foot of free board. It was determined that 280 lbs. of lead weight should be attached to the bottom plate of each board for proper ballasting. After this was accomplished the entire apparatus was assembled onshore and then loaded on board the VENTURE.

The test plan for the first day of field testing consisted of three tasks: (1) to deploy the net and boards from the VENTURE, (2) to tow the apparatus at various speeds using the VENTURE as the towing vessel and visually assess

its performance and (3) to determine total drag force as a function of tow speed. At a pre-cruise conference in Miami in November it was decided to try an alternative deployment procedure in which the net would be folded and sandwiched between the tow boards so that the entire assembly would be placed as a unit in the water. Once in the water tie lines holding the apparatus together would be released. The first objective of the at-sea work was to determine the utility of this procedure. A second objective of the initial sea trials was to determine if the VENTURE would be capable of towing the net at sufficient speed to attain significant wave attenuation. If this proved feasible then tests could be accomplished with just one chartered vessel at a substantial reduction in cost.

The alternative deployment procedure did not work well. Lines, net and boards became miserably entangled and the apparatus had to be hauled piecemeal back aboard the VENTURE and redeployed using essentially the same procedure which proved successful in the mesoscale tests. Following redeployment, the net was towed at 3/4 and full throttle while drag and tow speed measurements were obtained. In order to avoid any possibility of the propeller wash interfering with the net the entire 600' towing hawer was employed. At 3/4 power, the tension in the towing line was 4,500 lbs while at full power the tension increased to 6,000 lbs. At this tension the measured tow speed was about 2 ft/s,

substantially less than the tow speed of 3.8 ft/s which could be calculated on the assumption that the drag coefficient derived in the model tests was applicable at full-scale.

The visual observations of the net and boards while under tow gave rise to the following conclusions:

(1) The boards appeared to tow stably with no tendency to rise up out of the water.

(2) The net was pulled below the surface of the water despite the effect of 11 large, inflatable boat fenders tied along the top of the net. Vertical stiffeners were not used in these initial tests.

(3) In following waves, there was no visual impression of wave attenuation in the wake.

In view of the results of the first day of sea trials it was determined that the HOLMES would be used as the tow vessel in order to increase the available pulling force and to increase the speed of tow through the water. Current meter measurements, load cell measurements, and wave measurements in the wake of the net would all be made from the HOLMES. Wave measurements outside of the wake would be made from the VENTURE. To insure that the top of the net remains at the sea surface, three vertical wooden stiffeners (4" x 4" x 14') were attached to the net and nine 40-inch circumference inflatable rubber spheres were distributed along the top of the net to augment the buoyancy pro-

vided by the eleven inflatable boat fenders.

The second day of sea trials began with a very successful and quick deployment of the net and boards using essentially the method developed in the mesoscale tests. Initial tow tests were made without the towing hawser. Wave records were obtained inside and outside the wake. It was readily apparent that the net was being towed too close to the propeller wash of the HOLMES and that this wash was overpowering the wake produced by the net. Subsequent analysis of the wave records confirmed this impression since waves were higher behind the net than those measured to the side of the net. Before adding the towing hawser to eliminate the effect of the propeller wash a series of tests were undertaken to determine the behavior of the net at increased towing speeds. At a towing force of between 10,000 and 12,000 lbs. the net and boards were observed to submerge. After reducing the tow line tension the apparatus returned to the surface. At 15,000 lbs pull the net parted from the boards. Subsequent inspection of the net revealed that the tabs on each end of the attachment to the boards had not been sewn properly. A temporary "fix" to reattach the net to the boards was made and the apparatus was redeployed with the 600' towing hawser in place.

A series of tests to compare tow force with tow speed was made. The results are shown in

the following table:

TABLE 1

Tow Speed ft/sec	Tow Line Tension lbs
2.1	6,000
2.5	8,500
2.9	10,000

It is apparent from these results that our estimate of the required tow force based on both model scale and mesoscale tests were substantially less than that found in the full-scale tests. Recall that we had anticipated a tow speed of 5 ft/sec for a tow force of 10,000 lbs.

Near the conclusion of the test at 10,000 lbs. tension the towed apparatus became unstable with the result that it dived swiftly below the water surface. Retrieval of the apparatus was a slow and difficult procedure. It was determined that rather than risk a recurrence of this phenomenon the field tests would be postponed until adequate reserve buoyancy could be added to each board.

The modification of the boards to add reserve buoyancy was accomplished in Miami as was the repair to the net. Figure 29 shows this modification. It was also decided that the cable from the model boat used for wave measurements behind the net was too cumbersome. The wave measurement system was modified such that the accelerometer output could be transmitted by a radio link. This modification was accomp-

lished by Ocean Electronic Applications Inc. Power for the excitation to the accelerometer and for the transmitter was provided by a lithium battery installed in the model. The output signal from the accelerometer was converted to frequency by a voltage controlled oscillator. At the receiving end the transmitted frequency signal was reconverted to a voltage level and the signal conditioner was used to vary the gain of the signal to the TEAC recorder.

4.3. Full-Scale Tests: Second Series, May 1980.

Following completion of the modifications of the full-scale test apparatus a second series of field trials were conducted during 12-14 May, 1980. The boards and net were deployed and retrieved from the MOBY 11. All wave measurements were also obtained from on board the MOBY 11.

The outside-the-wake wave measurements were made with the boat model towed behind the MOBY 11 as the captain carefully kept pace with the towed net. The inside-the-wake wave measurements were transmitted to the receiver on board the MOBY 11.

The two pages of photographs at the front of this report show, on the first page, the deployment of the boards and net from the afterdeck of the MOBY 11 and on the second page the board and nets under tow. In the lower photograph on the second page an attenuated region behind the net is clearly discernable. One change in the apparatus was to substitute 4-inch

diameter PVC tubing for the vertical stiffeners. Two of these stiffeners can be seen on the lower photograph on the first page.

All of the modifications proved successful and boards towed stably at all towline tensions and the radio transmission of data from the accelerometer in the boat model behind the net was accomplished in a highly satisfactory manner. The chief difficulty encountered in the tests was the absence of waves with heights greater than about 2 feet. Despite the lack of high waves seven data runs were taken to compare wave spectra inside and outside of the net wake region.

A summary of the test conditions is presented in Table 2.

TABLE 2

SUMMARY OF TEST CONDITIONS

May 1980

Run No.	Tow Line Tension (Lbs)	Speed of Tow (ft/s)	Distance of Wave Sensor aft of net (ft)
301	10,500	2.5	60
302	13,000	-	60
303	12,500	-	60
304	10,500	3.0	30
305	7,500	2.6	15
306	13,500	3.3	15
307	13,500	-	15

Note: Current meter failed to function properly during Runs 302, 303 and 307.

From Table 2, it is apparent that the measured drag is again, as in the first full-scale tests, substantially greater than calculated estimates based on model scale results. These drag and speed measurements are, however, wholly consistent with the previous full-scale results which were summarized in Table 1.

The comparison of the wave spectra obtained within and outside the wake for the seven runs are shown in Figures 30, 32, 34, 36, 38, 40 and 42. The time histories of the acceleration and wave elevations are presented in Figures 31, 33, 35, 37, 39 and 43. For the first three runs with wave measurements 60 feet behind the net there was no significant attenuation: For Run No. 304 with the boat model towed 30-feet behind the net there was again no significant attenuation. For the final three runs there was substantial attenuation of the peak spectral densities within the wake. In these three cases the peak in the spectrum was reduced in the wake to between 40 and 60% of the peak spectral ordinate measured outside the wake. It should be noted that a 50% reduction in a spectral ordinate represents an attenuation in wave height at that frequency of 25%

4.4. Discussion of Full-Sacle Test Results.

There are two striking results of the full-scale tests. First, the region behind the net where the waves were clearly attenuated was limited to a distance of between 15 and 30 feet.

Second, the drag of the full-scale net and boards was appreciably higher than that predicted from model scale results. No satisfactory explanation of this second result has been found. For the first noted result, there would appear to be two complementary explanations. As mentioned in the previous section, wave conditions were light during the test period. In the absence of a clearly defined seaway with strong directionality of the dominant waves we would expect to have a somewhat broad range of wave directions. Although best efforts were expended to tow the net in the direction of the prevailing waves we must allow for considerable wave energy to be incident at oblique angles to the line of tow.

At this point it is useful to recall the salient features of the model scale tests in oblique seas. The wave attenuation was less than expected and, most importantly, the region of maximum attenuation was found not on the centerline but towards the downwave side of the wake region. If we now consider a confused and variable seaway with waves approaching at oblique angles from either side of the wake region it seems likely that the region of attenuation will be eroded. We should note here that during a test the slick-like attenuated patch behind the net (such as shown on the lower photograph on the second page of photographs) was not a constant feature but transitory. This lends support to the supposition that the

net was effective for following seas but that the directionality of the waves was variable.

5. CONCLUSIONS AND RECOMMENDATIONS.

All of the major objectives of the experimental program were met save for a convincing demonstration of the methods applicability at sea. The model scale tests served to extend the basic study reported in Reference 1. The semi-empirical formula for predicting wave attenuation developed in Reference 1 proved adequate for collapsing most of the towing tank test results. The only case where this failed was for the tests in oblique waves. The development of a practical system proceeded in a trial-and-error mode from model scale to mesoscale to full-scale. The final configuration used in the May, 1980 field trials appeared satisfactory.

The at-sea demonstration of the system was hampered by the prevailing low sea state. It seems likely that a far more convincing demonstration could be obtained with either the mesoscale or full-scale apparatus operating in substantially higher waves. In view of the high costs associated with full-scale testing, it would appear reasonable to conduct future testing with the mesoscale net and boards.

One aspect of the field work which was startingly apparent was the force and extent of the propeller wash when the vessel's forward speed was retarded by the net. The velocity field in this wash appeared far stronger than that induced in the wake of the net. It would be interesting to consider the use of this

propeller wash to attenuate waves. In this case the sole purpose of the net and boards would be to retard the tow vessel's forward speed. Such tests could be conducted sequentially with addition field tests of the effectiveness of the net wake in attenuating waves.

REFERENCES:

1. Hires R. I. "An Experimental Study of a Method To Attenuate Surface Waves Over a Limited Region of the Open Ocean".
Report SIT-DL-78-2020, Davidson Laboratory, Stevens Institute of Technology, Hoboken, N.J. June 1978.

2. Taylor G. I., "The Action of a Surface Current Used as a Breakwater". Proc. Roy Soc. Series A. Vol. 231. 1955.

3. Food and Agriculture Organization of the U.N. Otter Board Design and Performance, Rome, Italy, 1974.

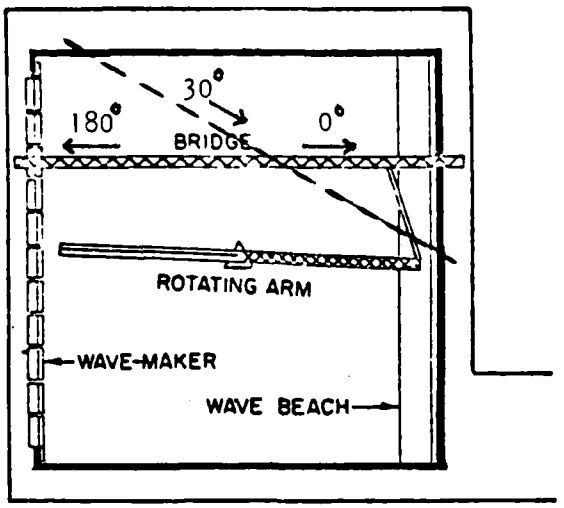

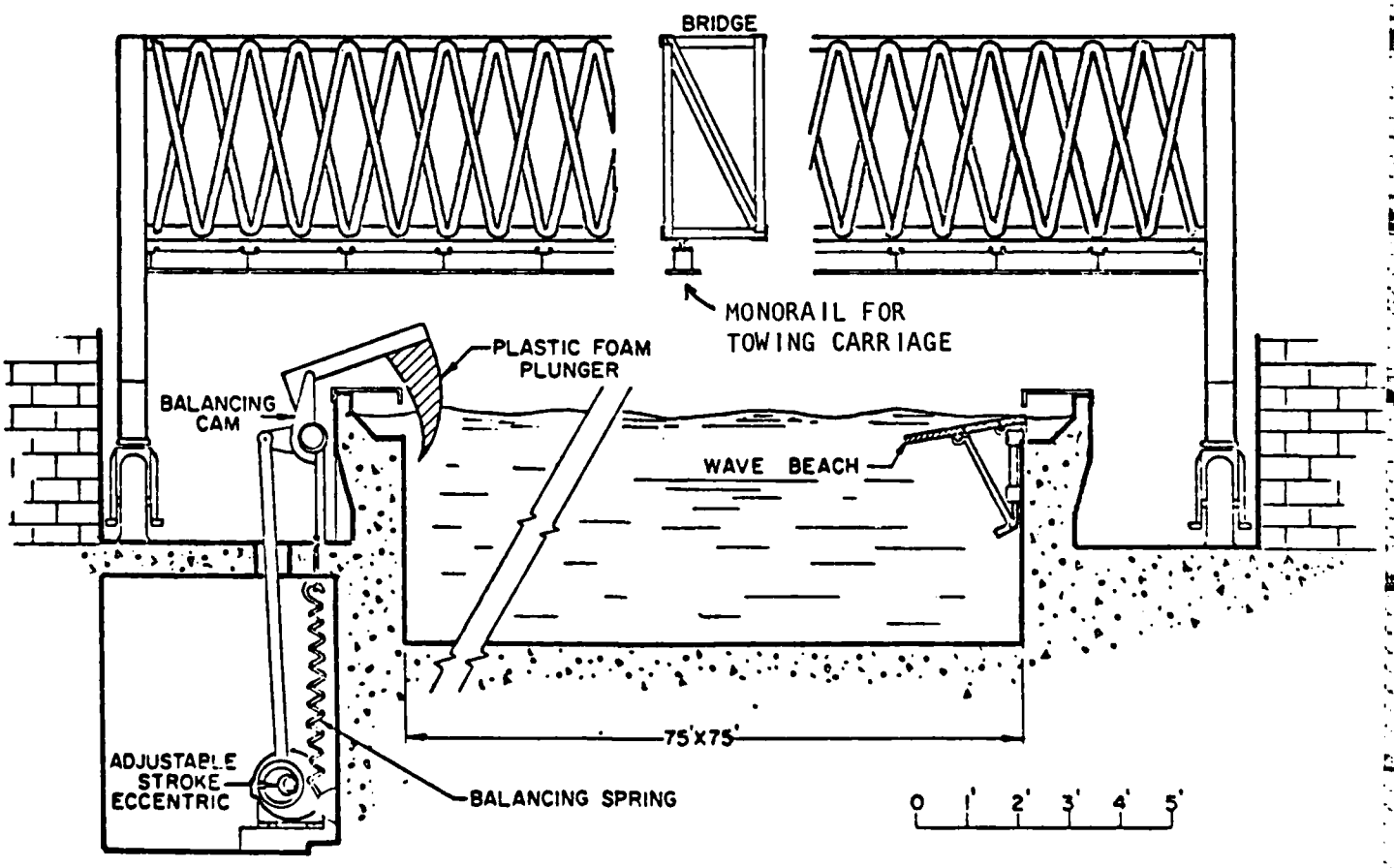

FIGURE 1. DAVIDSON LABORATORY TANK NO.2.

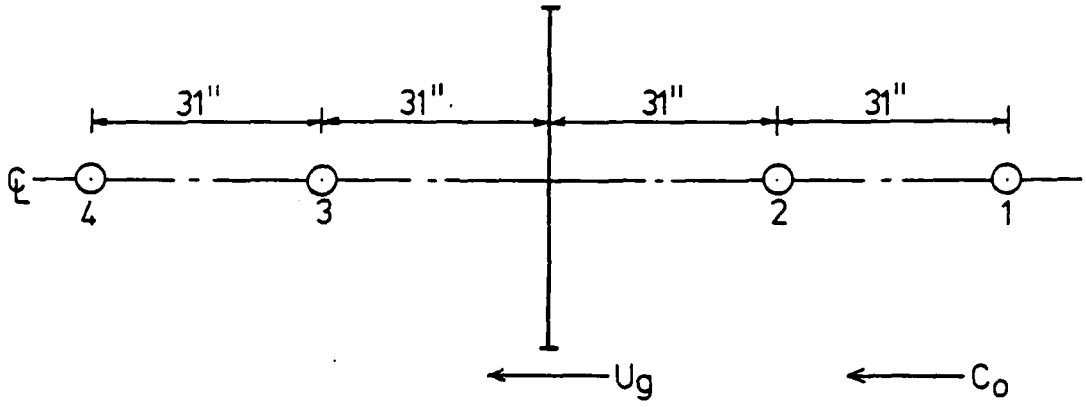

Figure 2A. Single Grid With Following Seas

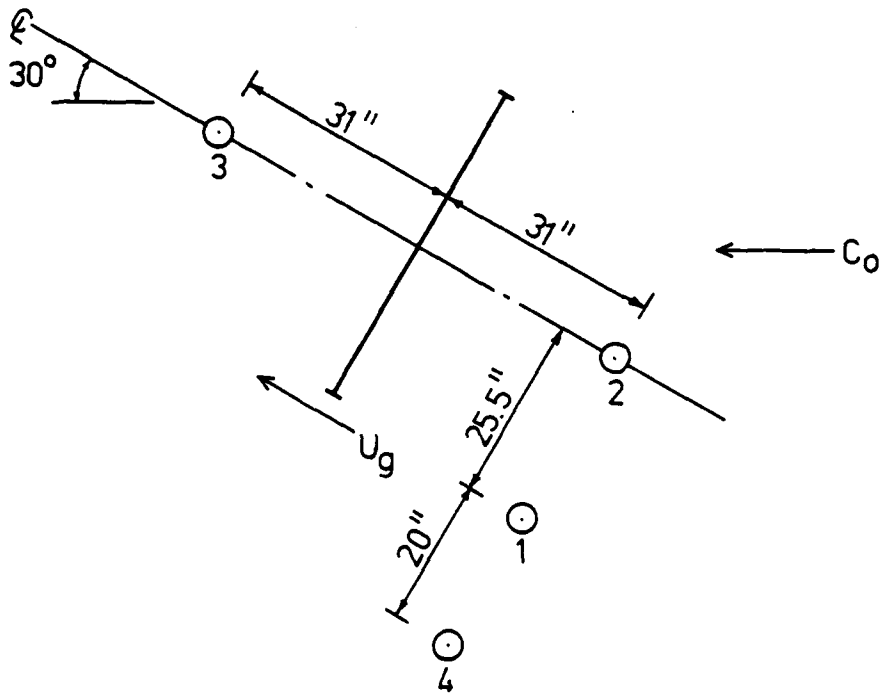

Figure 2B. Oblique Heading Tests With Regular Waves

FIGURE 2. ARRANGEMENT OF WAVE PROBES FOR VARIOUS MODEL TESTS

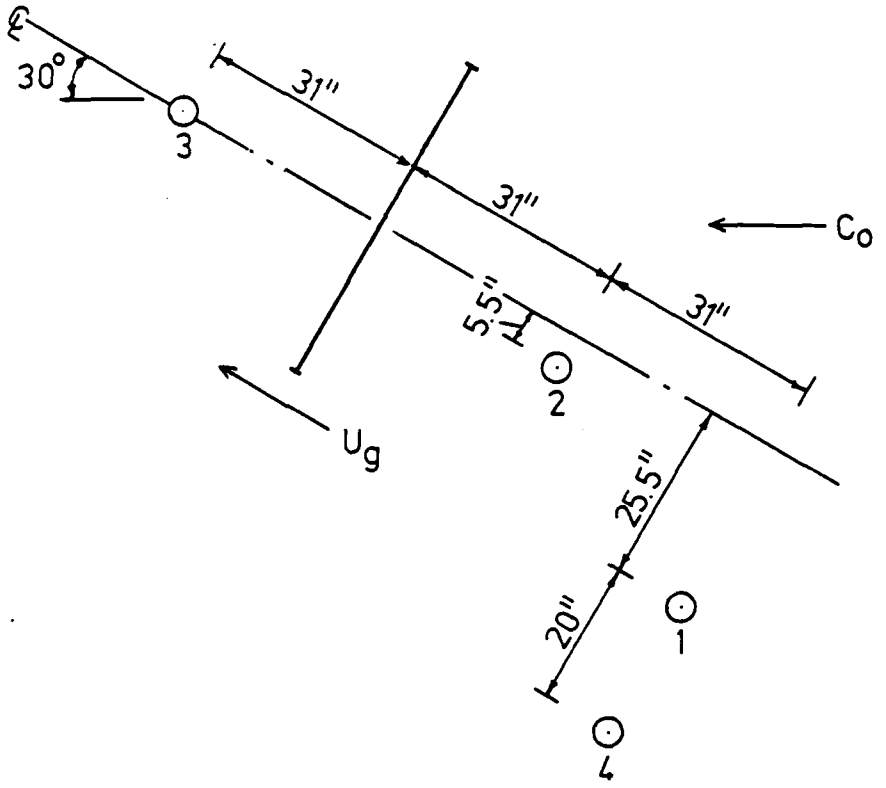

Figure 2C. Obliqe Heading Tests With Random Waves

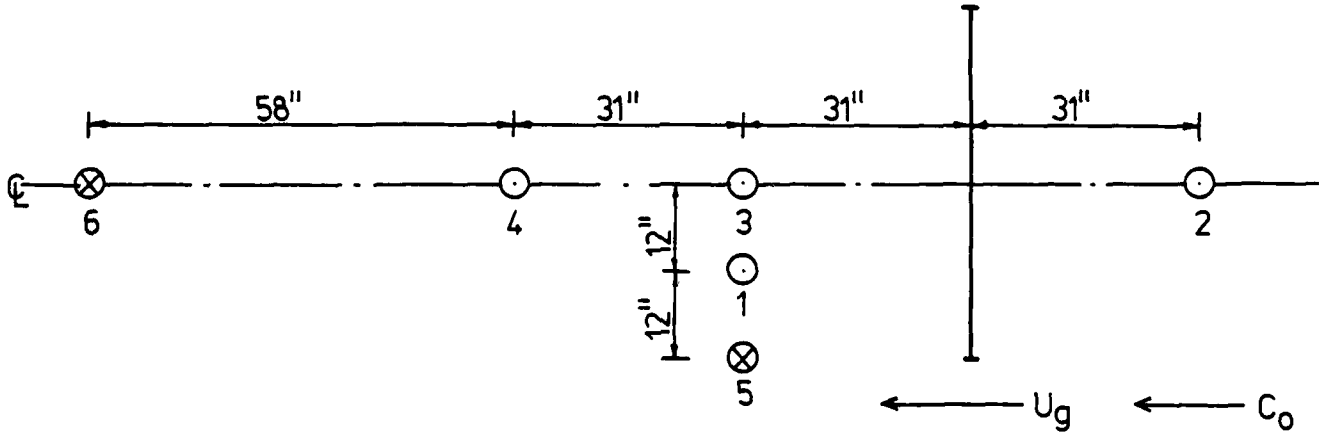

Figure 2D. Scenario I

FIGURE 2. ARRANGEMENT OF WAVE PROBES FOR VARIOUS MODEL TESTS

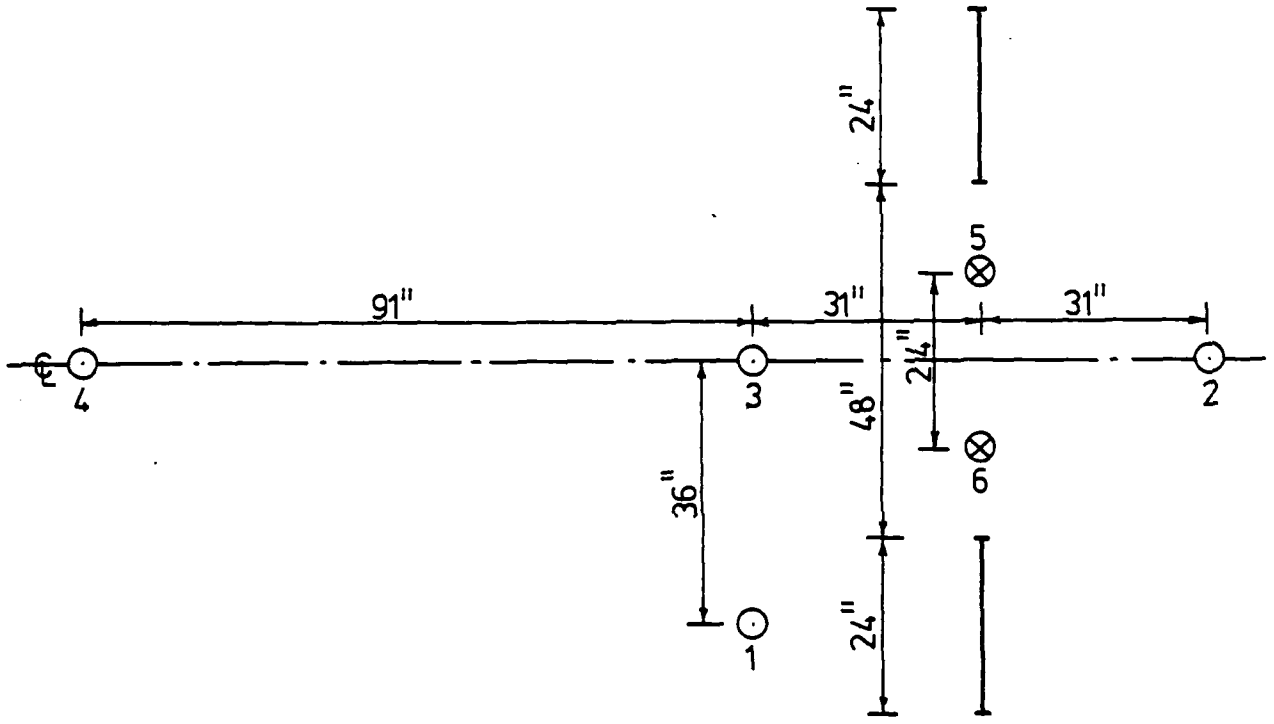

Figure 2E. Scenario II With Two 2-Foot Grids

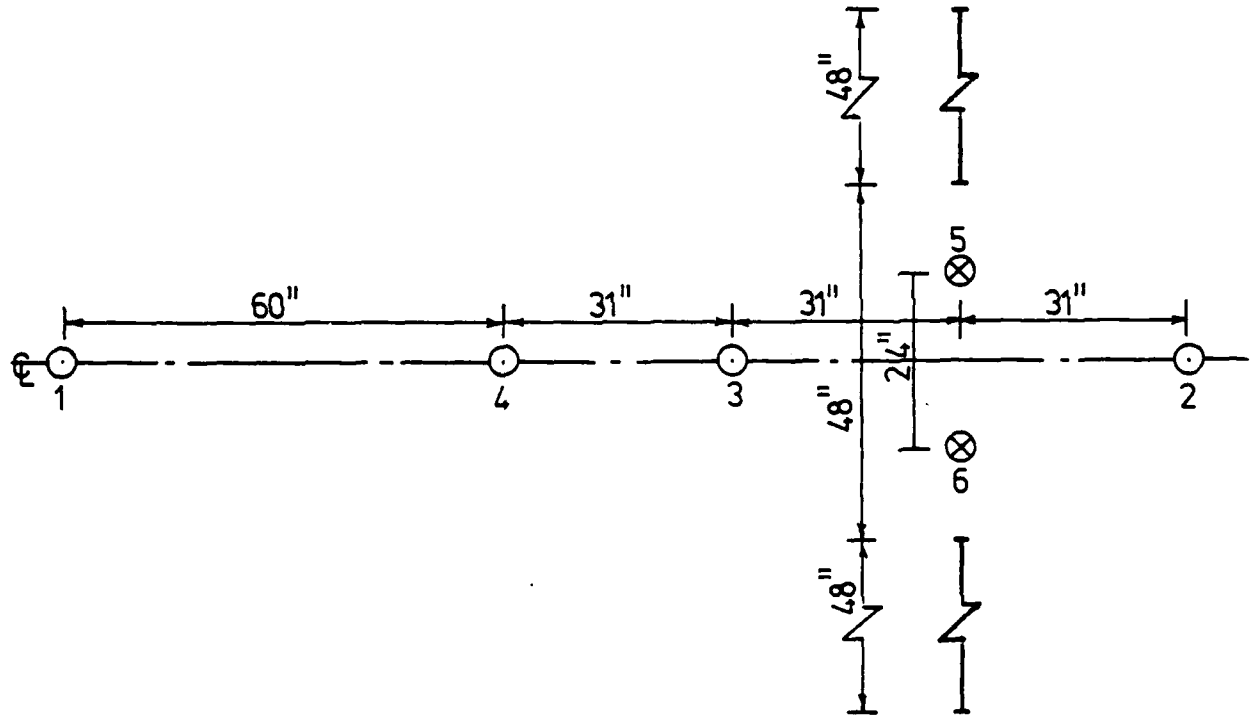

Figure 2F. Scenario II With Two 4-Foot Grids

FIGURE 2. ARRANGEMENT OF WAVE PROBES FOR VARIOUS MODEL TESTS

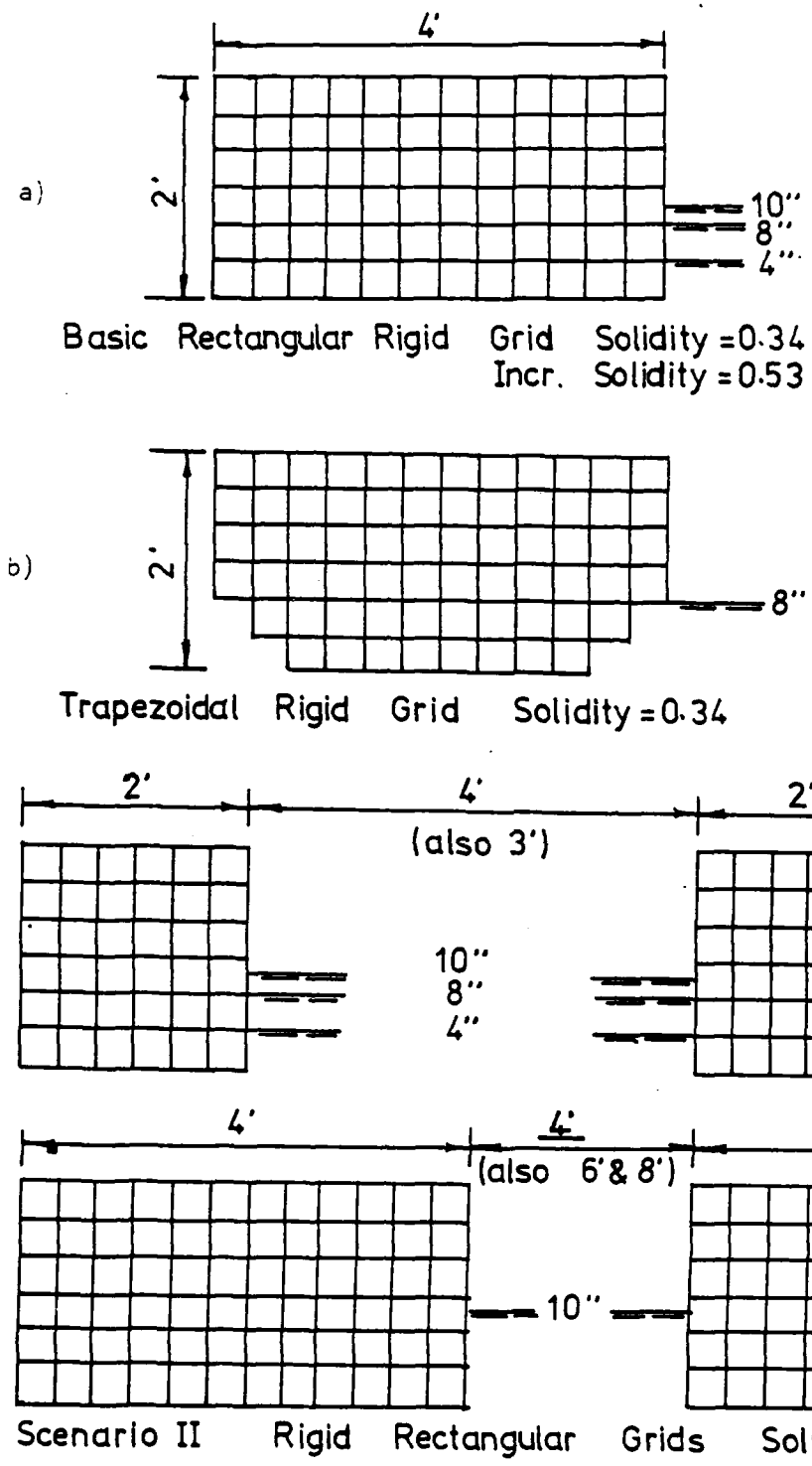

FIGURE 3. GRID CONFIGURATIONS.

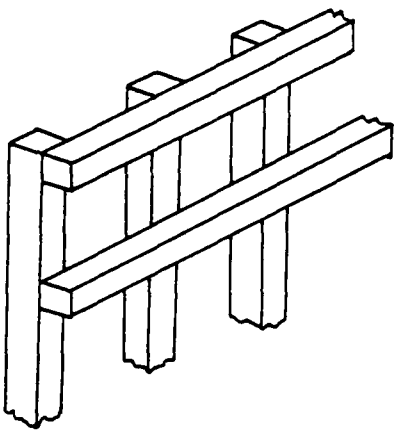

Rigid Wooden Grids

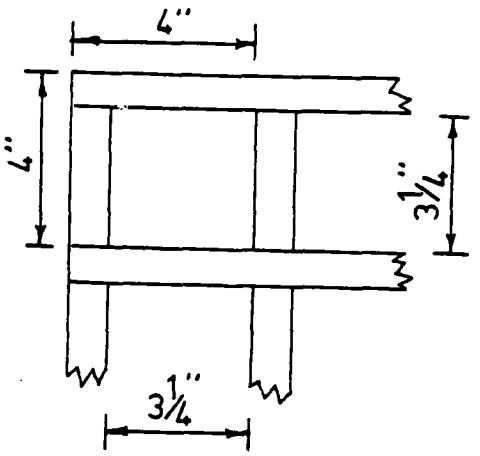

Basic Solidity = 0.34

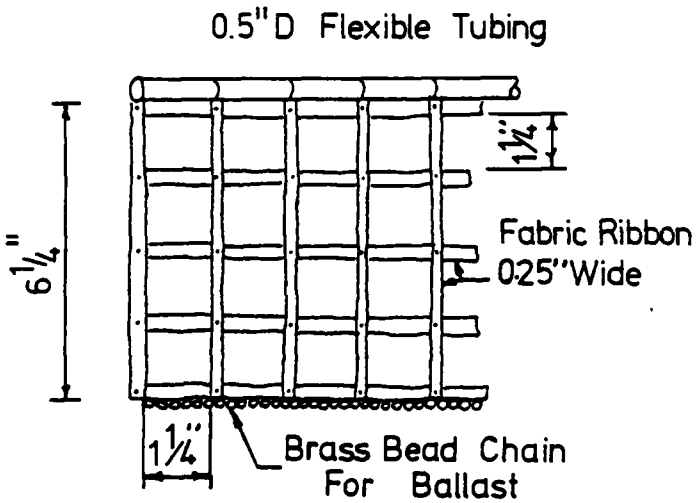

Flexible Ribbon Grid
Solidity = 0.31

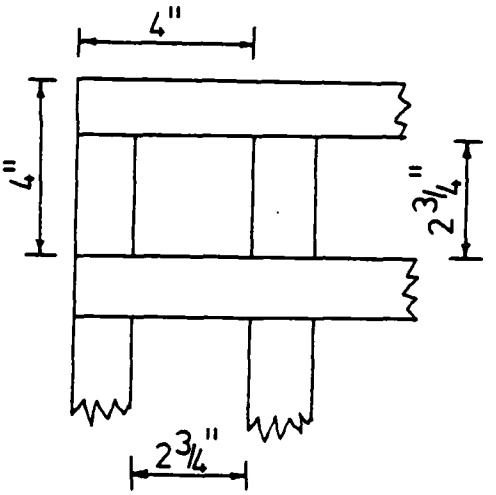

Increased Solidity = 0.53

FIGURE 4. DETAILS OF GRID CONSTRUCTION.

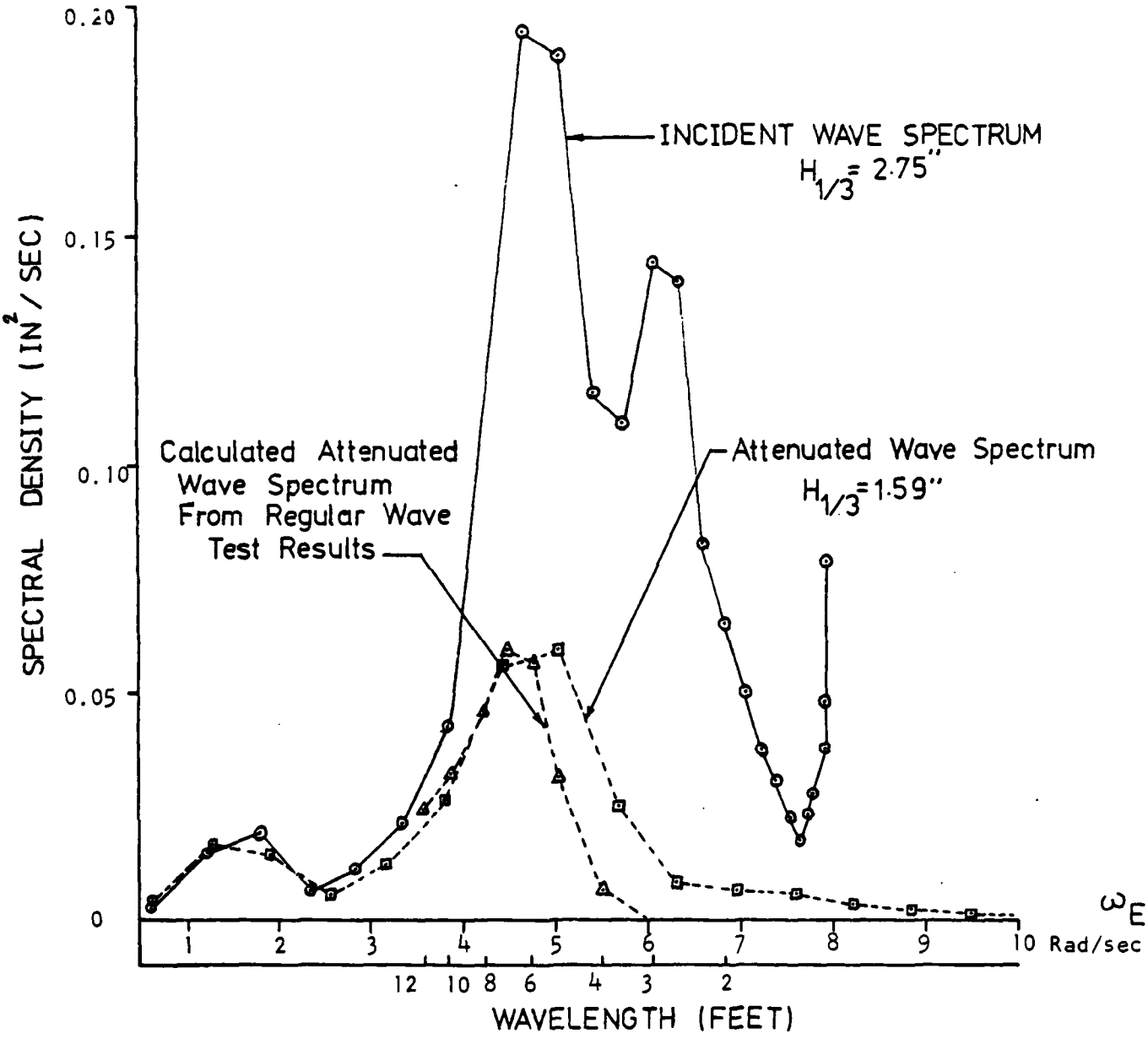

FIGURE 5. COMPARISON OF INCIDENT AND ATTENUATED SPECTRA FOR FOLLOWING SEAS. THE GRID TOW SPEED WAS 1.03 FEET/SECOND.

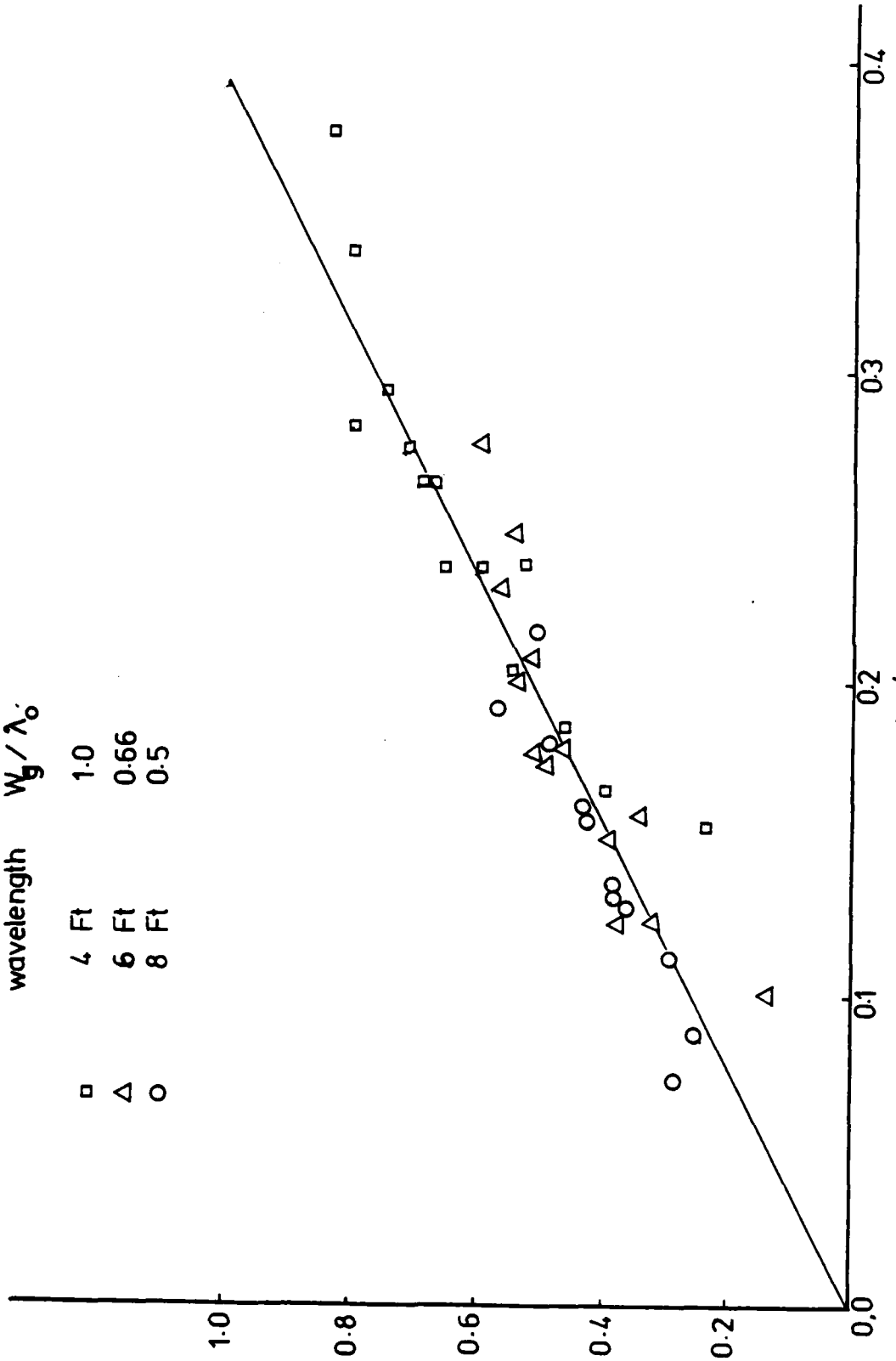

FIGURE 6. SUMMARY OF TEST RESULTS FOR OBLIQUE WAVES.

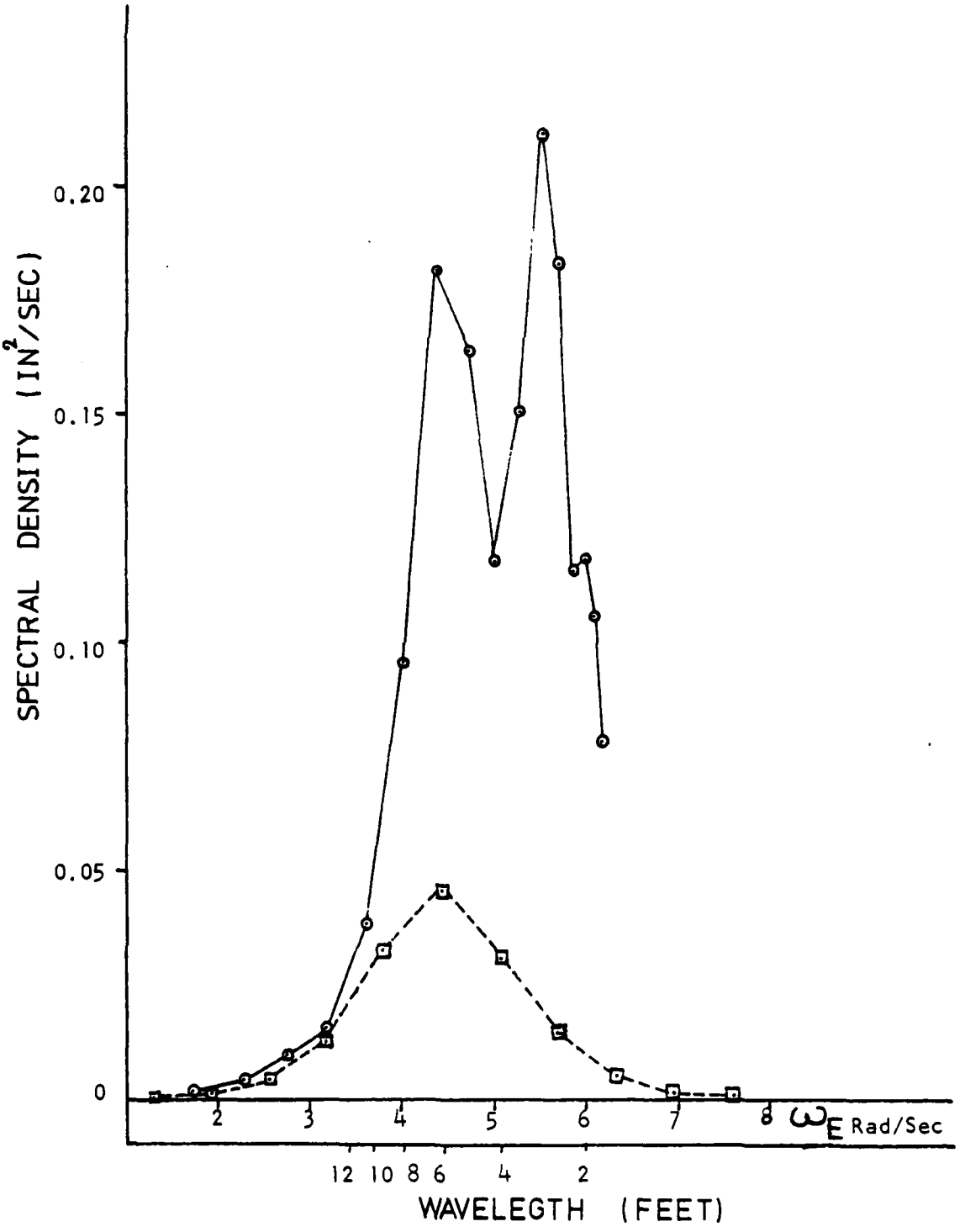

FIGURE 7. COMPARISON OF INCIDENT AND ATTENUATED WAVE SPECTRA FOR 30° HEADING. THE GRID TOW SPEED WAS 1.5 FEET PER SECOND.

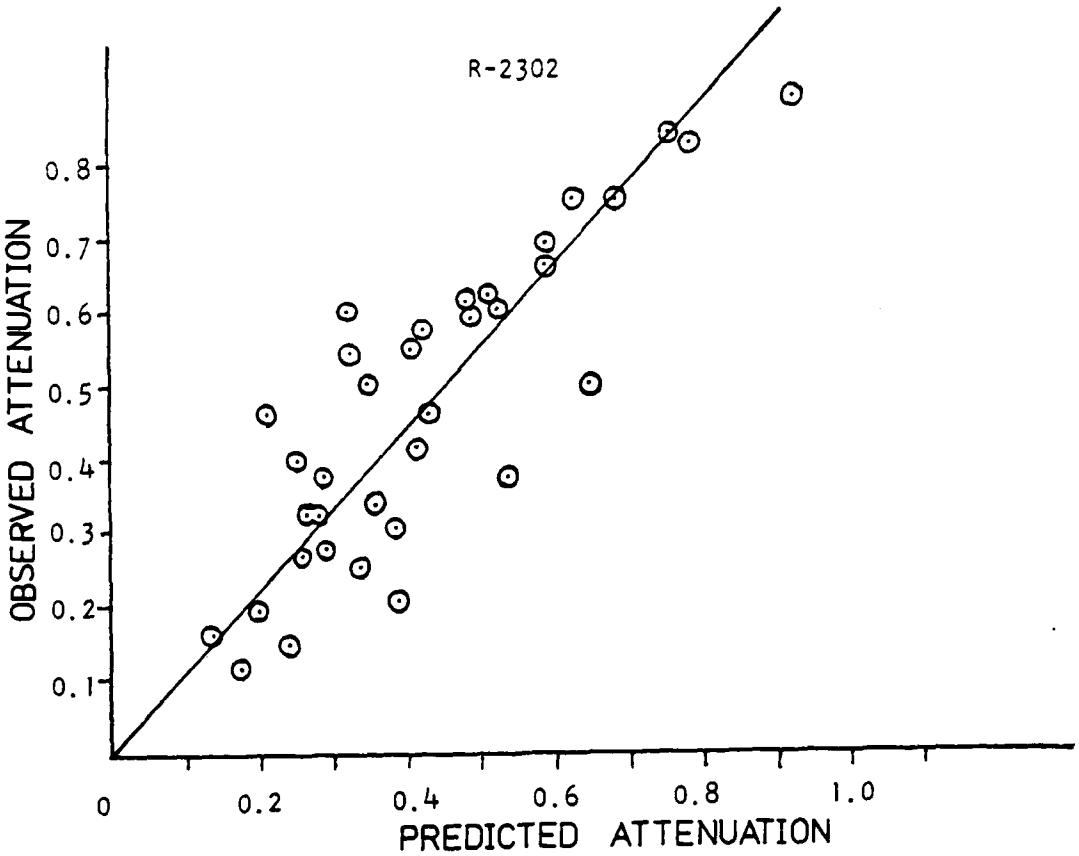

Figure 8A. Wave Wire No. 2

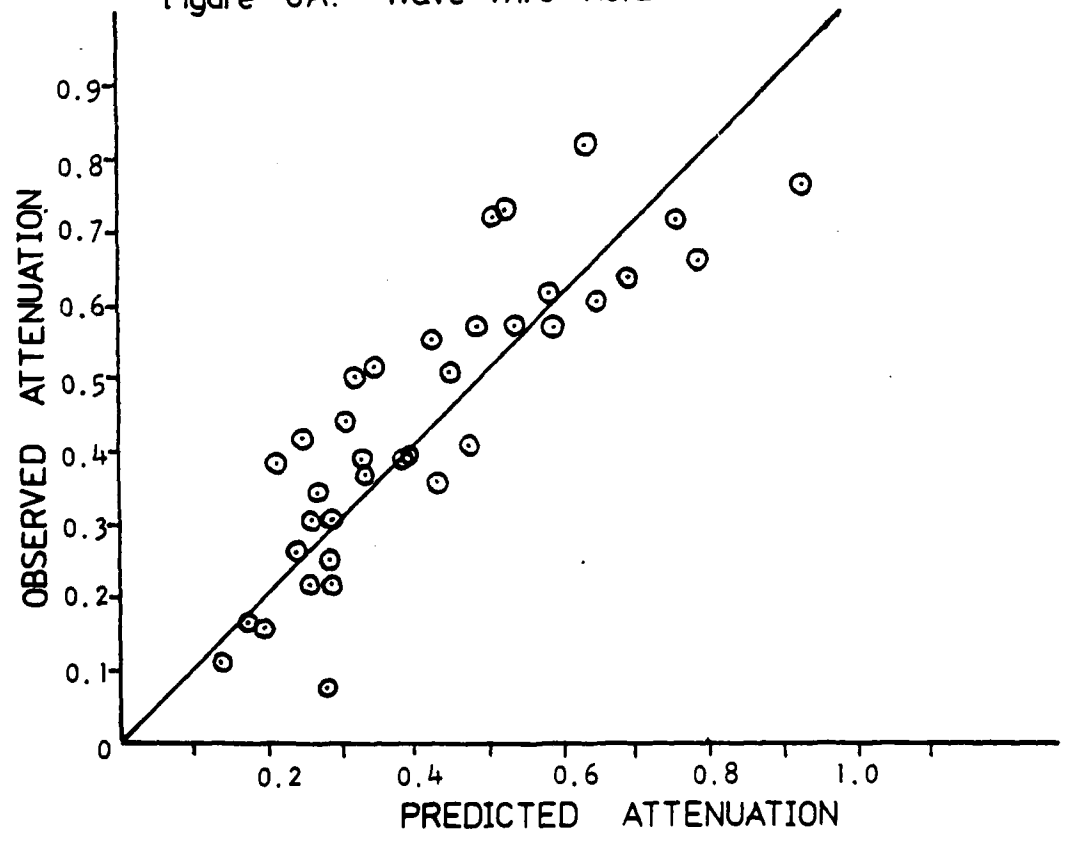

Figure 8B. Wave Wire No. 3

FIGURE 8. COMPARISON OF PREDICTED AND OBSERVED ATTENUATION RATIOS FOR SCENARIO I TEST RESULTS.

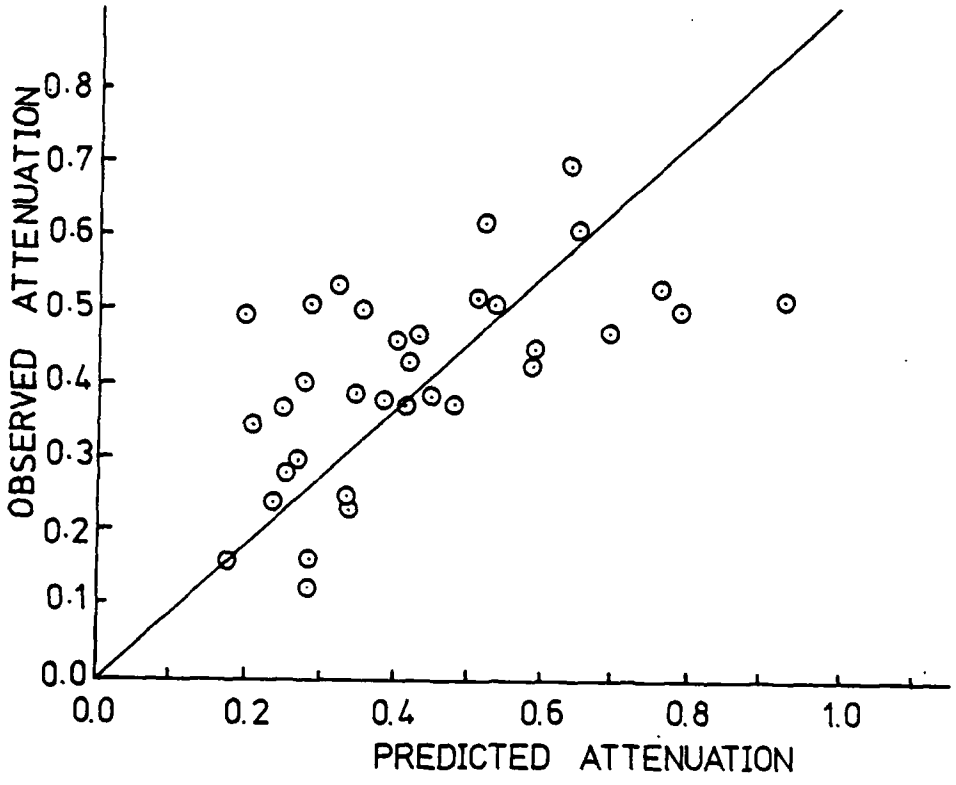

Figure 9 A. Wave Wire No. 4

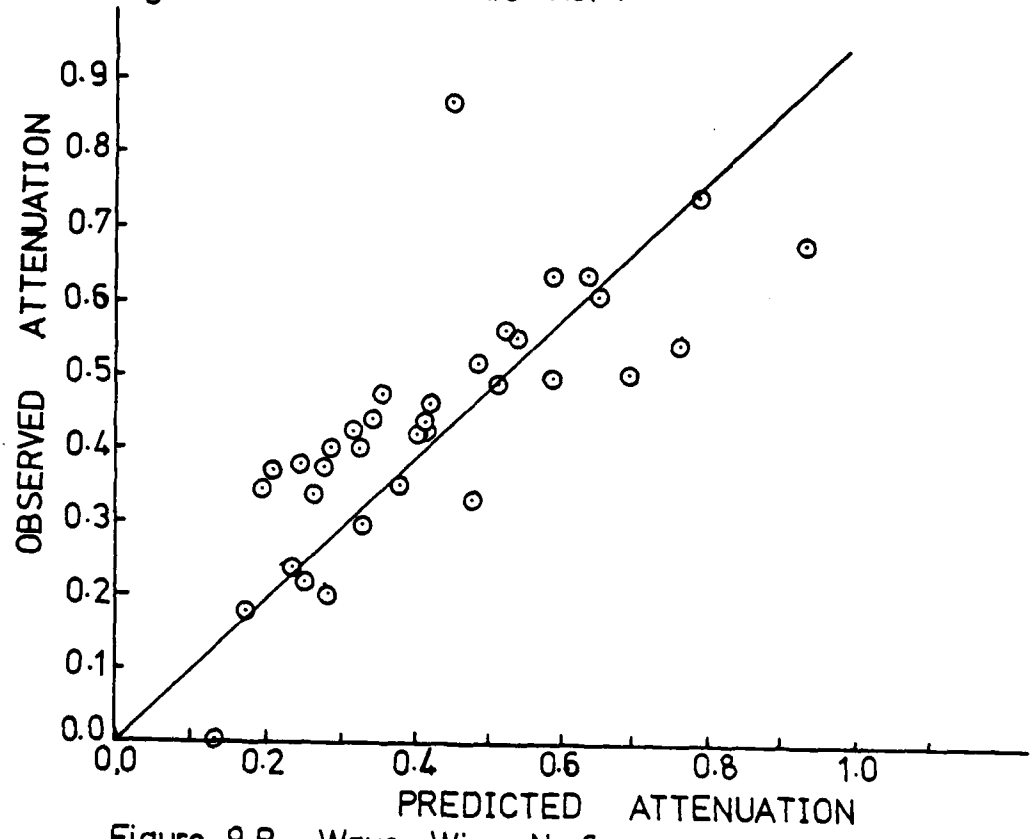

Figure 9 B Wave Wire No.6.

FIGURE 9. COMPARISION OF PREDICTED AND OBSERVED ATTENUATION RATIOS FOR SCENARIO I TEST RESULTS.

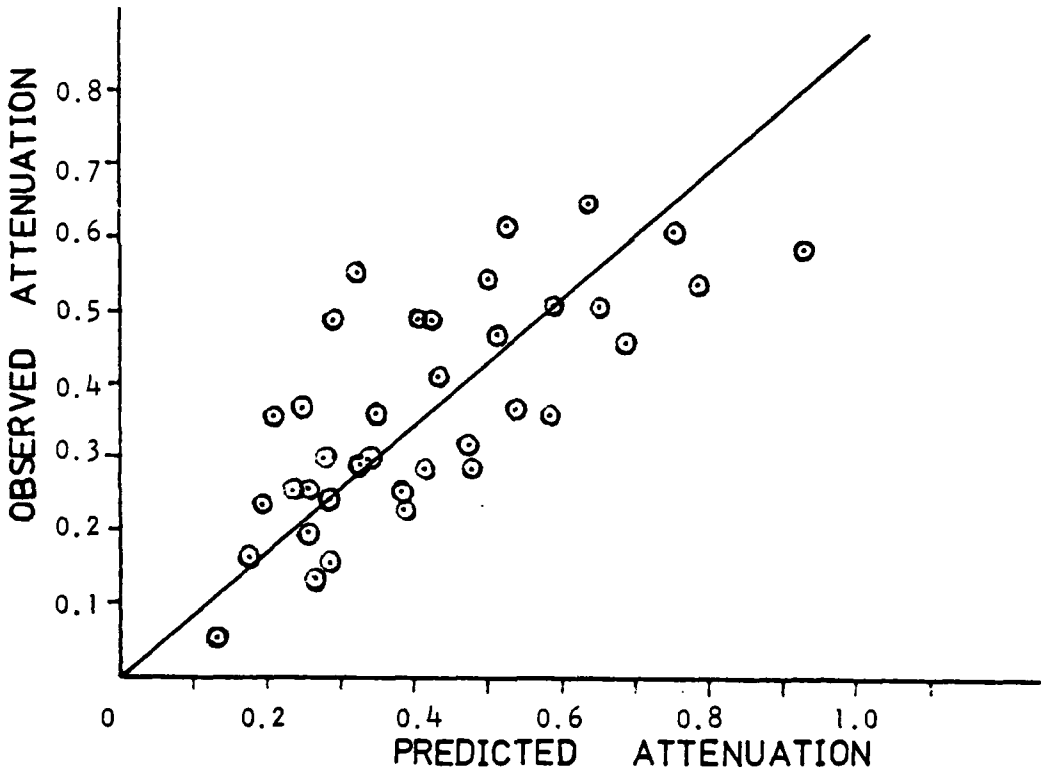

Figure 10A. Wave Wire NO.1

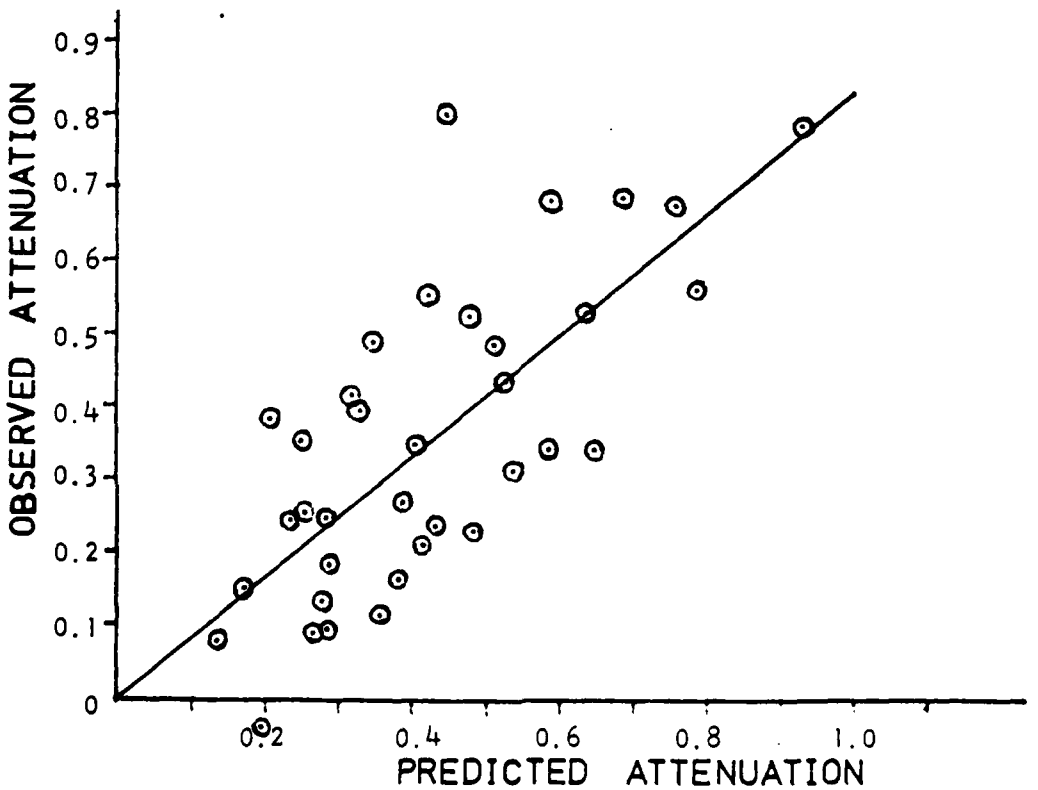

Figure 10B Wave Wire NO.5

FIGURE 10. COMPARISON OF PREDICTED AND OBSERVED ATTENUATION RATIOS FOR SCENARIOI TEST RESULTS

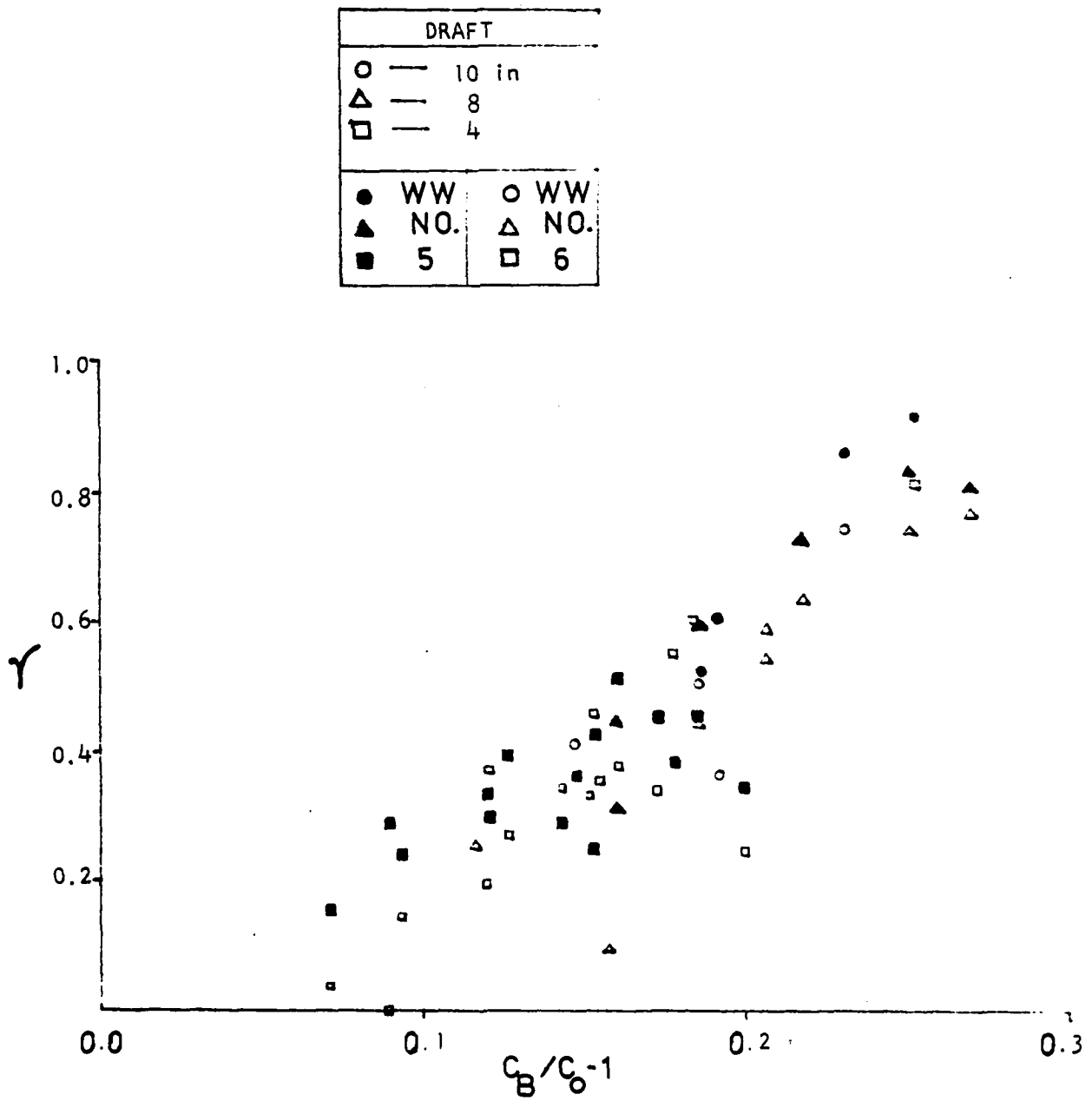

FIGURE 11. SCENARIO II TEST RESULTS FOR INCIDENT WAVELENGTHS OF 4 FEET.

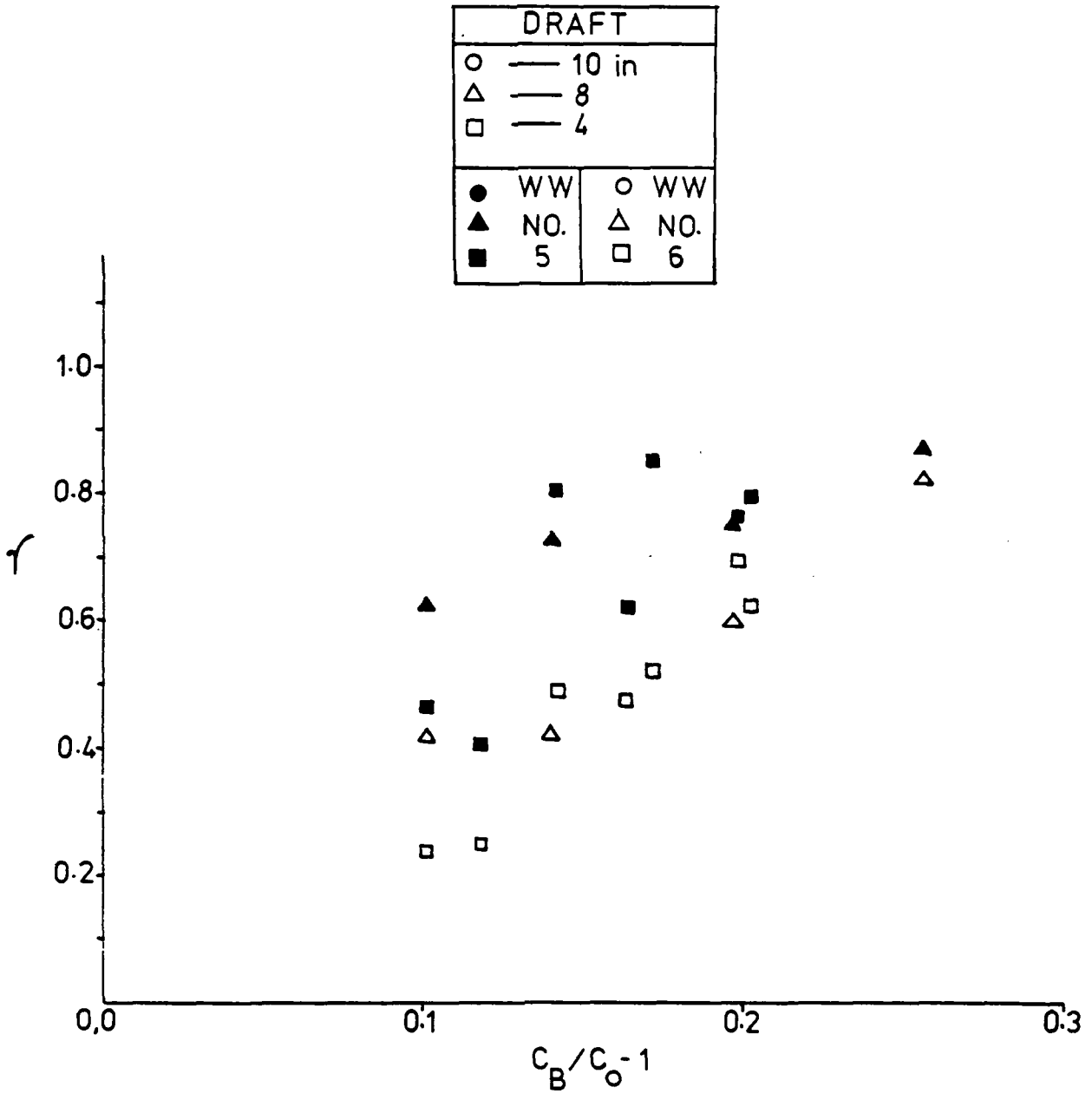

FIGURE 12. SCENARIO II TEST RESULTS FOR INCIDENT WAVELENGTHS OF 3 FEET.

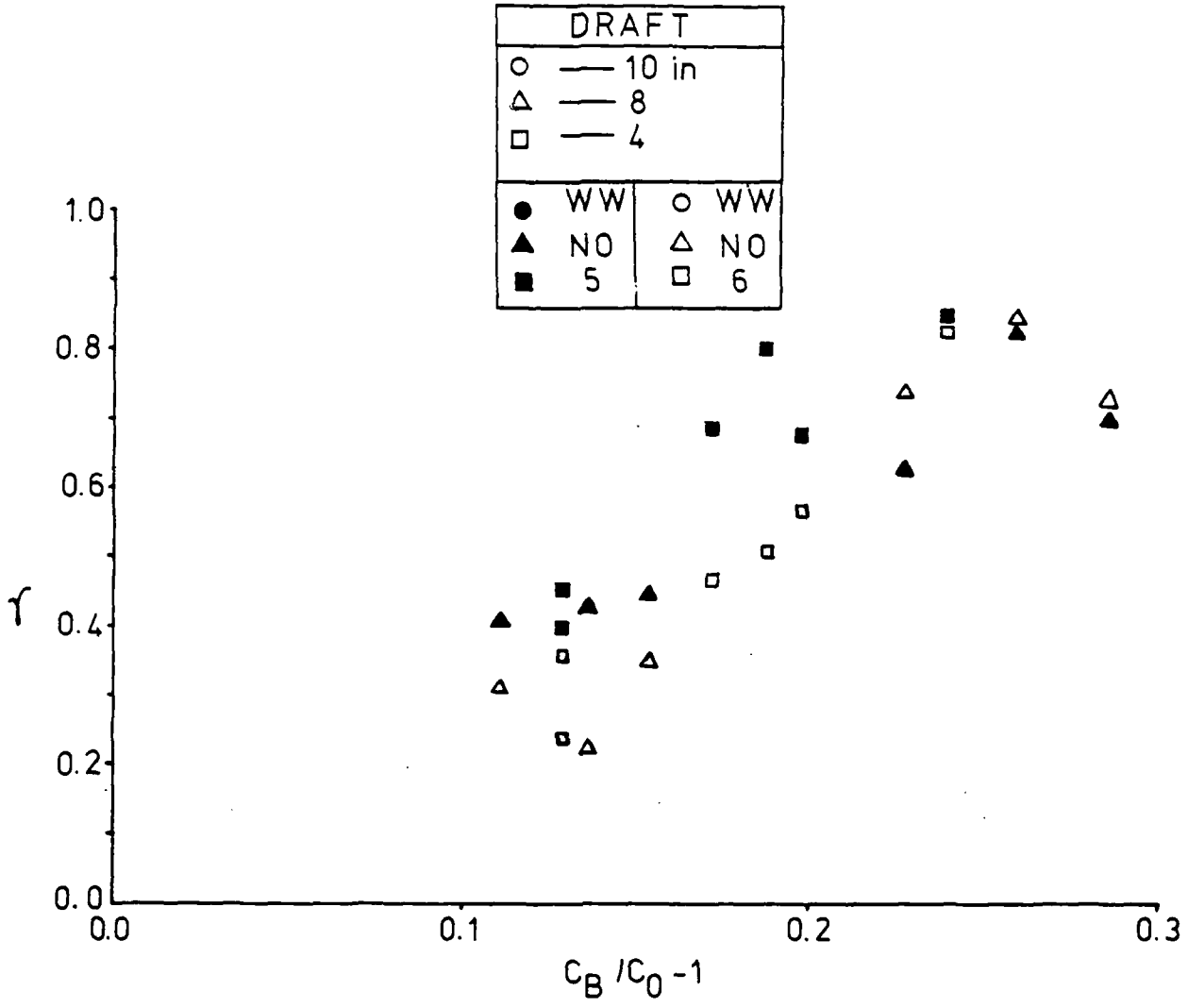

FIGURE 13. SCENARIO II TEST RESULTS FOR INCIDENT WAVELENGTHS OF 2.5 FEET.

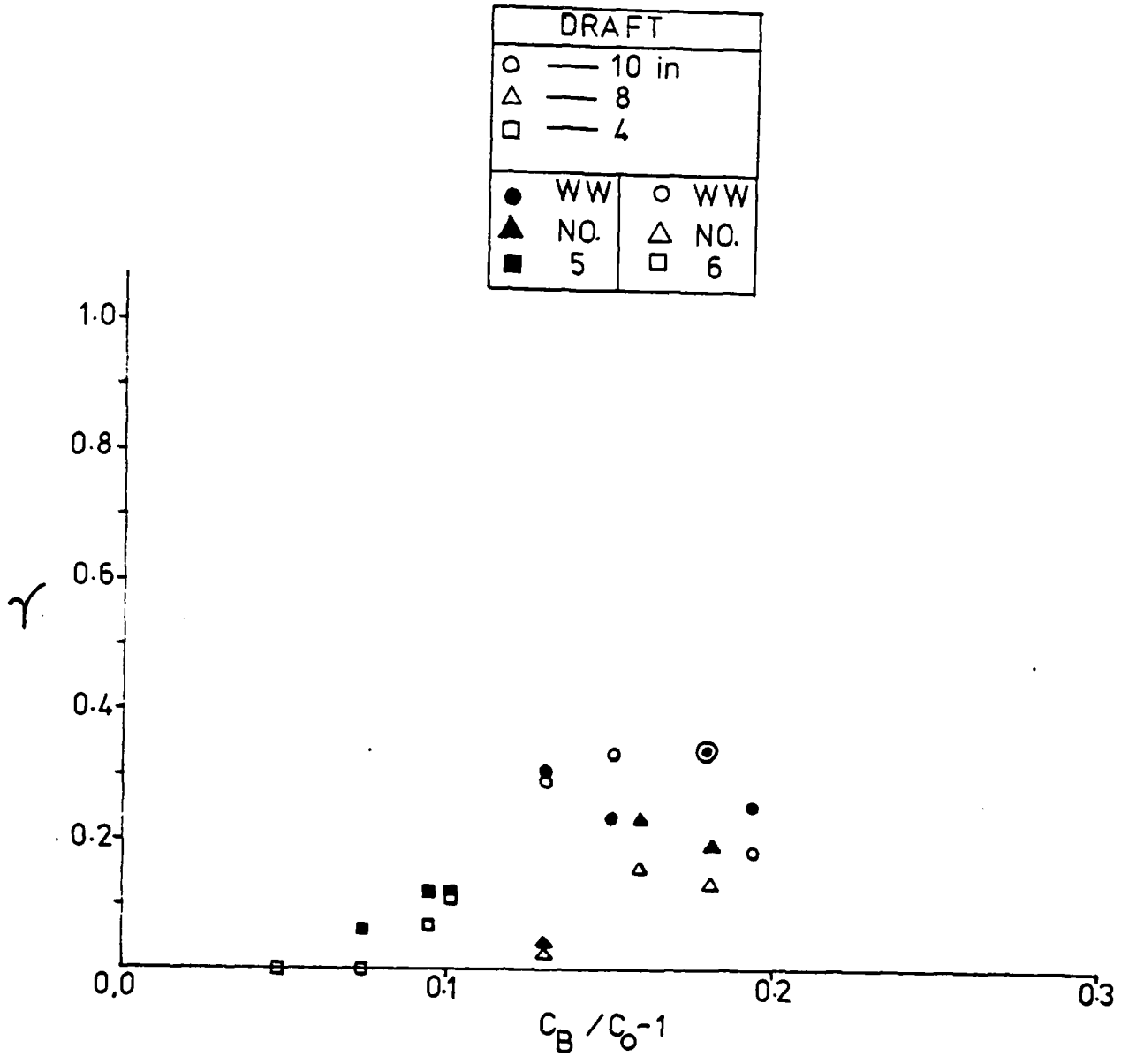

FIGURE 14A. SCENARIO II TEST RESULTS FOR INCIDENT WAVELENGTHS OF 6 FEET.

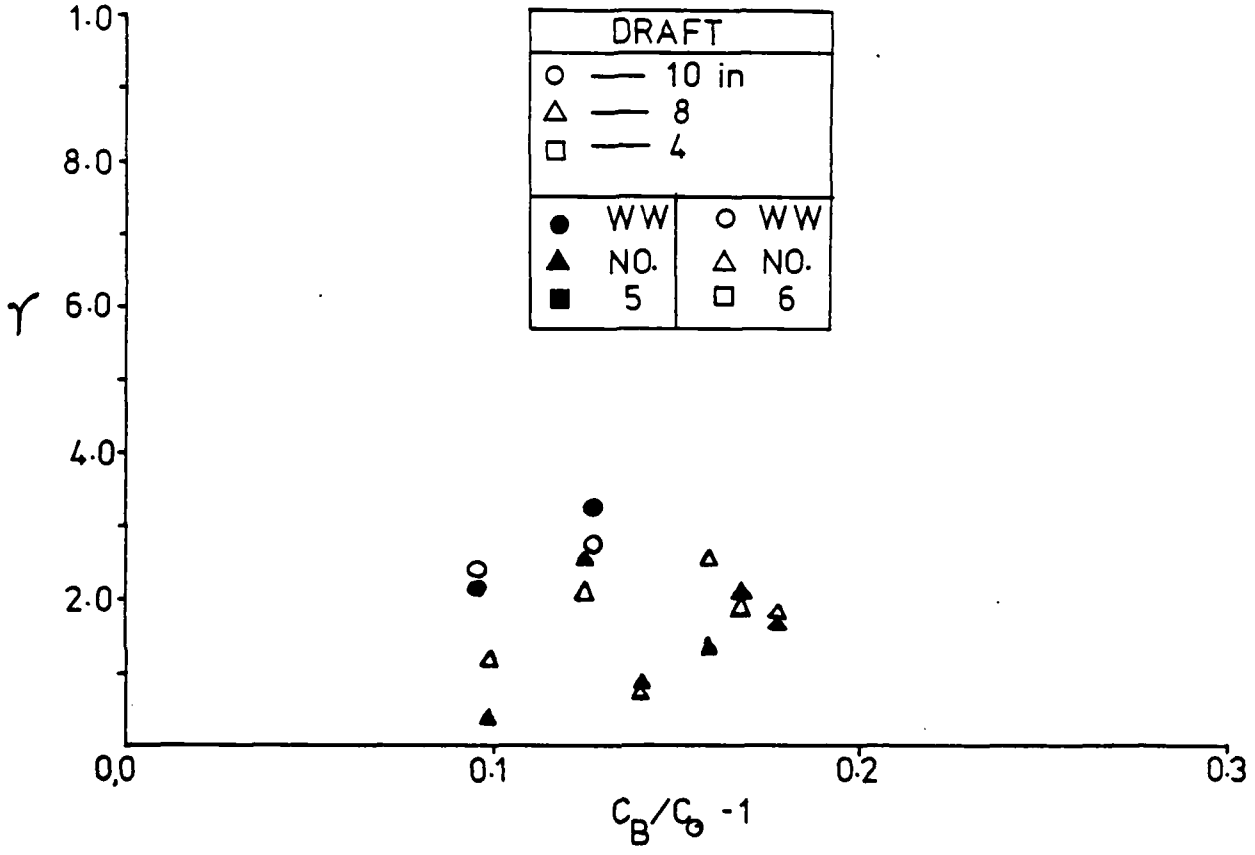

FIGURE 14 B SCENARIO II TEST RESULTS FOR INCIDENT WAVELENGTHS OF 8 FEET.

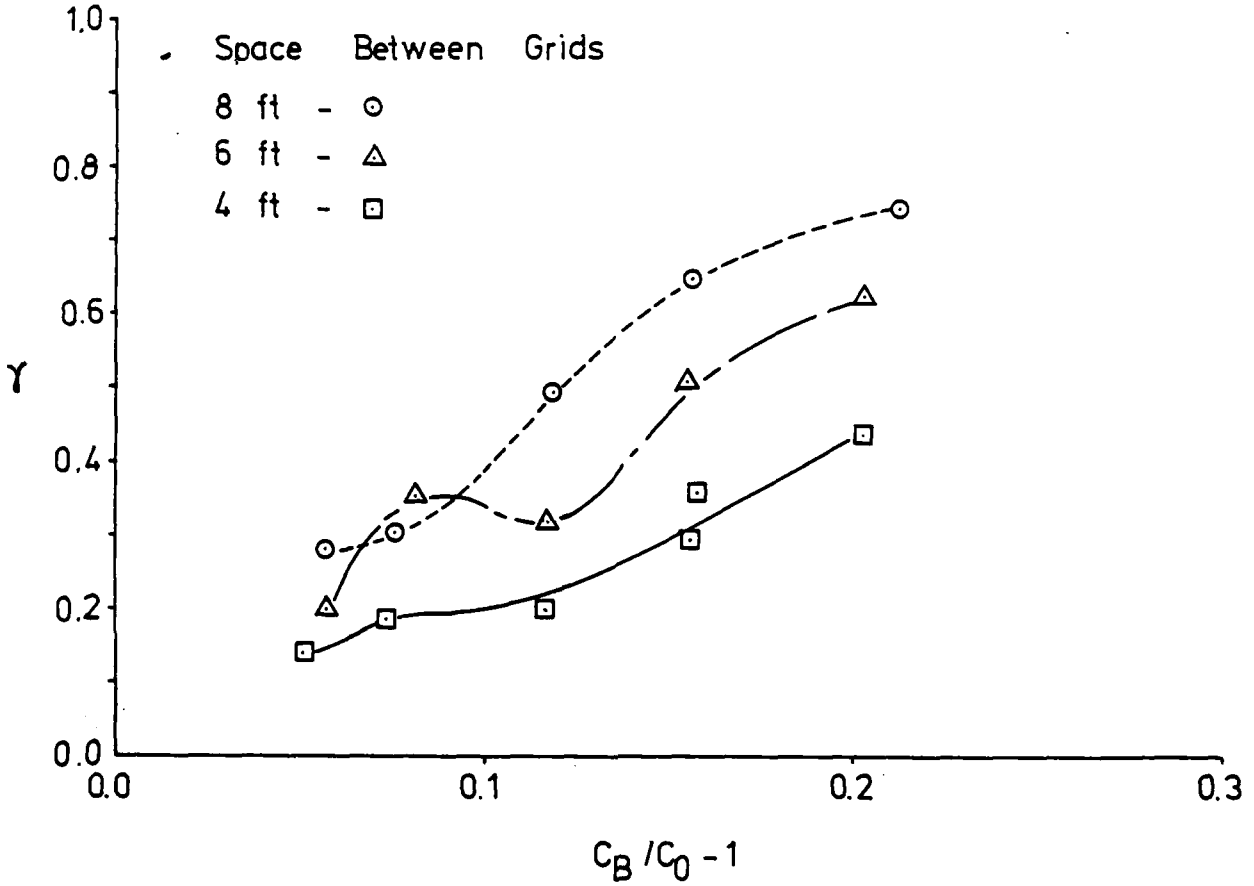

FIGURE 15. TEST RESULTS FOR SCENARIO II WITH TWO 4-FOOT GRIDS SEPARATED BY 4, 6 AND 8-FOOT SPACE. THE INCIDENT WAVELENGTH WAS 8 FEET.

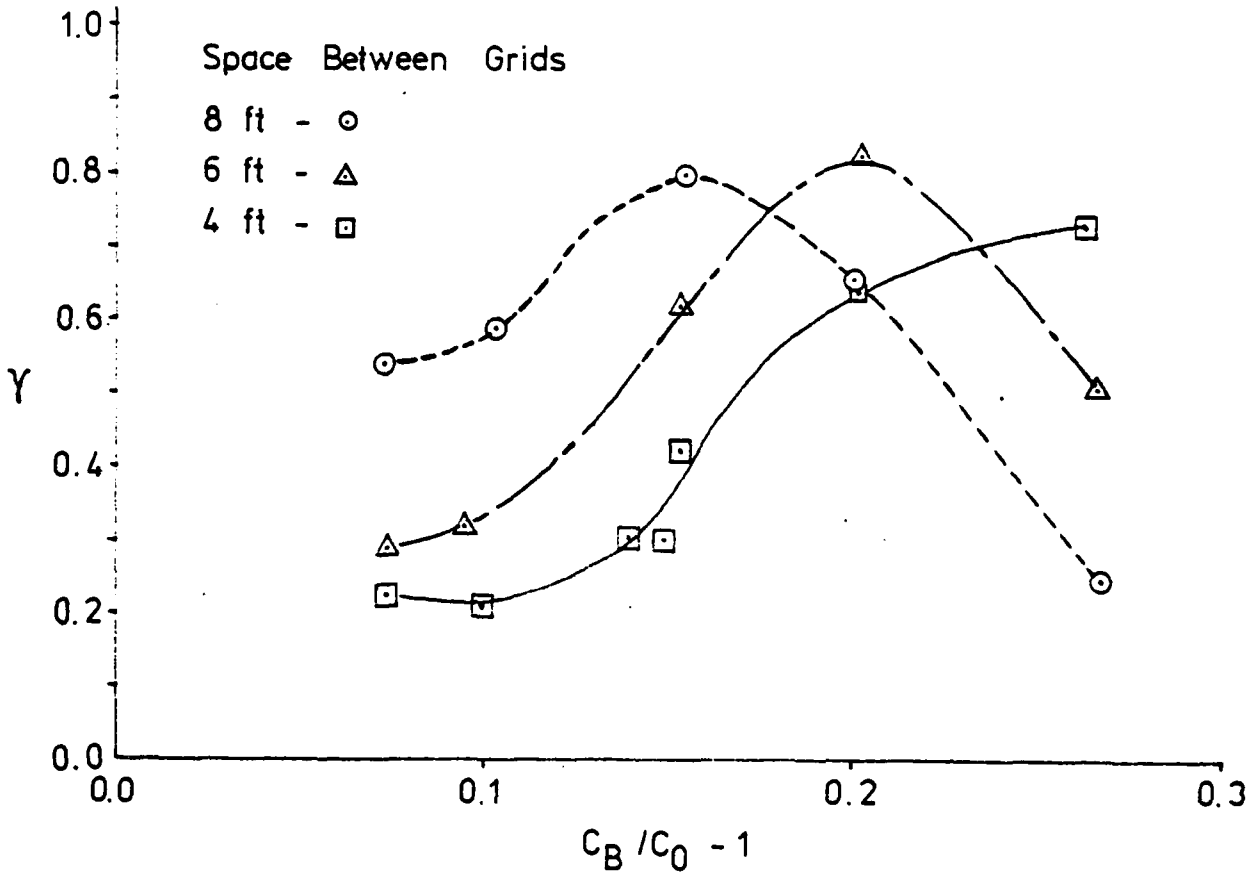

FIGURE 16. TEST RESULTS FOR SCENARIO II WITH TWO 4-FOOT GRIDS SEPARATED BY 4, 6 AND 8-FOOT SPACE. THE INCIDENT WAVELENGTH WAS 6 FEET.

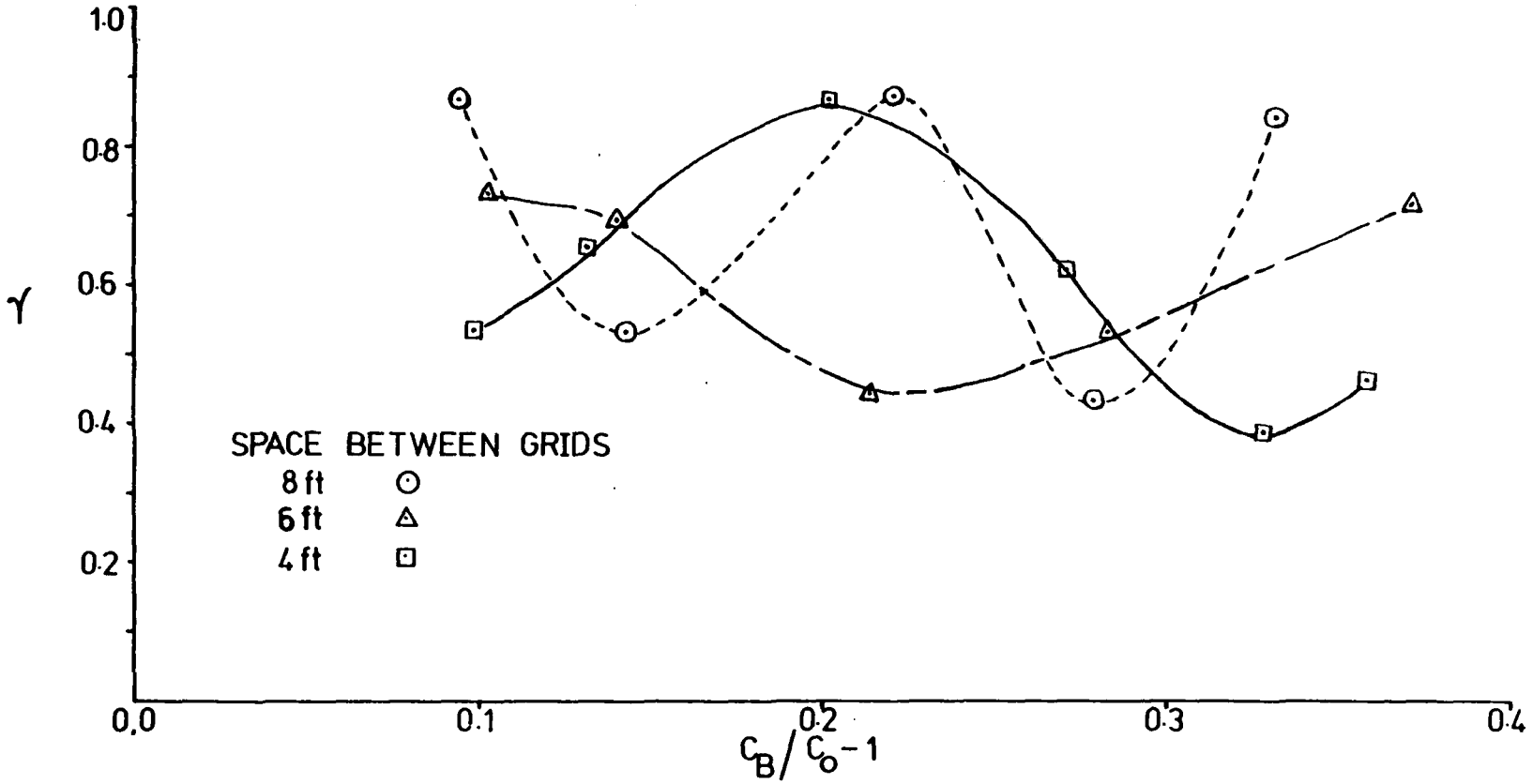

FIGURE 17: TEST RESULTS FOR SCENARIO II WITH TWO 4-FOOT GRIDS SEPARATED BY 4, 6 & 8-FOOT SPACE. THE INCIDENT WAVELENGTH WAS 4 FEET.

R-2302

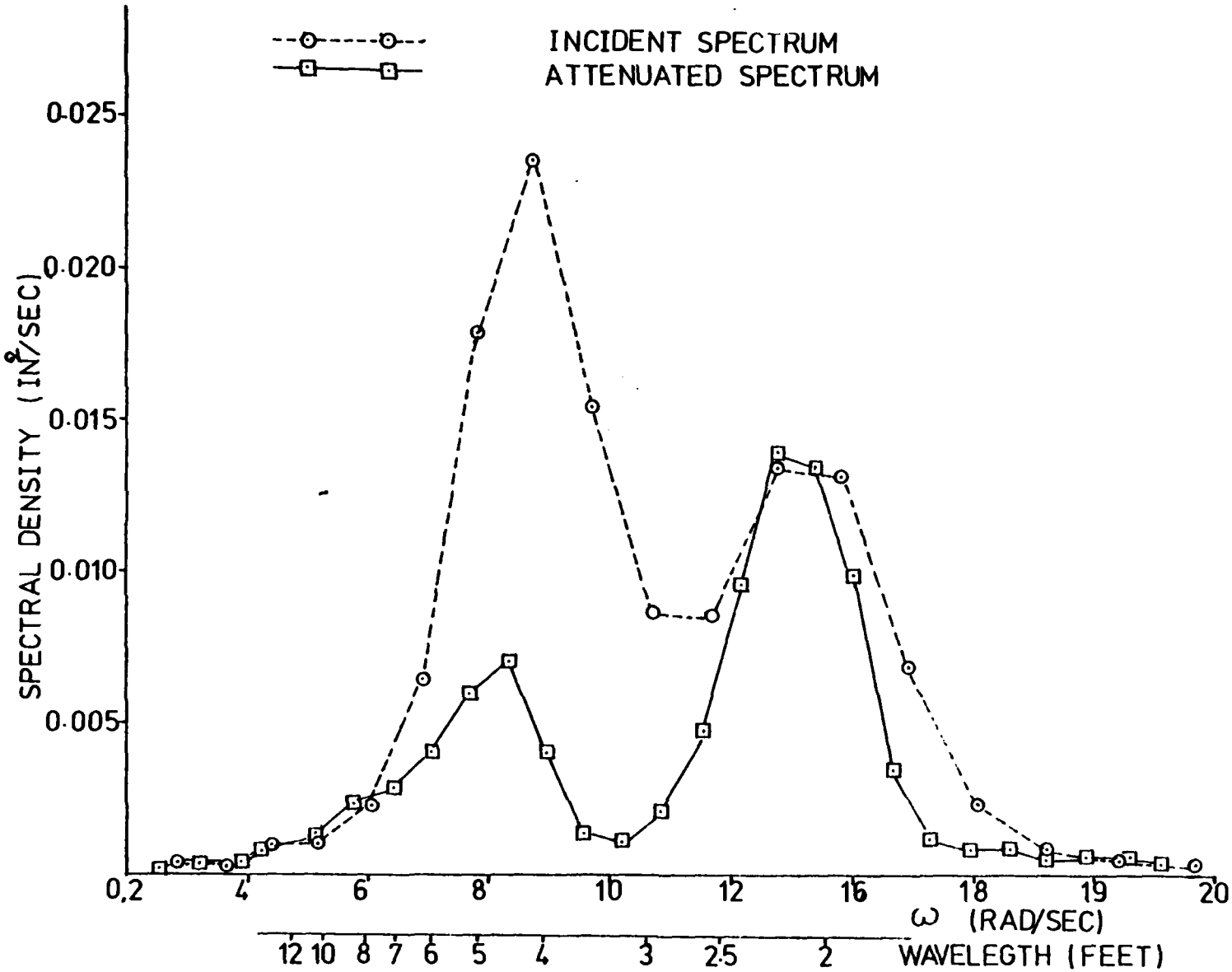

FIGURE 18. TEST RESULTS IN RANDOM WAVES FOR SCENARIO II WITH TWO 2-FOOT GRIDS SEPARATED BY A 4-FOOT SPACE.

R-2302

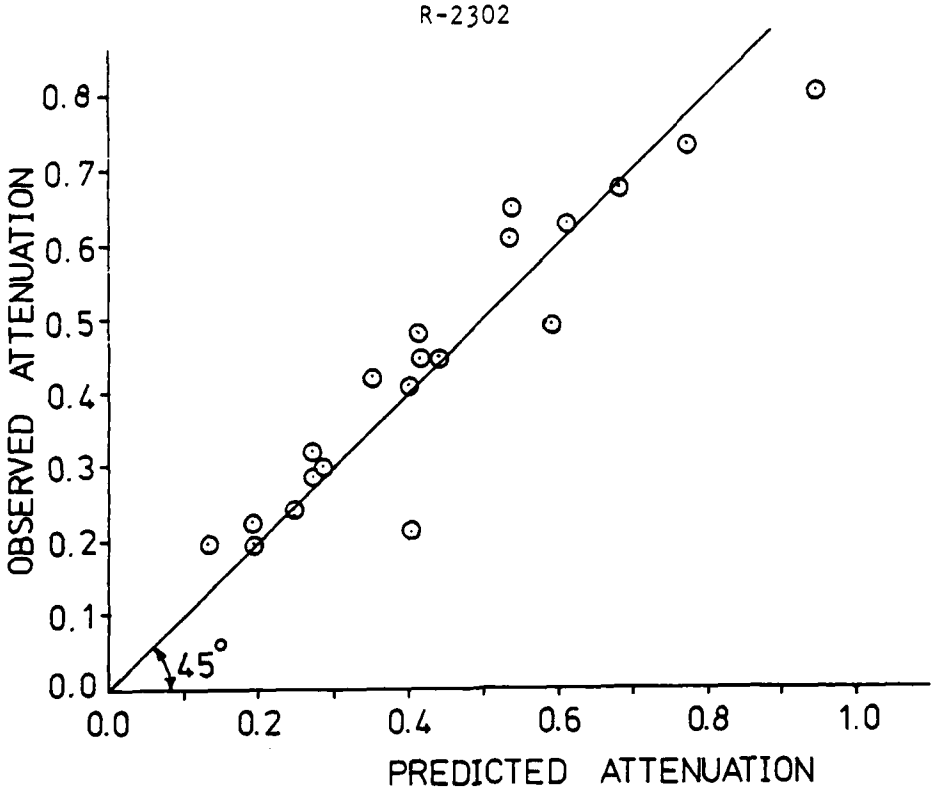

Figure 19 A. Wave Wire No. 1.

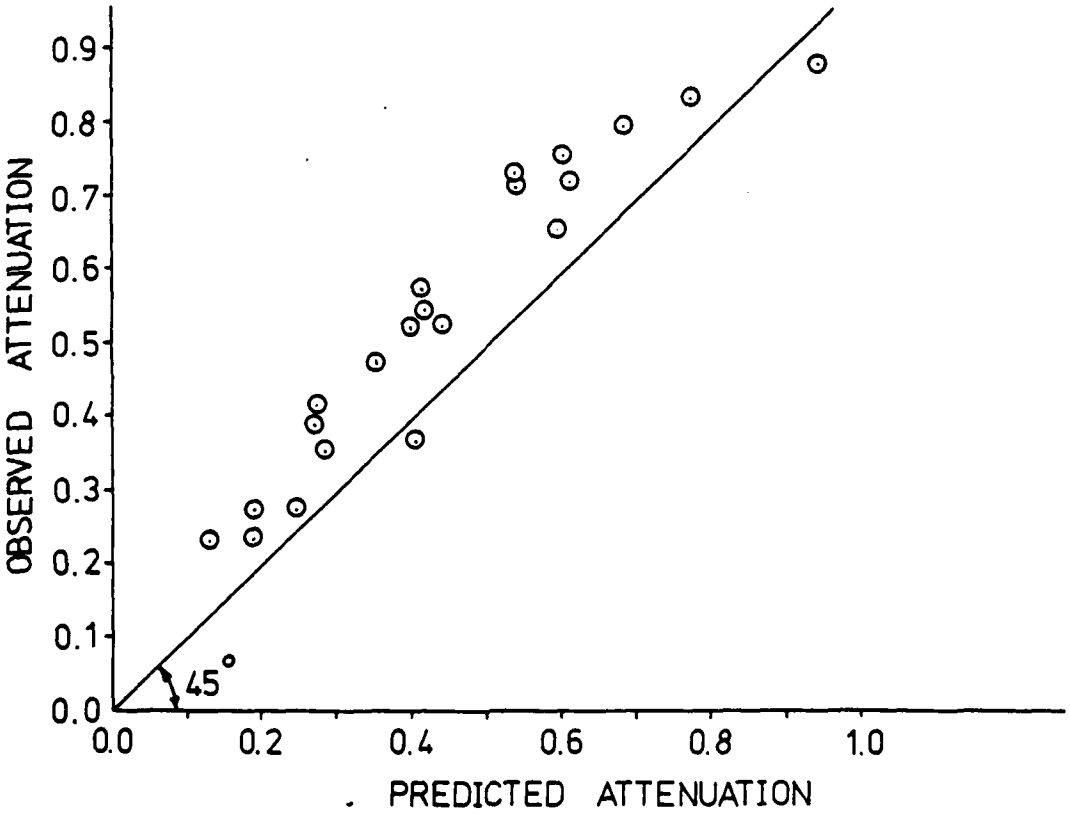

Figure 19 B. Wave Wire No. 2

FIGURE 19. OBSERVED ATTENUATION FOR GRID SOLIDITY OF 0.53 PLOTTED AGAINST PREDICTED ATTENUATION FOR GRID SOLIDITY OF 0.34

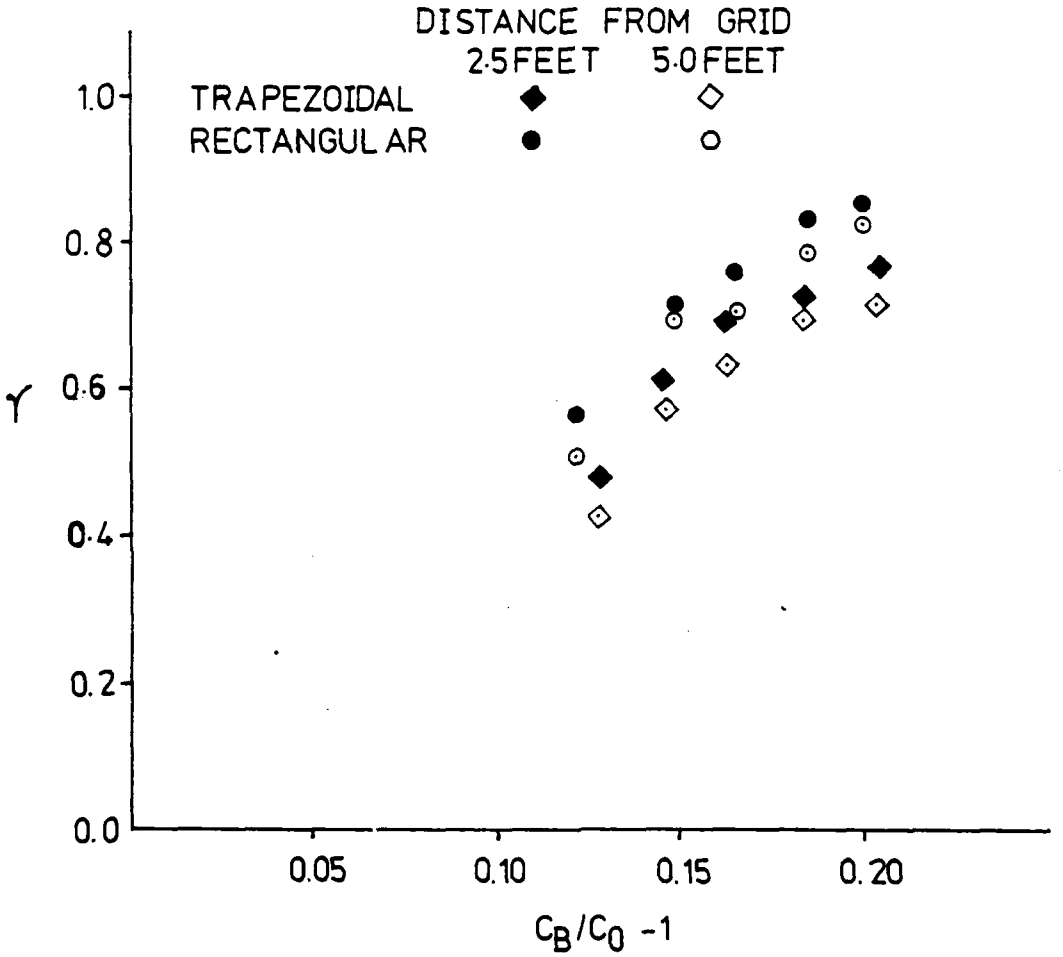

FIGURE 20. COMPARISON OF WAVE ATTENUATION FOR RECTANGULAR AND TRAPEZOIDAL GRIDS.

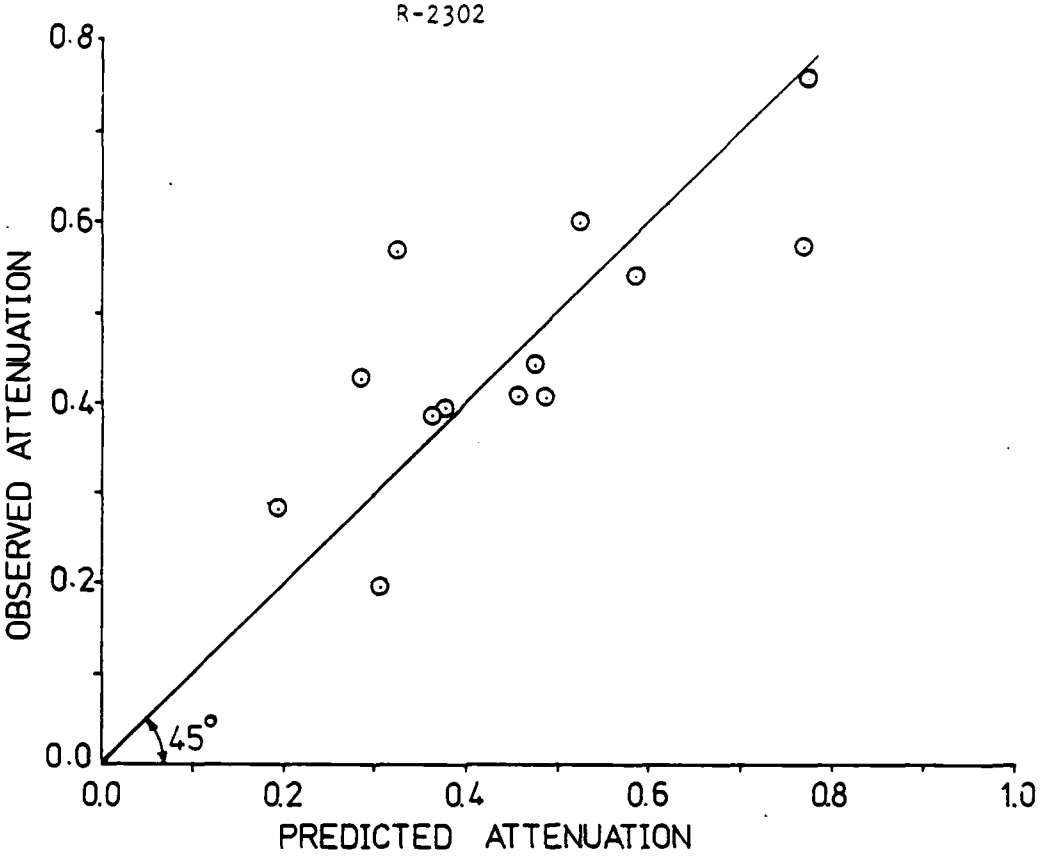

Figure 21A. Wave Wire No. 1

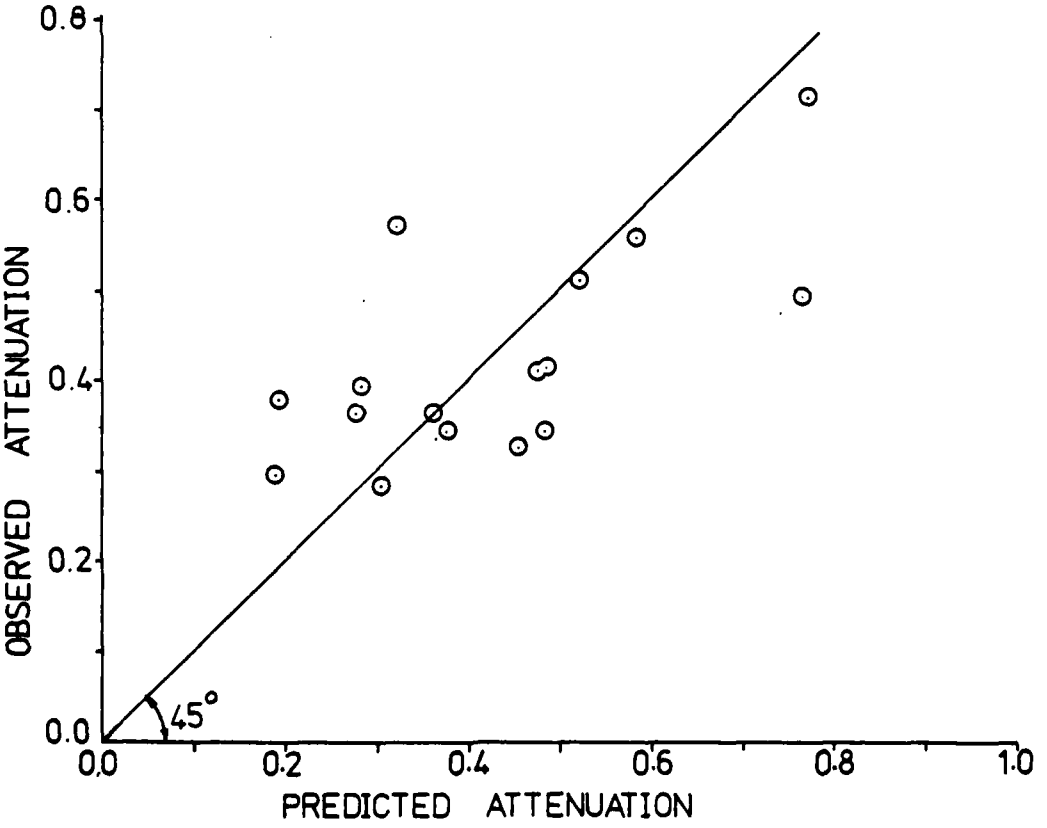

Figure 21B. Wave Wire No. 2

FIGURE 21. COMPARISON OF OBSERVED AND PREDICTED ATTENUATION FOR THE RIBBON GRID IN A RIGID FRAME.

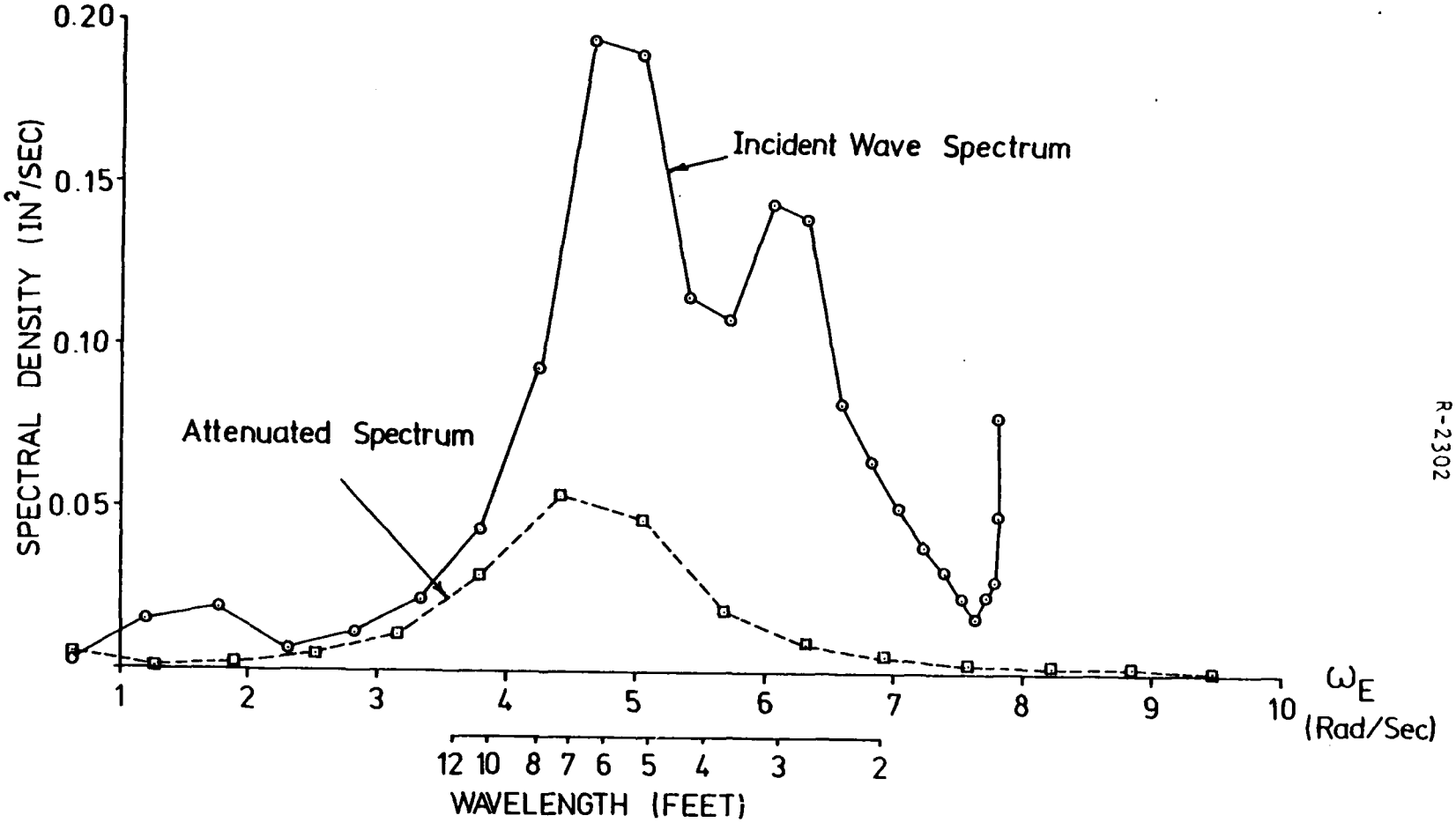

FIGURE 22. RESULTS OF RANDOM WAVE TESTS WITH THE RIBBON GRID IN A RIGID FRAME.

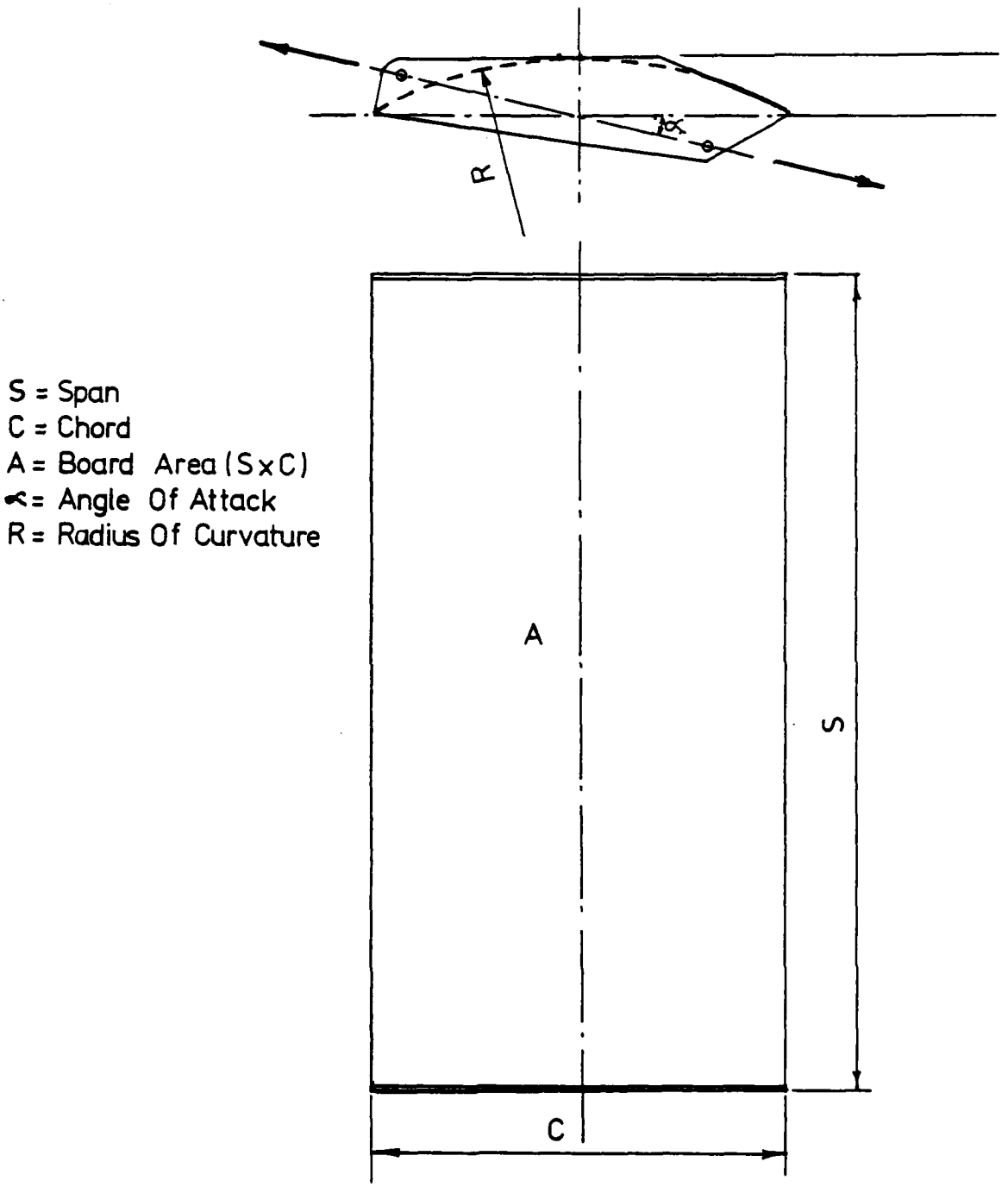

S = Span
C = Chord
A = Board Area (S x C)
α = Angle Of Attack
R = Radius Of Curvature

FIGURE 23. SUBERKRUB BOARD CONFIGURATION.

Tow Warp Total Length

Model Scale	96	Inches
Meso Scale	94	Feet
Full Scale	161	Feet

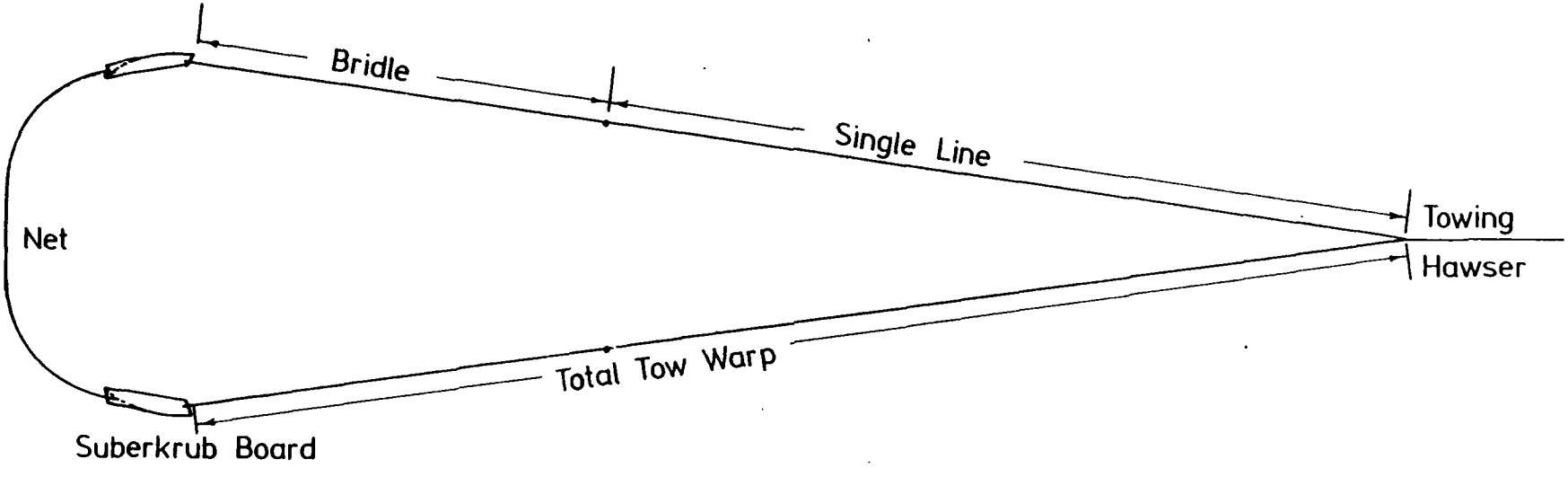

R-2302

FIGURE 24 PLAN VIEW OF TOWING CONFIGURATION OF SUBERKRUB BOARDS AND NET.

Length Of Bridle (B)

Model	Scale	20 Inches
Meso	Scale	24 Feet
Full	Scale	42 Feet

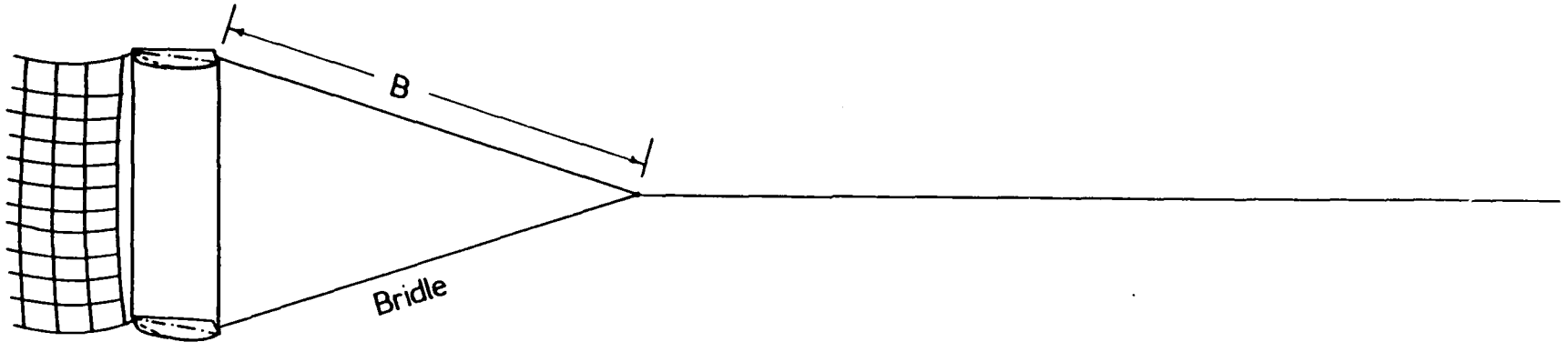

R-2302

FIGURE 25. PROFILE VIEW OF TOWING CONFIGURATION OF SUBERKRUB BOARDS AND NET.

AD-A132 470 AN EXPERIMENTAL STUDY OF A METHOD TO ATTENUATE SURFACE WAVES USING ARTIFI.. (U) STEVENS INST OF TECH HOBOKEN NJ DAVIDSON LAB R I HIRES APR 83 SIT-DL-82-2302 2/2

UNCLASSIFIED N00014-78-C-0740 F/G 8/3 NL

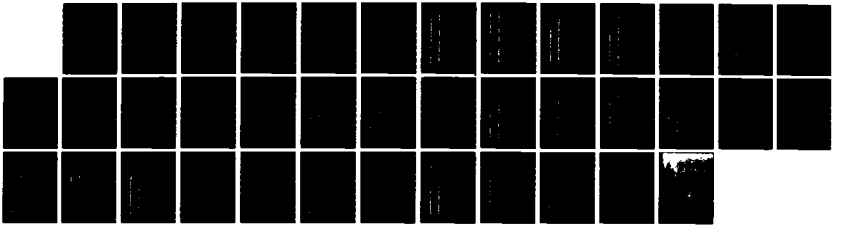

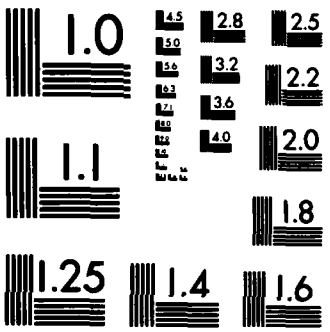

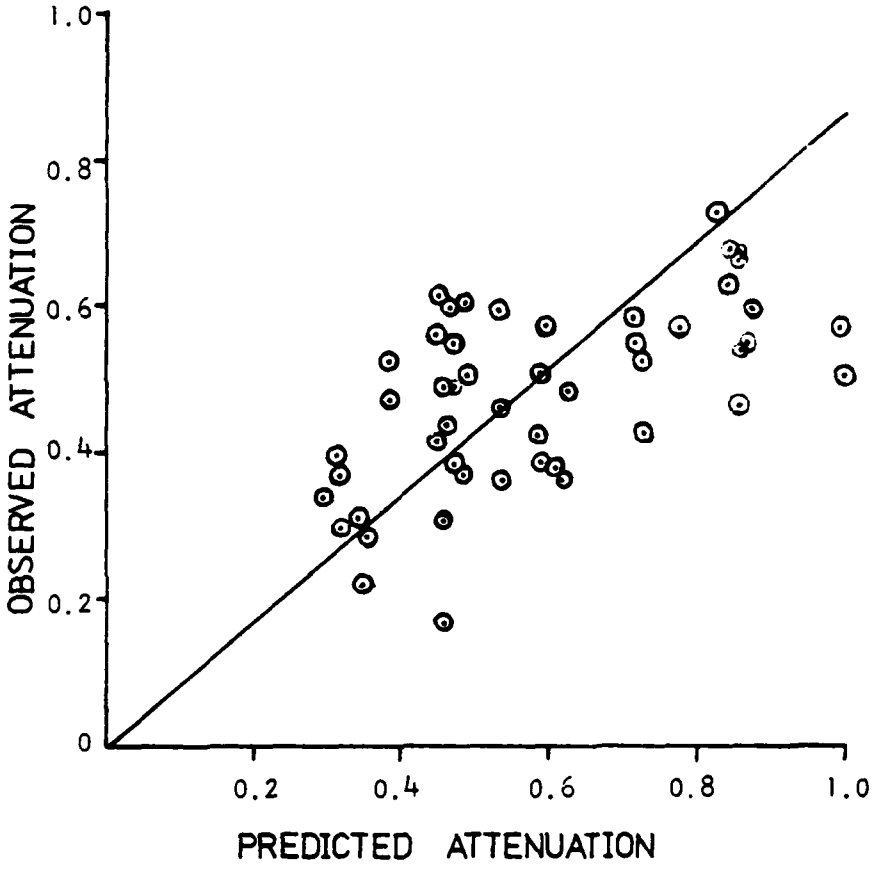

FIGURE 26 . SUMMARY OF TEST RESULTS FOR THE RIBBON GRID WITH BOARDS. THE PREDICTED ATTEN--UATION WAS OBTAINED UNDER THE ASSUMT--ION THAT THE EFFECTIVE WIDTH AND DRAFT OF THE GRID WERE 80 % OF THE ACTUAL GRID DIMENSIONS

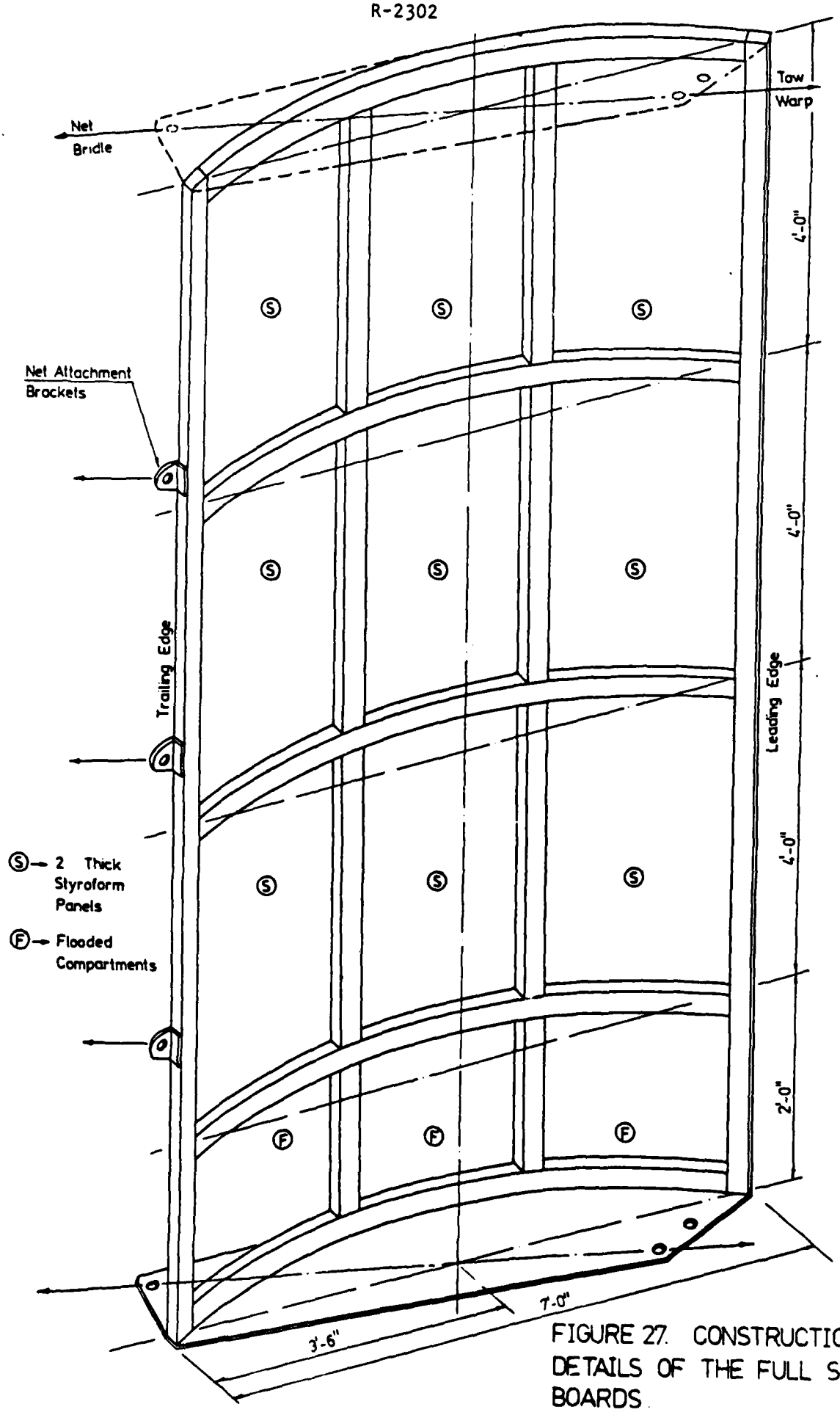

FIGURE 27. CONSTRUCTION DETAILS OF THE FULL SCALE BOARDS

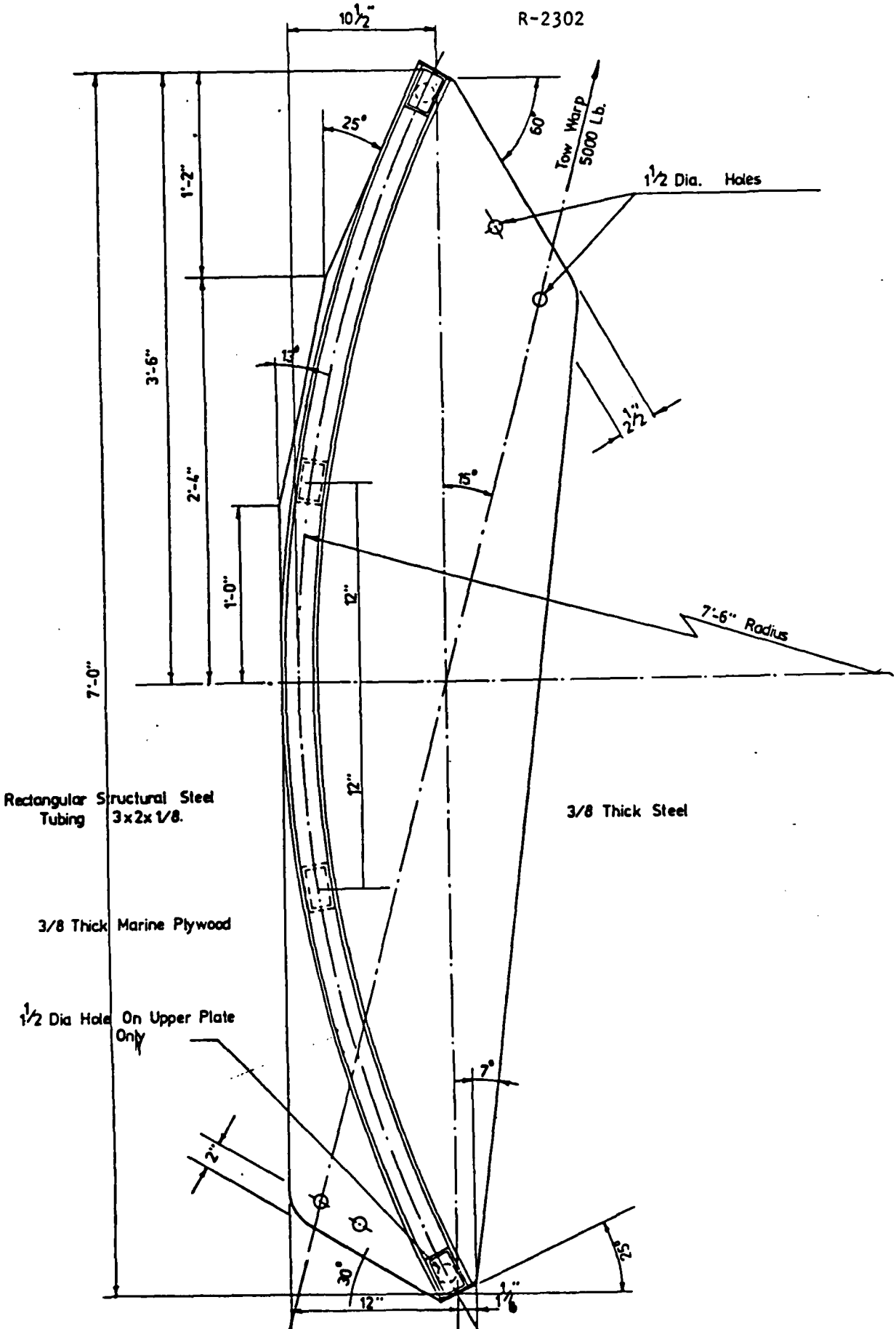

FIGURE 28. CONSTRUCTION DETAILS FOR TOP AND BOTTOM PLATES OF THE FULL SCALE BOARDS.

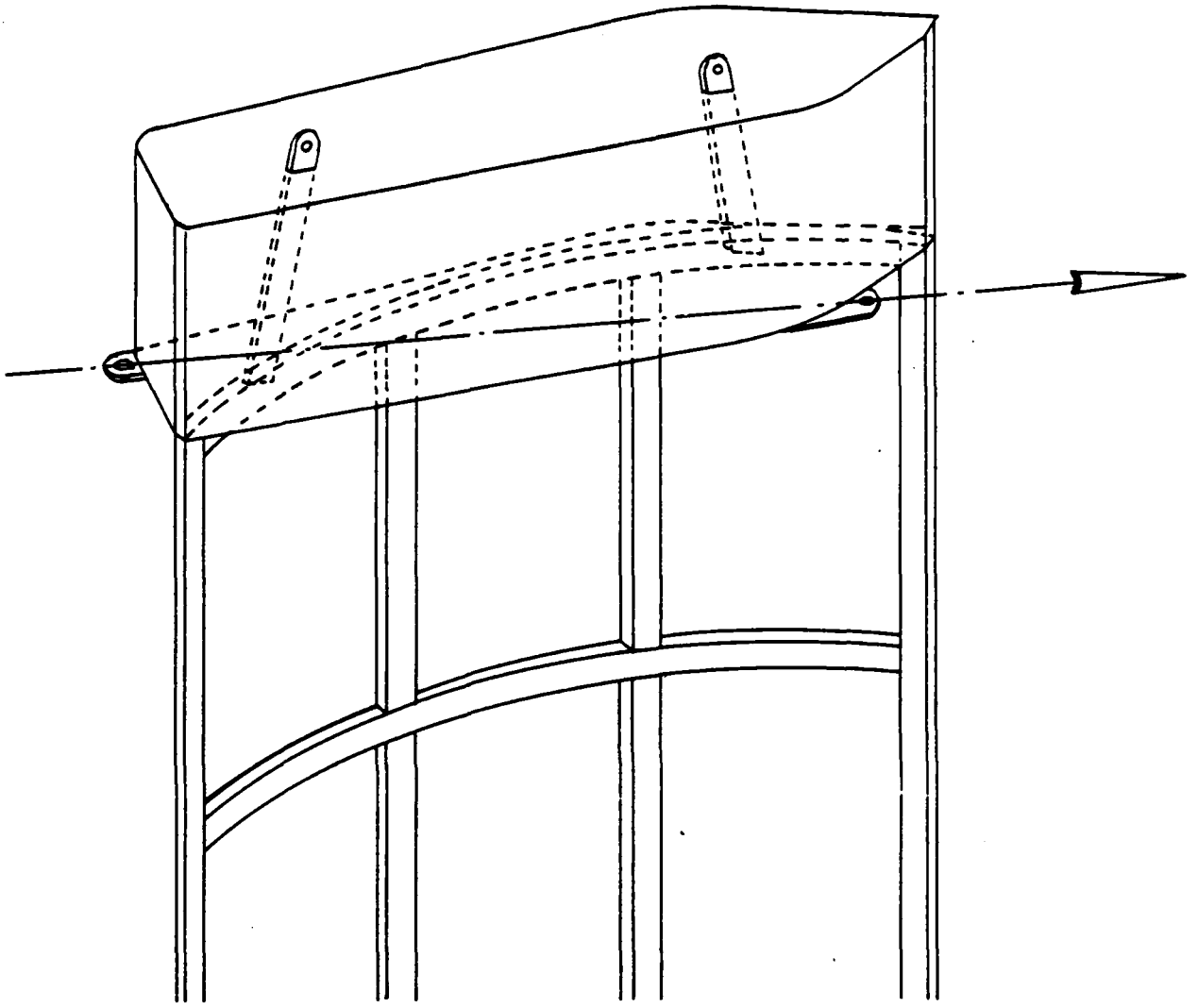

Tank made from 0.125" mild steel 24" high.

Displacement : 17 cu.ft. x 62 lbs./cu.ft. = 1052 lbs.
Weight of Tank : = 194 lbs.
Total Additional Buoyancy = 860 lbs.

FIGURE 29. MODIFICATION OF FULL SCALE SUBERKRUB BOARD TO ADD BUOYANCY TANKS ON TOP OF EACH BOARD.

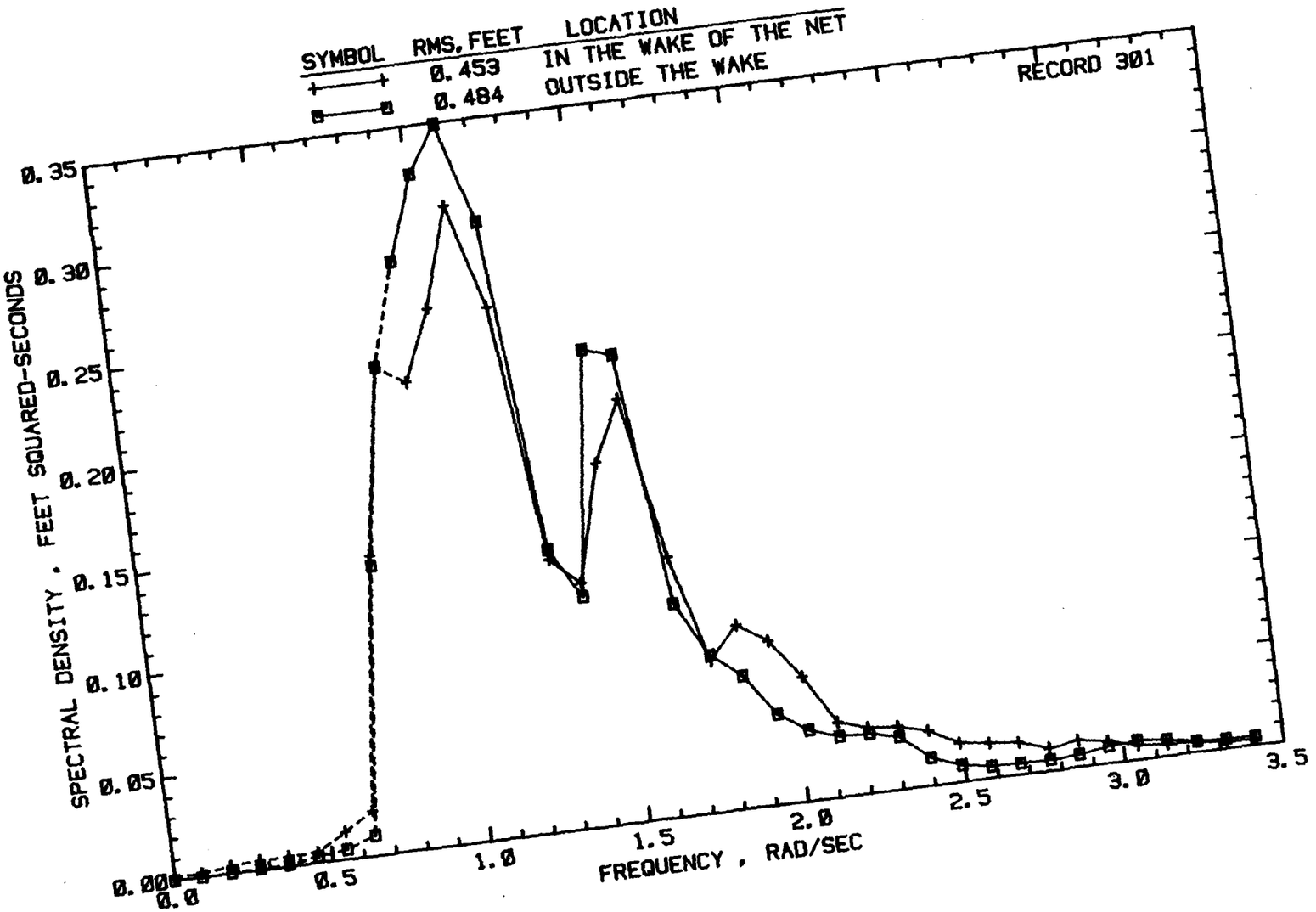
SYMBOL RMS, FEET LOCATION
0.453 IN THE WAKE OF THE NET
0.484 OUTSIDE THE WAKE
RECORD 301
SPECTRAL DENSITY , FEET SQUARED-SECONDS
0.35
0.30
0.25
0.20
0.15
0.10
0.05
0.00
0.0
0.5
1.0
1.5
2.0
2.5
3.0
3.5
FREQUENCY , RAD/SEC

FIGURE 30.

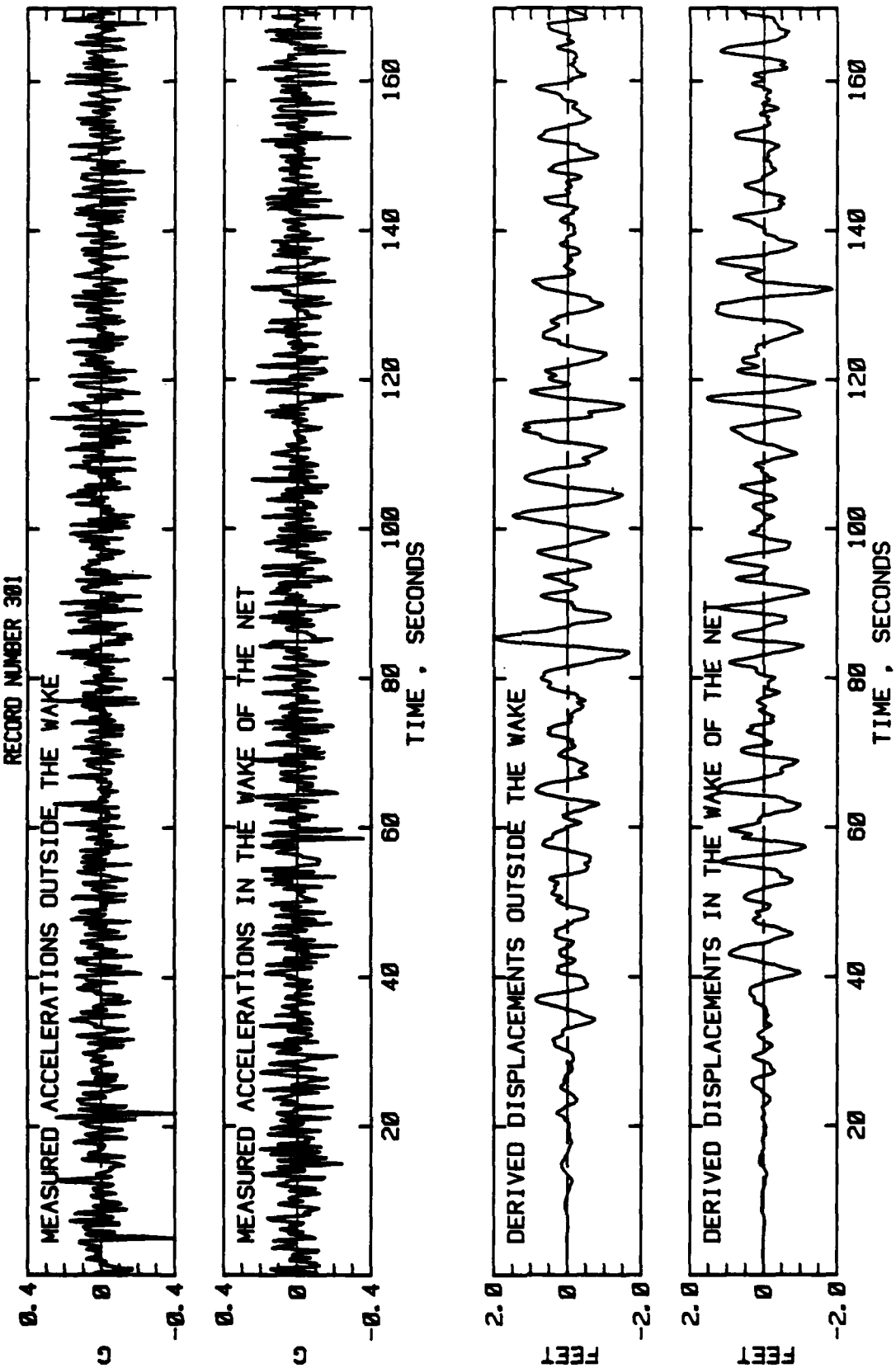
RECORD NUMBER 301
MEASURED ACCELERATIONS OUTSIDE THE WAKE
MEASURED ACCELERATIONS IN THE WAKE OF THE NET
DERIVED DISPLACEMENTS OUTSIDE THE WAKE
DERIVED DISPLACEMENTS IN THE WAKE OF THE NET
G
FEET
TIME, SECONDS
0.4
0
-0.4
2.0
-2.0
20
40
60
80
100
120
140
160

FIGURE 31A.

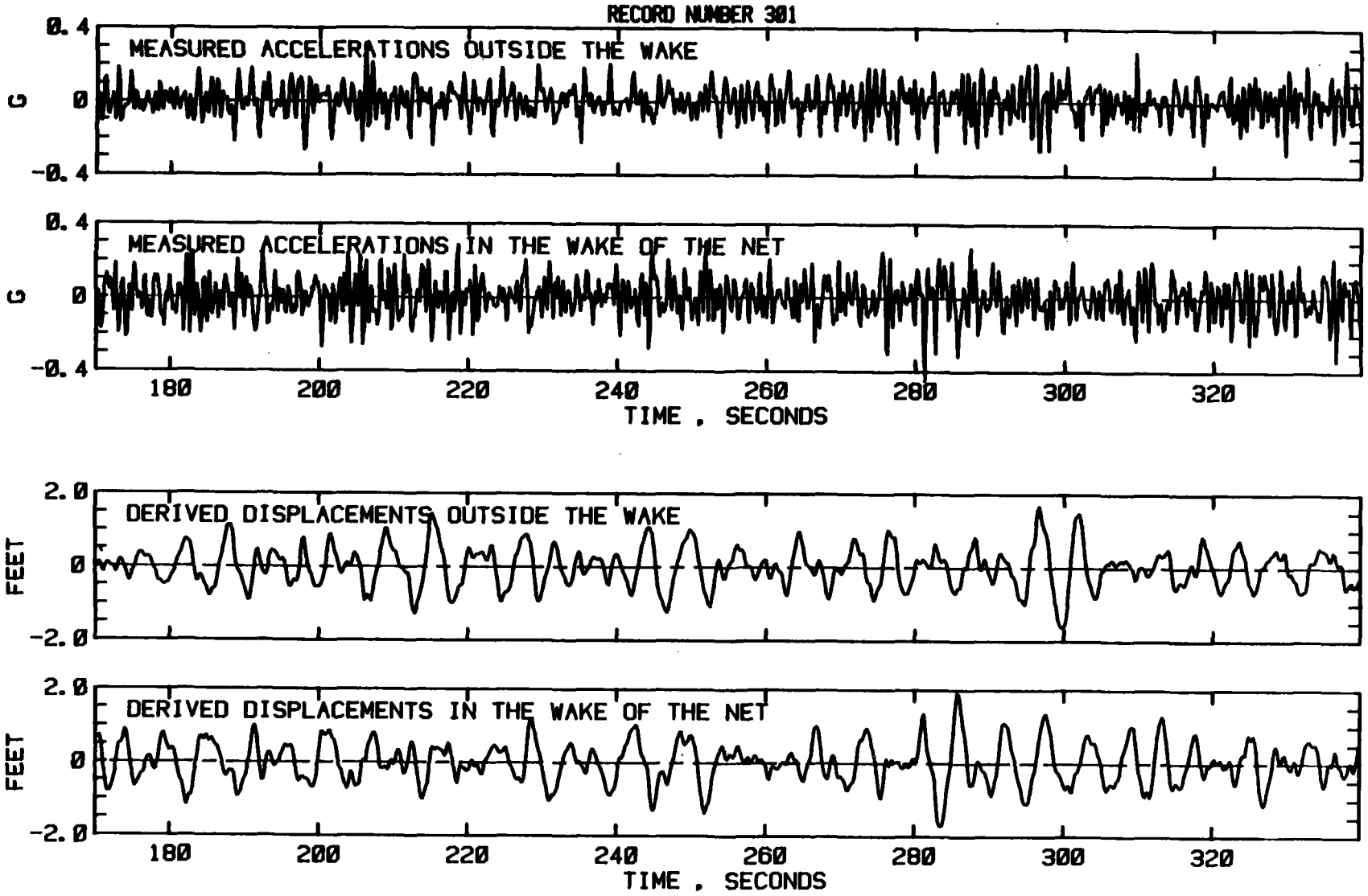

FIGURE 31 B.

R-2302

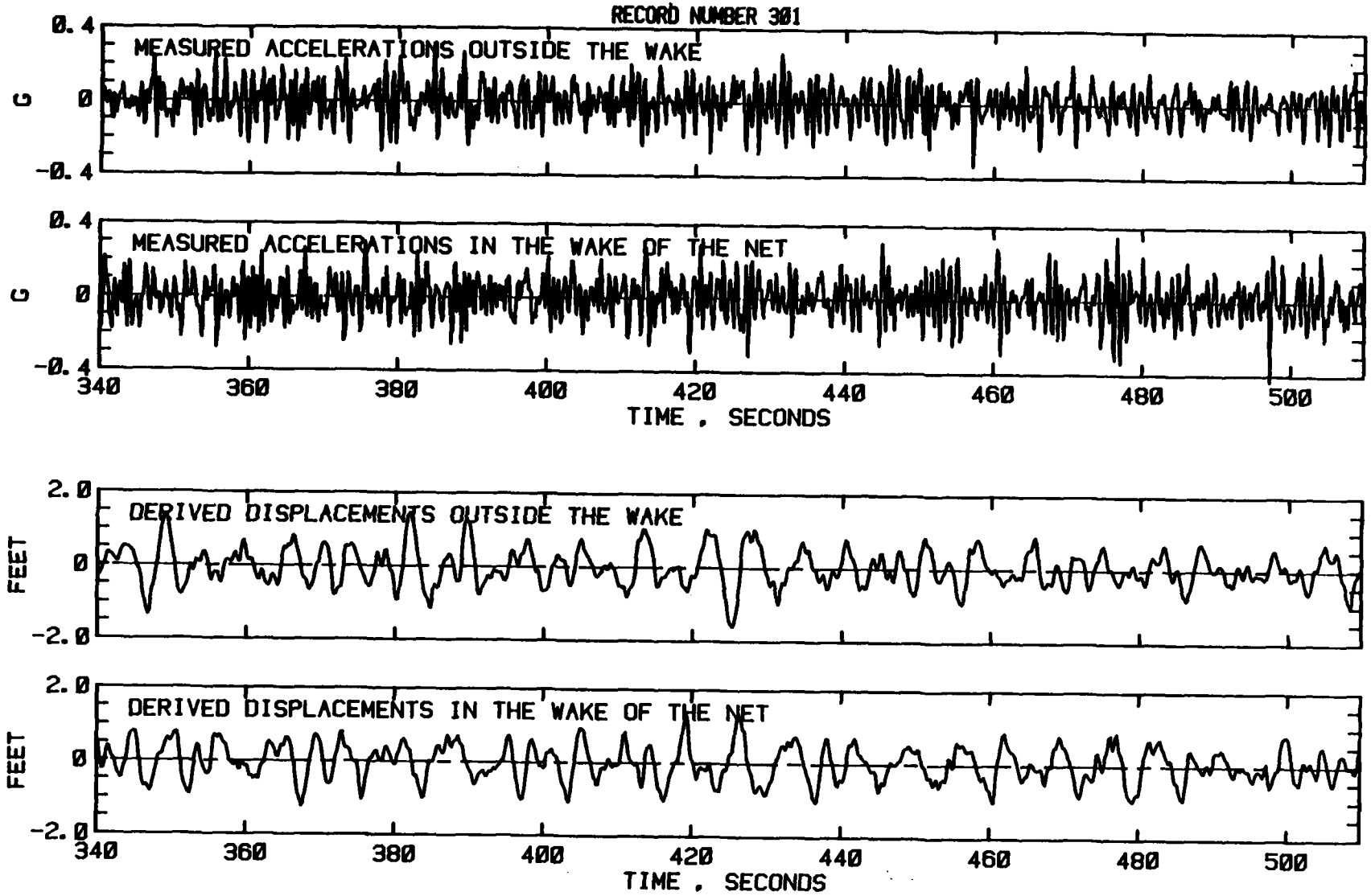
RECORD NUMBER 301
MEASURED ACCELERATIONS OUTSIDE THE WAKE
MEASURED ACCELERATIONS IN THE WAKE OF THE NET
G
0.4
0
-0.4
340
360
380
400
420
440
460
480
500
TIME , SECONDS
DERIVED DISPLACEMENTS OUTSIDE THE WAKE
DERIVED DISPLACEMENTS IN THE WAKE OF THE NET
FEET
2.0
0
-2.0

FIGURE 31 C.

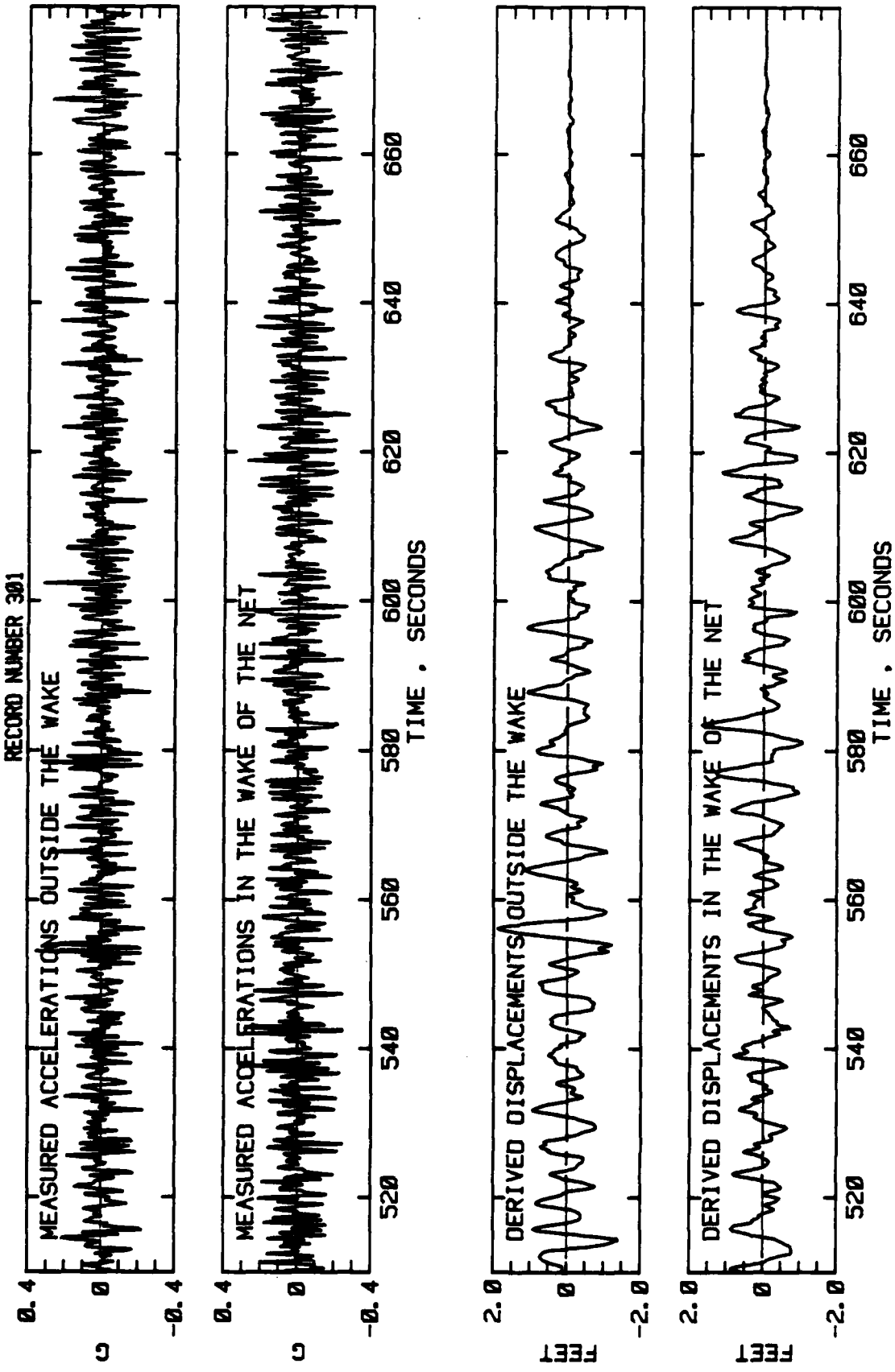
RECORD NUMBER 301
MEASURED ACCELERATIONS OUTSIDE THE WAKE
MEASURED ACCELERATIONS IN THE WAKE OF THE NET
DERIVED DISPLACEMENTS OUTSIDE THE WAKE
DERIVED DISPLACEMENTS IN THE WAKE OF THE NET
G
FEET
TIME . SECONDS
0.4
0
-0.4
2.0
-2.0
520
540
560
580
600
620
640
660

FIGURE 31 D.

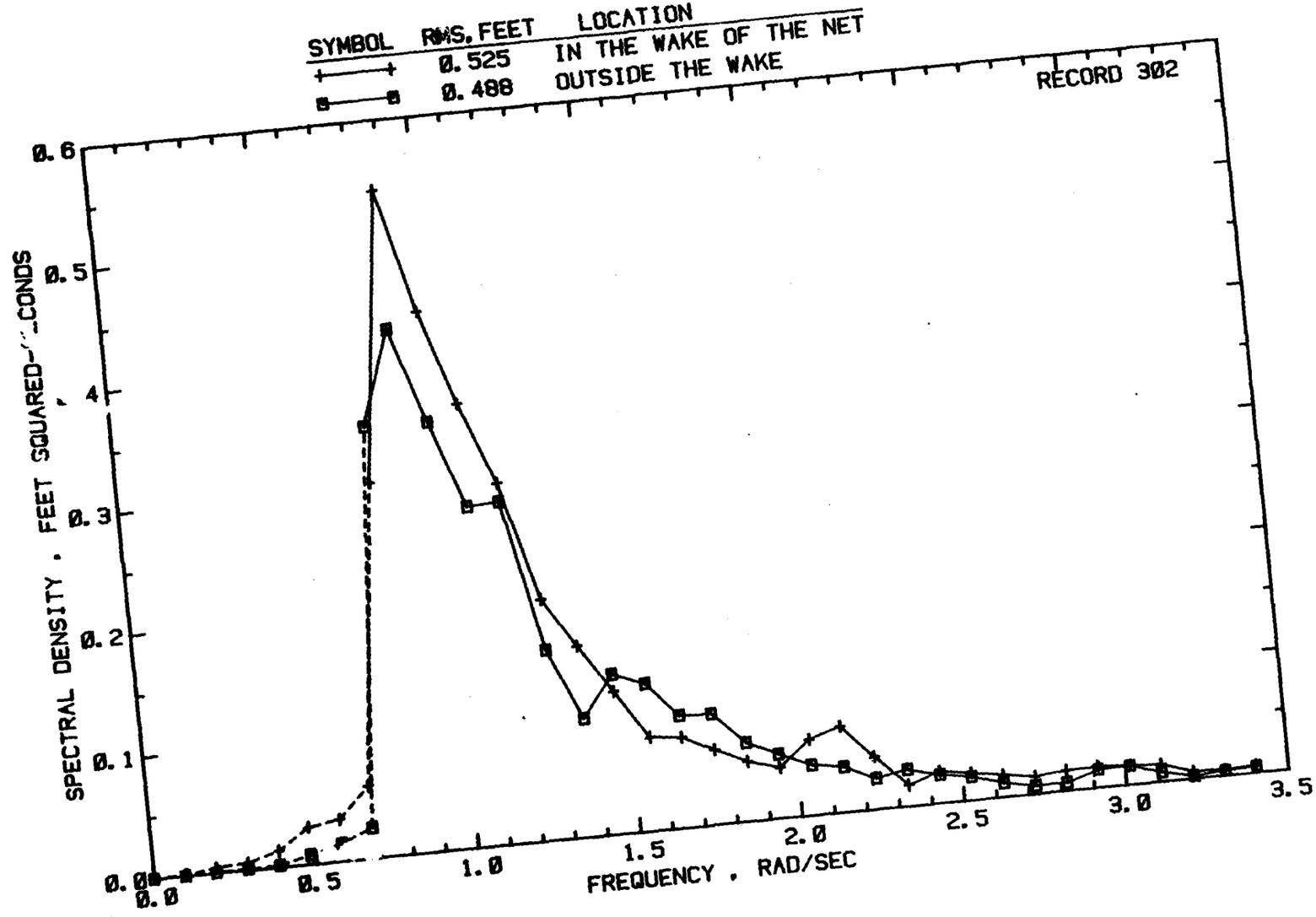
SYMBOL RMS, FEET LOCATION
0.525 IN THE WAKE OF THE NET
0.488 OUTSIDE THE WAKE
RECORD 302
SPECTRAL DENSITY , FEET SQUARED-~_CONDS
0.6
0.5
4
0.3
0.2
0.1
0.0
0.0
0.5
1.0
1.5
2.0
2.5
3.0
3.5
FREQUENCY , RAD/SEC

FIGURE 32

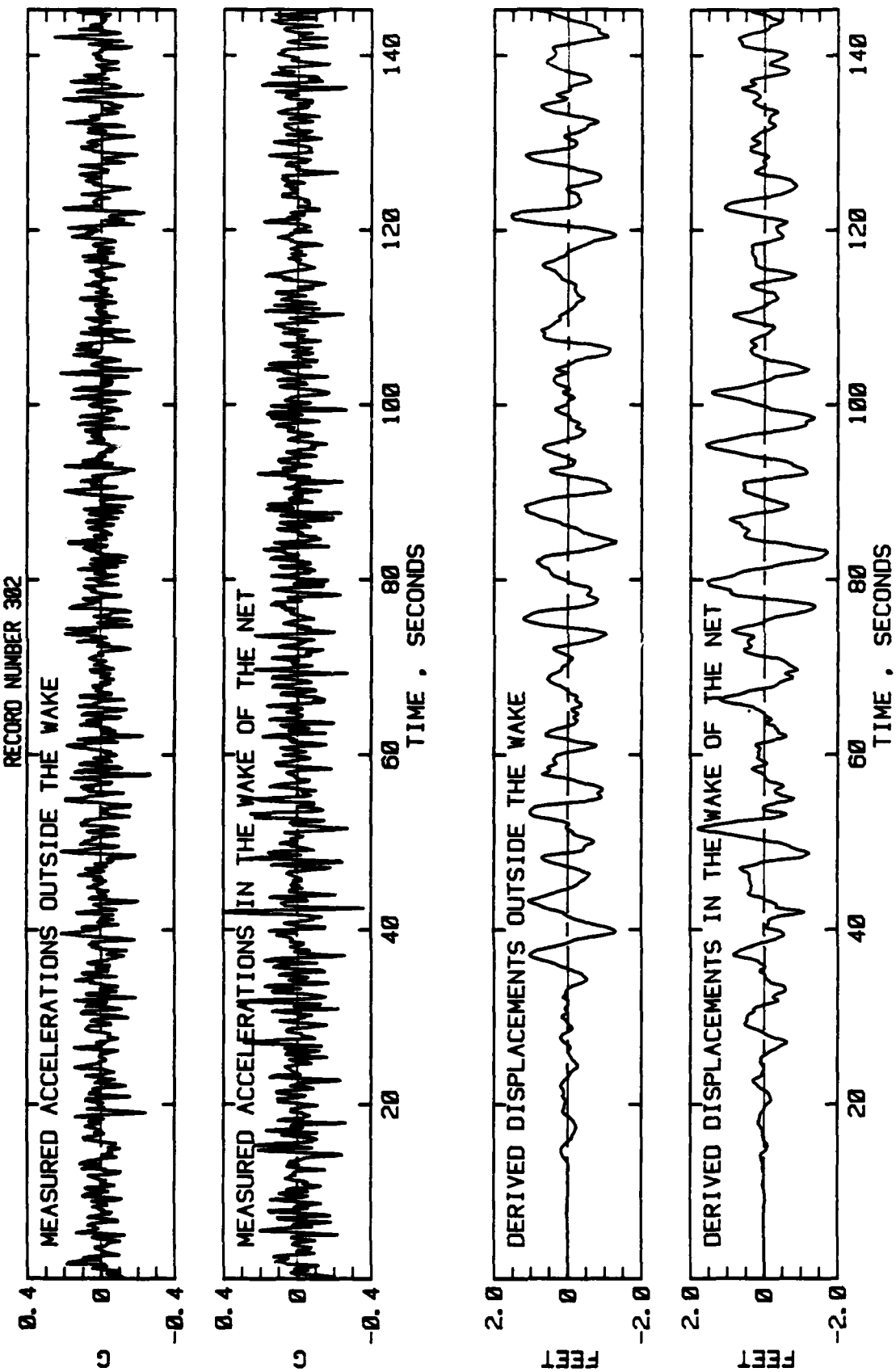
RECORD NUMBER 302
MEASURED ACCELERATIONS OUTSIDE THE WAKE
MEASURED ACCELERATIONS IN THE WAKE OF THE NET
DERIVED DISPLACEMENTS OUTSIDE THE WAKE
DERIVED DISPLACEMENTS IN THE WAKE OF THE NET
G
FEET
TIME , SECONDS
0.4
0
-0.4
2.0
-2.0
20
40
60
80
100
120
140

FIGURE 33A.

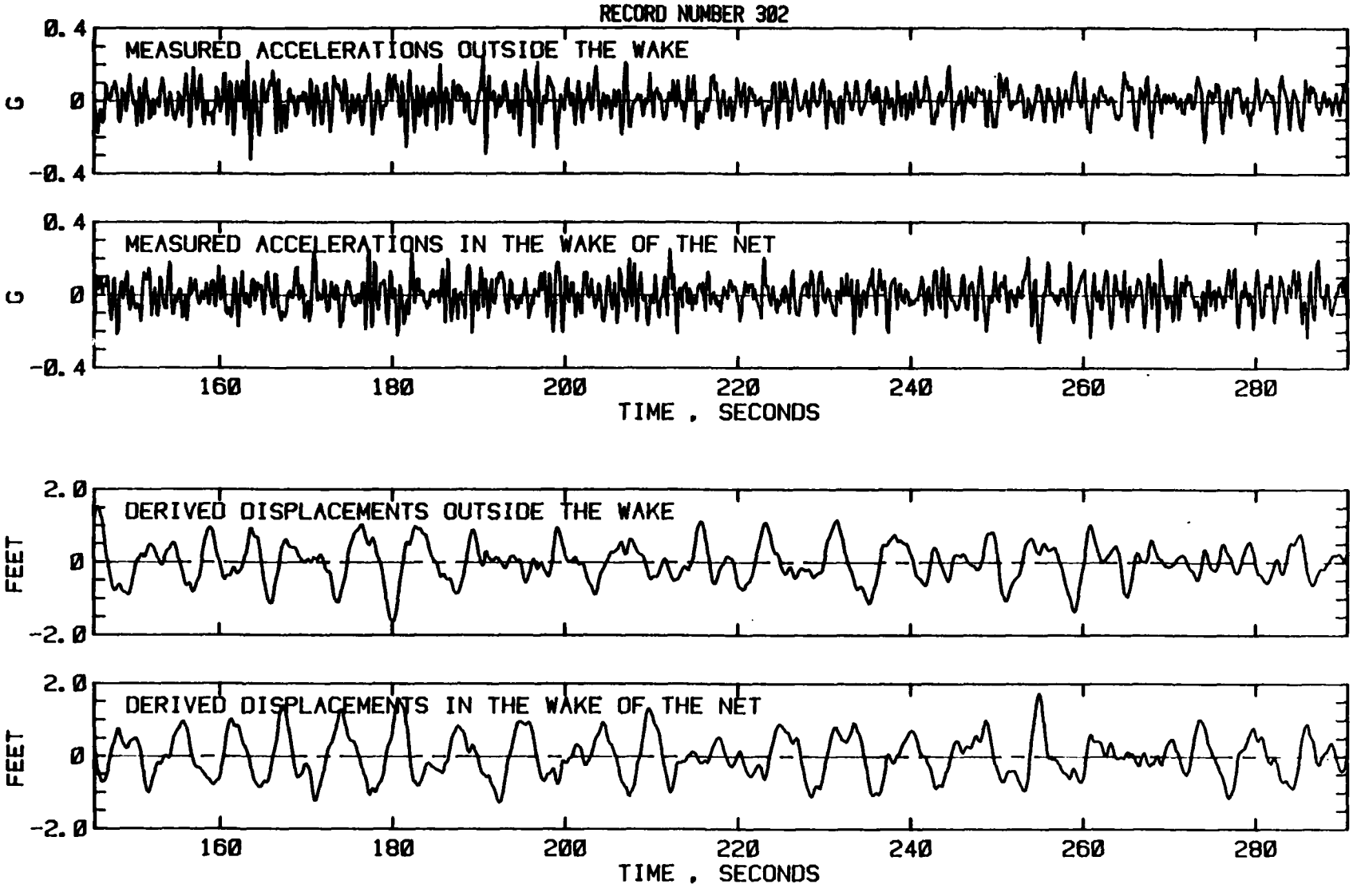
RECORD NUMBER 302
MEASURED ACCELERATIONS OUTSIDE THE WAKE
MEASURED ACCELERATIONS IN THE WAKE OF THE NET
G
0.4
0
-0.4
160
180
200
220
240
260
280
TIME , SECONDS
DERIVED DISPLACEMENTS OUTSIDE THE WAKE
DERIVED DISPLACEMENTS IN THE WAKE OF THE NET
FEET
2.0
0
-2.0

FIGURE 33 B.

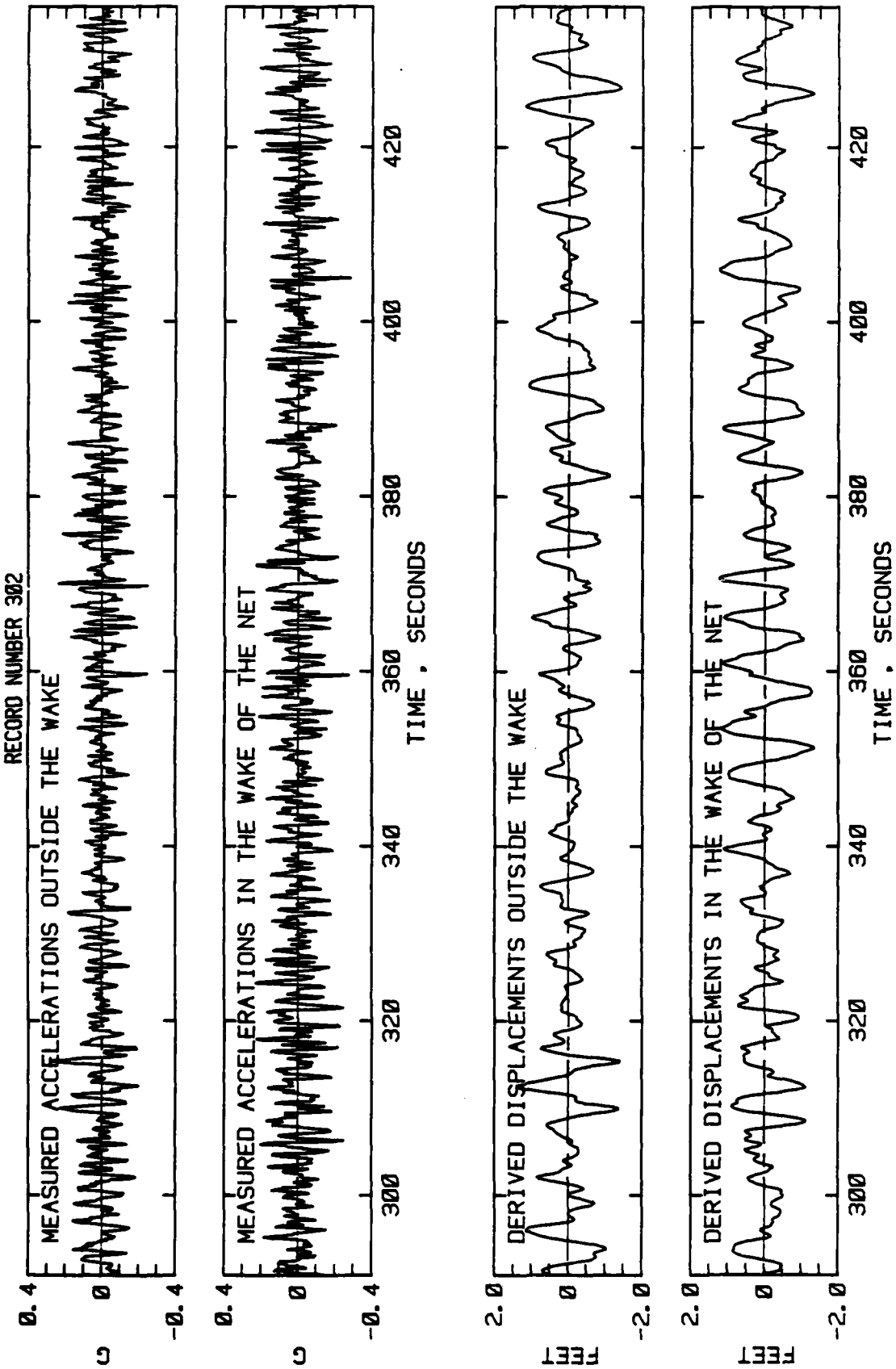
RECORD NUMBER 302
MEASURED ACCELERATIONS OUTSIDE THE WAKE
MEASURED ACCELERATIONS IN THE WAKE OF THE NET
DERIVED DISPLACEMENTS OUTSIDE THE WAKE
DERIVED DISPLACEMENTS IN THE WAKE OF THE NET
G
FEET
TIME • SECONDS
0.4
0
-0.4
2.0
-2.0
300
320
340
360
380
400
420

FIGURE 33 C.

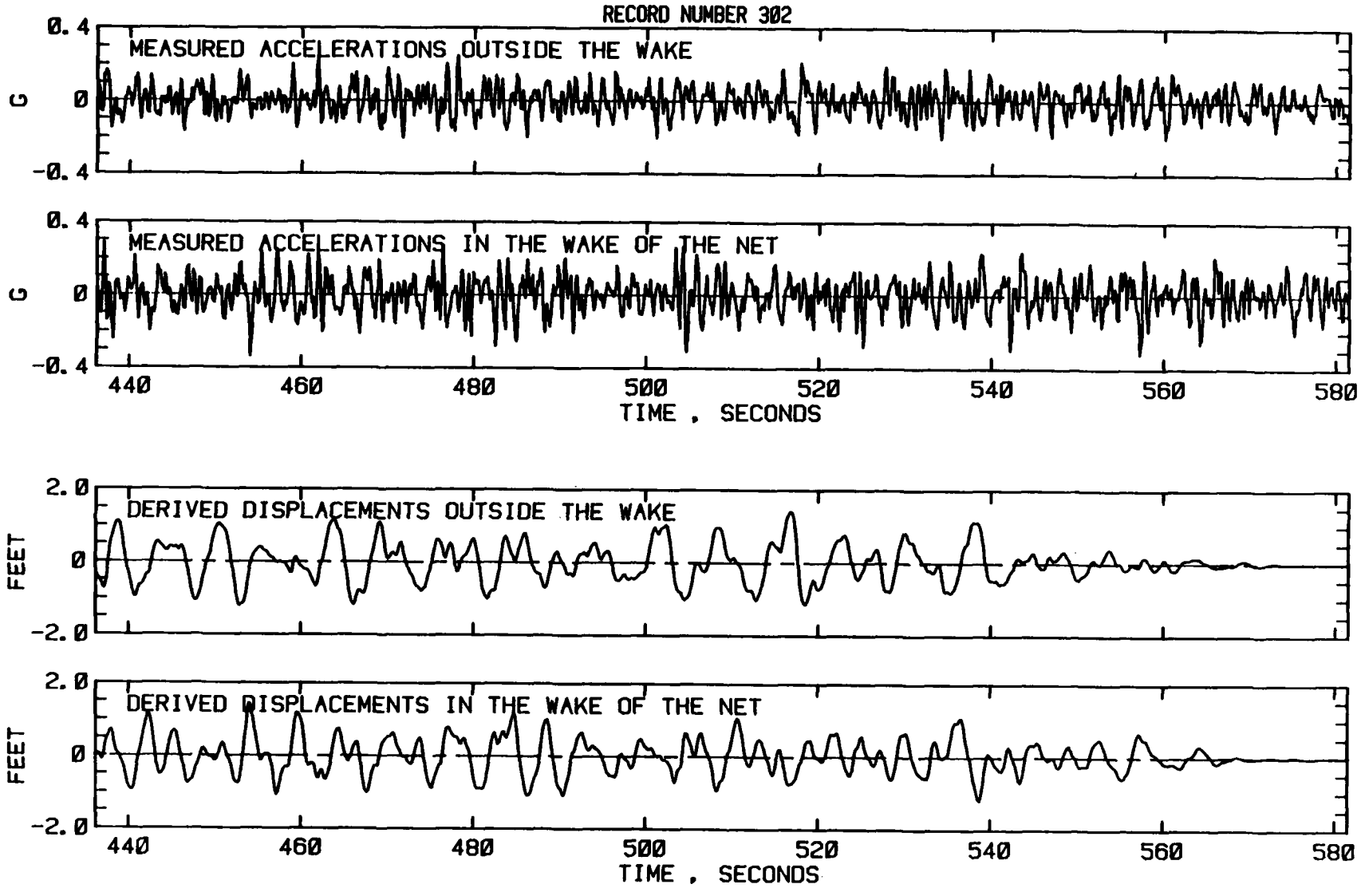
RECORD NUMBER 302
MEASURED ACCELERATIONS OUTSIDE THE WAKE
MEASURED ACCELERATIONS IN THE WAKE OF THE NET
G
0.4
0
-0.4
DERIVED DISPLACEMENTS OUTSIDE THE WAKE
DERIVED DISPLACEMENTS IN THE WAKE OF THE NET
FEET
2.0
0
-2.0
440
460
480
500
520
540
560
580
TIME , SECONDS

FIGURE 33 D.

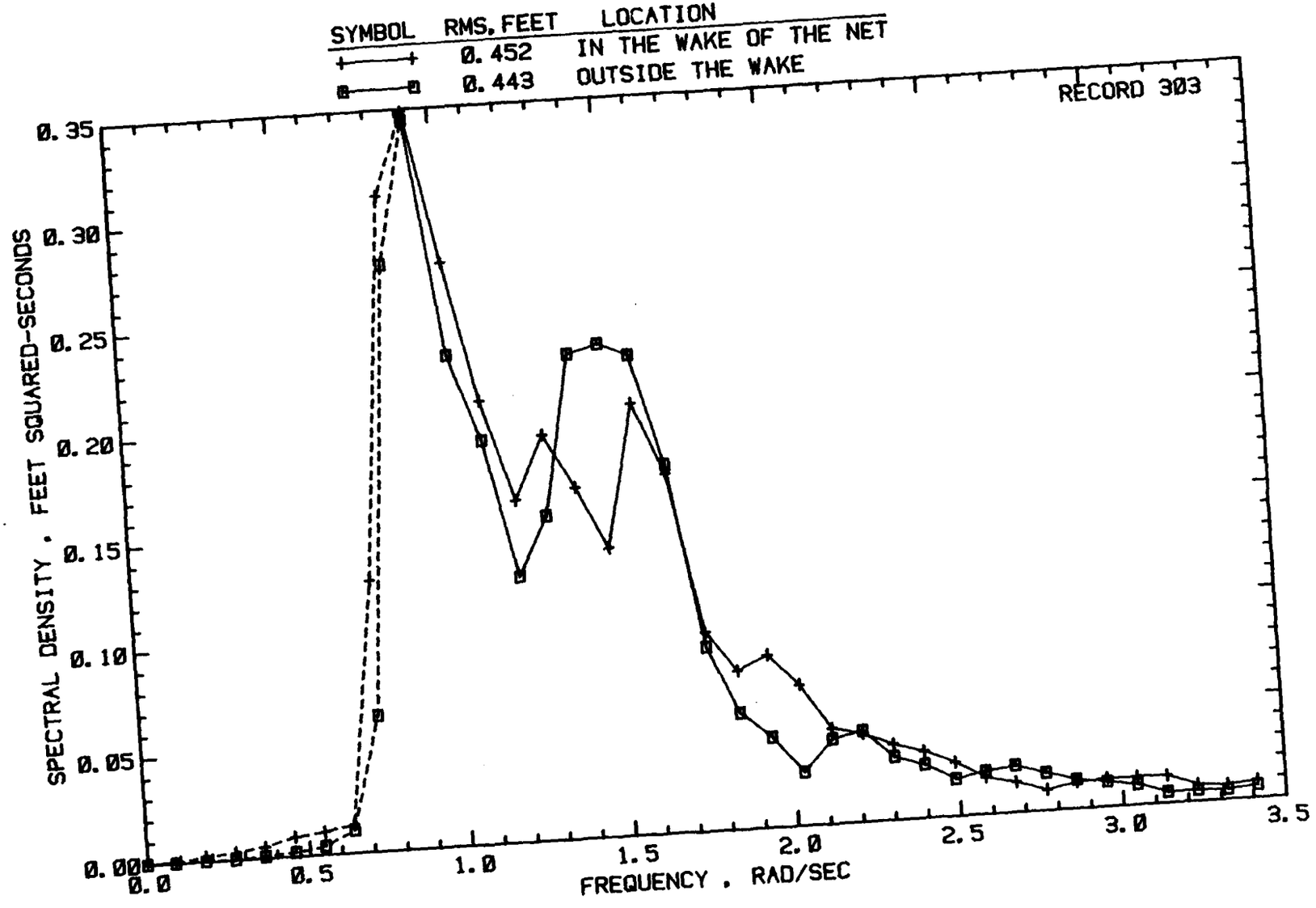
SYMBOL RMS, FEET LOCATION
0.452 IN THE WAKE OF THE NET
0.443 OUTSIDE THE WAKE
RECORD 303
SPECTRAL DENSITY , FEET SQUARED-SECONDS
0.35
0.30
0.25
0.20
0.15
0.10
0.05
0.00
0.0
0.5
1.0
1.5
2.0
2.5
3.0
3.5
FREQUENCY , RAD/SEC

FIGURE 34.

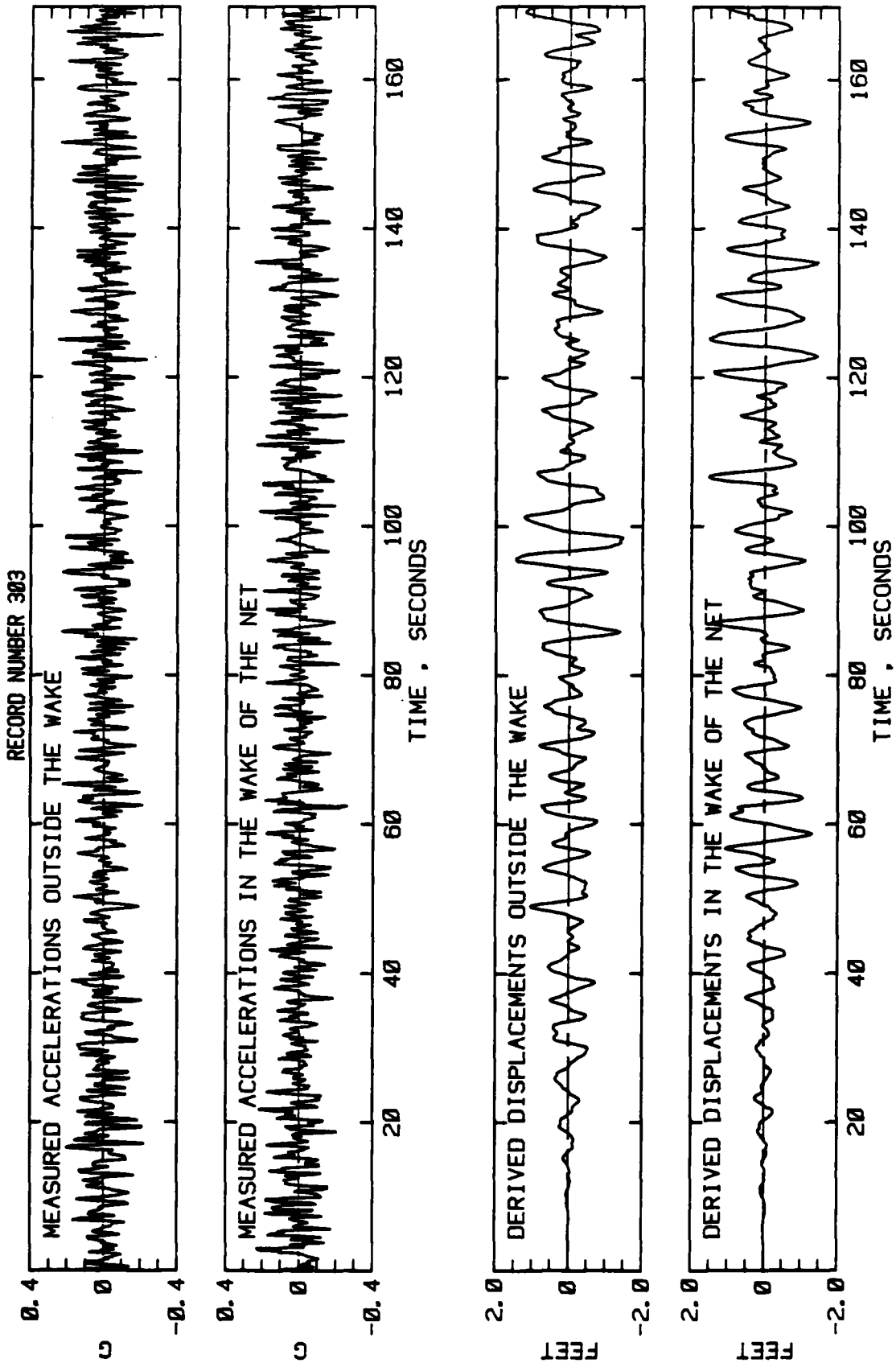
RECORD NUMBER 303
MEASURED ACCELERATIONS OUTSIDE THE WAKE
MEASURED ACCELERATIONS IN THE WAKE OF THE NET
DERIVED DISPLACEMENTS OUTSIDE THE WAKE
DERIVED DISPLACEMENTS IN THE WAKE OF THE NET
G
FEET
TIME , SECONDS
0.4
0
-0.4
2.0
-2.0
20
40
60
80
100
120
140
160

FIGURE 35A.

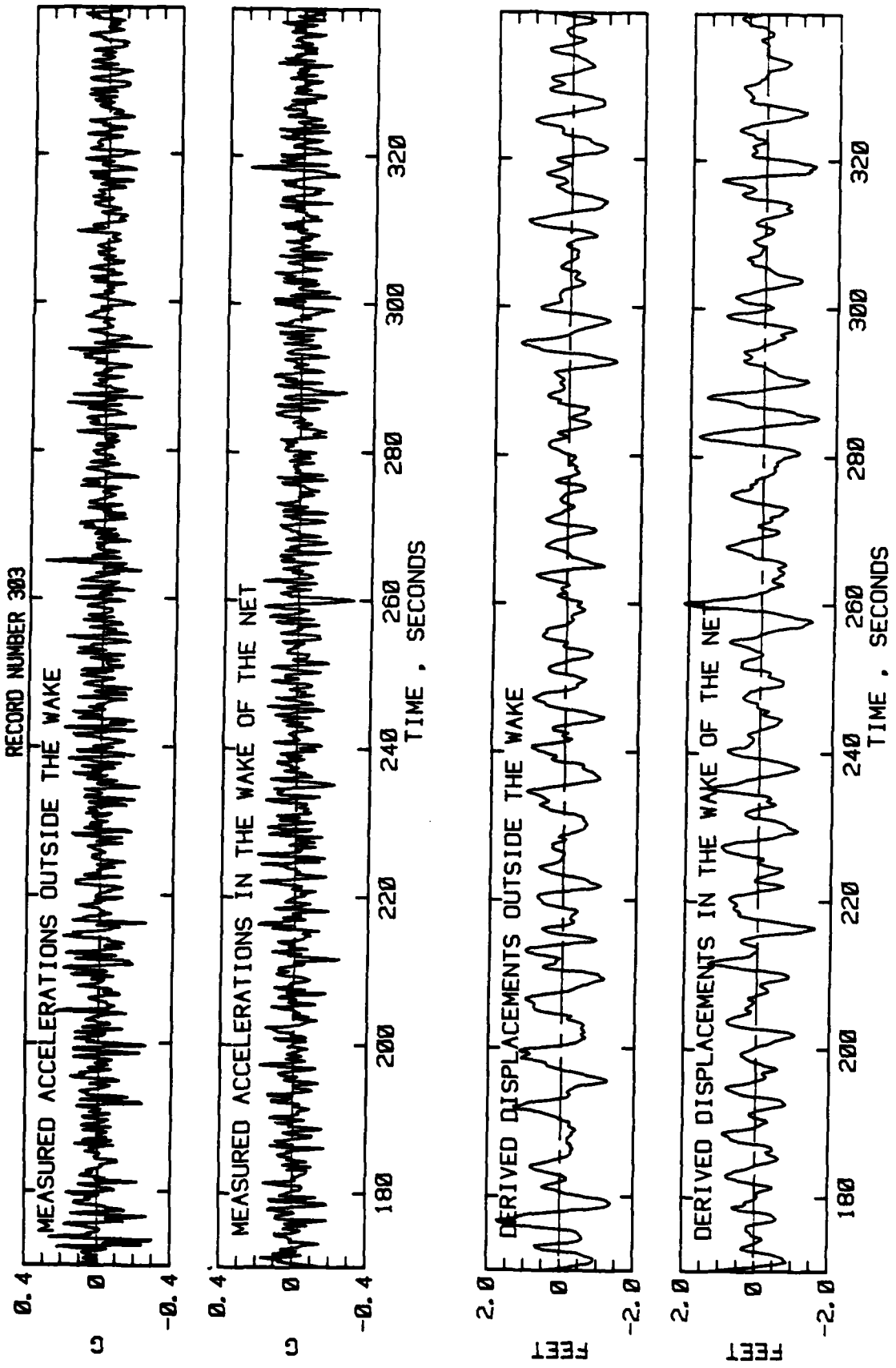
RECORD NUMBER 303
MEASURED ACCELERATIONS OUTSIDE THE WAKE
MEASURED ACCELERATIONS IN THE WAKE OF THE NET
DERIVED DISPLACEMENTS OUTSIDE THE WAKE
DERIVED DISPLACEMENTS IN THE WAKE OF THE NET
G
FEET
TIME , SECONDS
0.4
0
-0.4
2.0
-2.0
180
200
220
240
260
280
300
320

FIGURE 35 B.

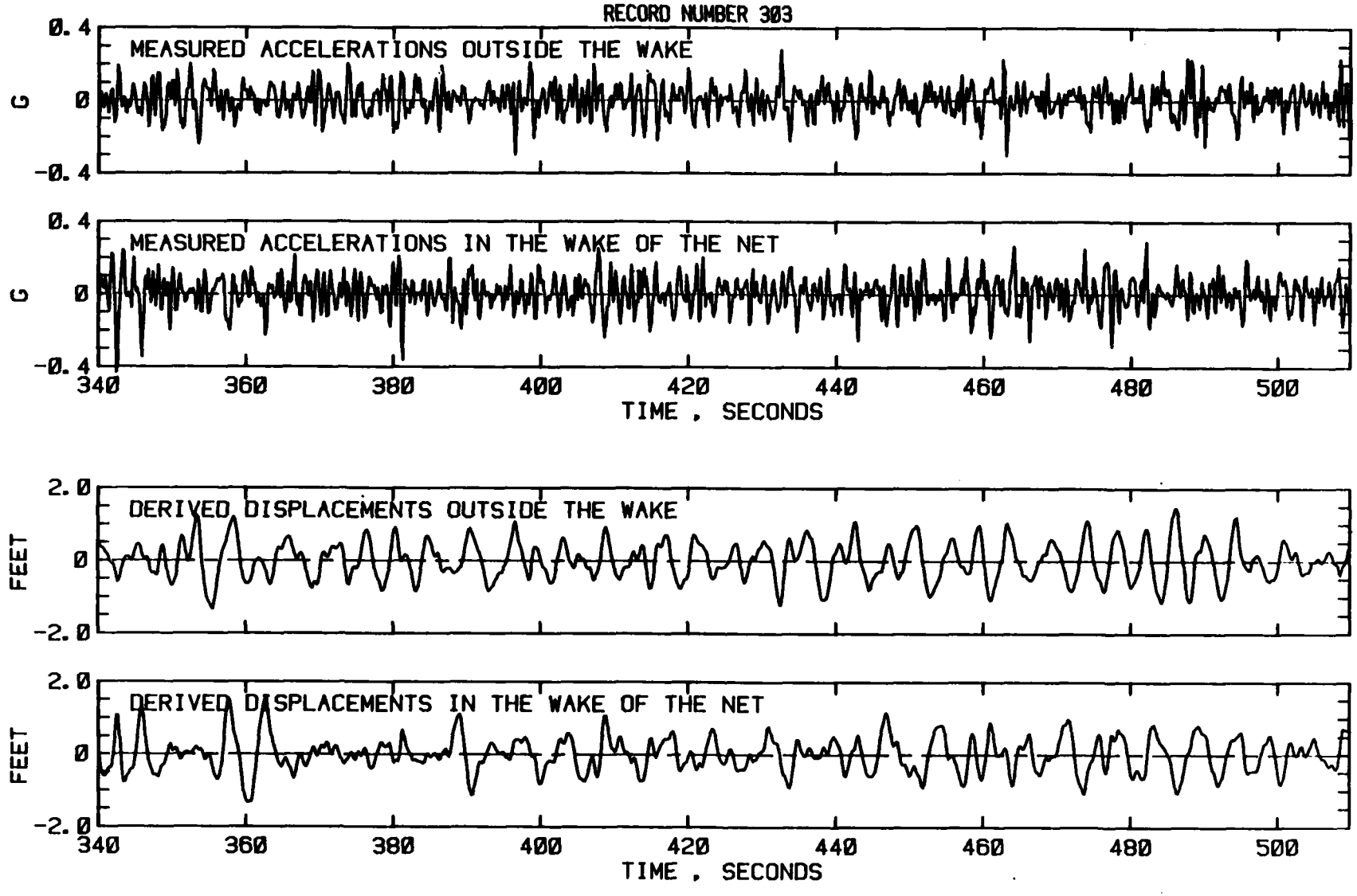

FIGURE 35 C

R-2302

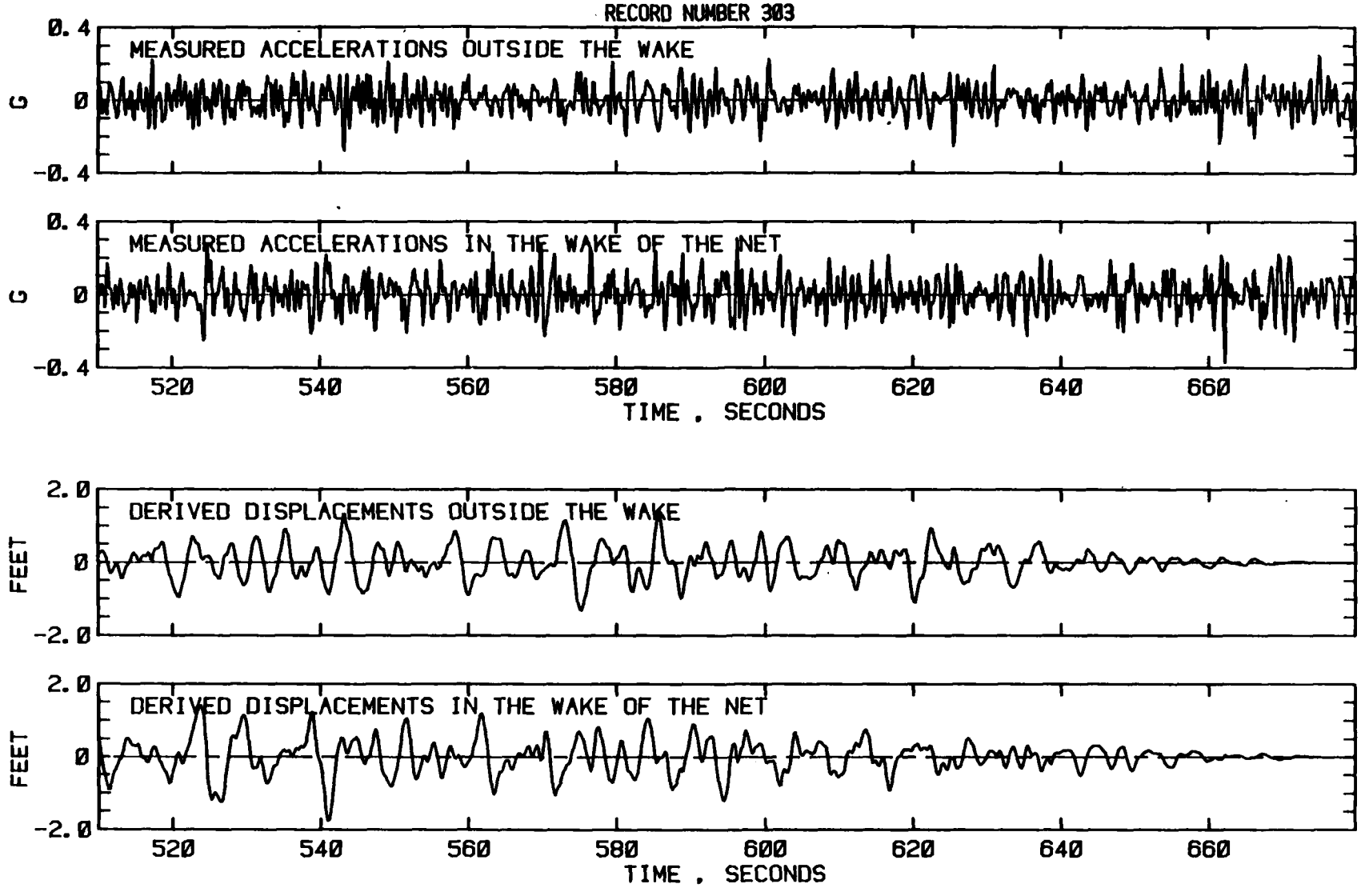

FIGURE 35 D.

R-2302

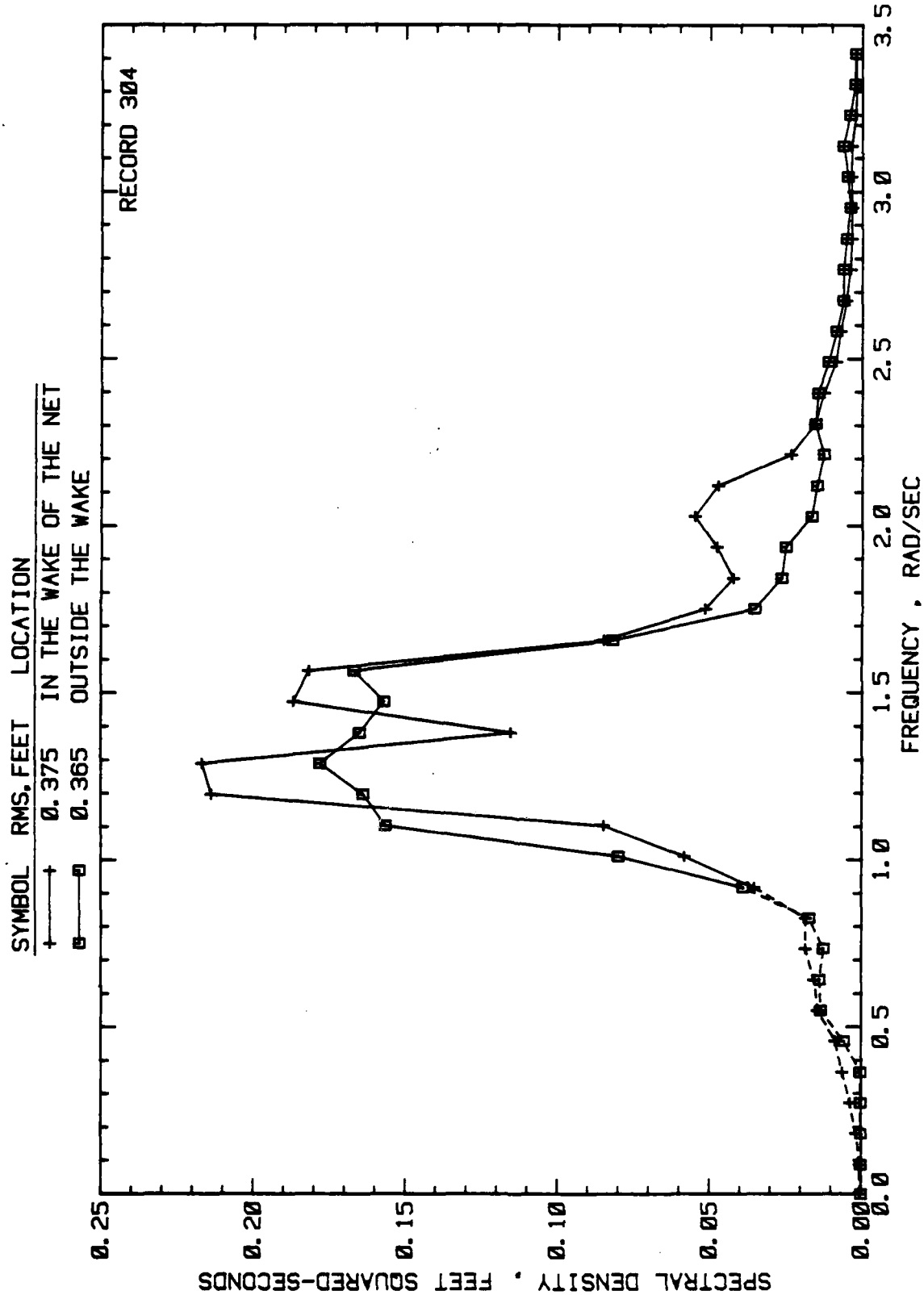
RECORD 304
SYMBOL RMS,FEET LOCATION
0.375 IN THE WAKE OF THE NET
0.365 OUTSIDE THE WAKE
SPECTRAL DENSITY , FEET SQUARED-SECONDS
0.25
0.20
0.15
0.10
0.05
0.00
0.0
0.5
1.0
1.5
2.0
2.5
3.0
3.5
FREQUENCY , RAD/SEC

FIGURE 36.

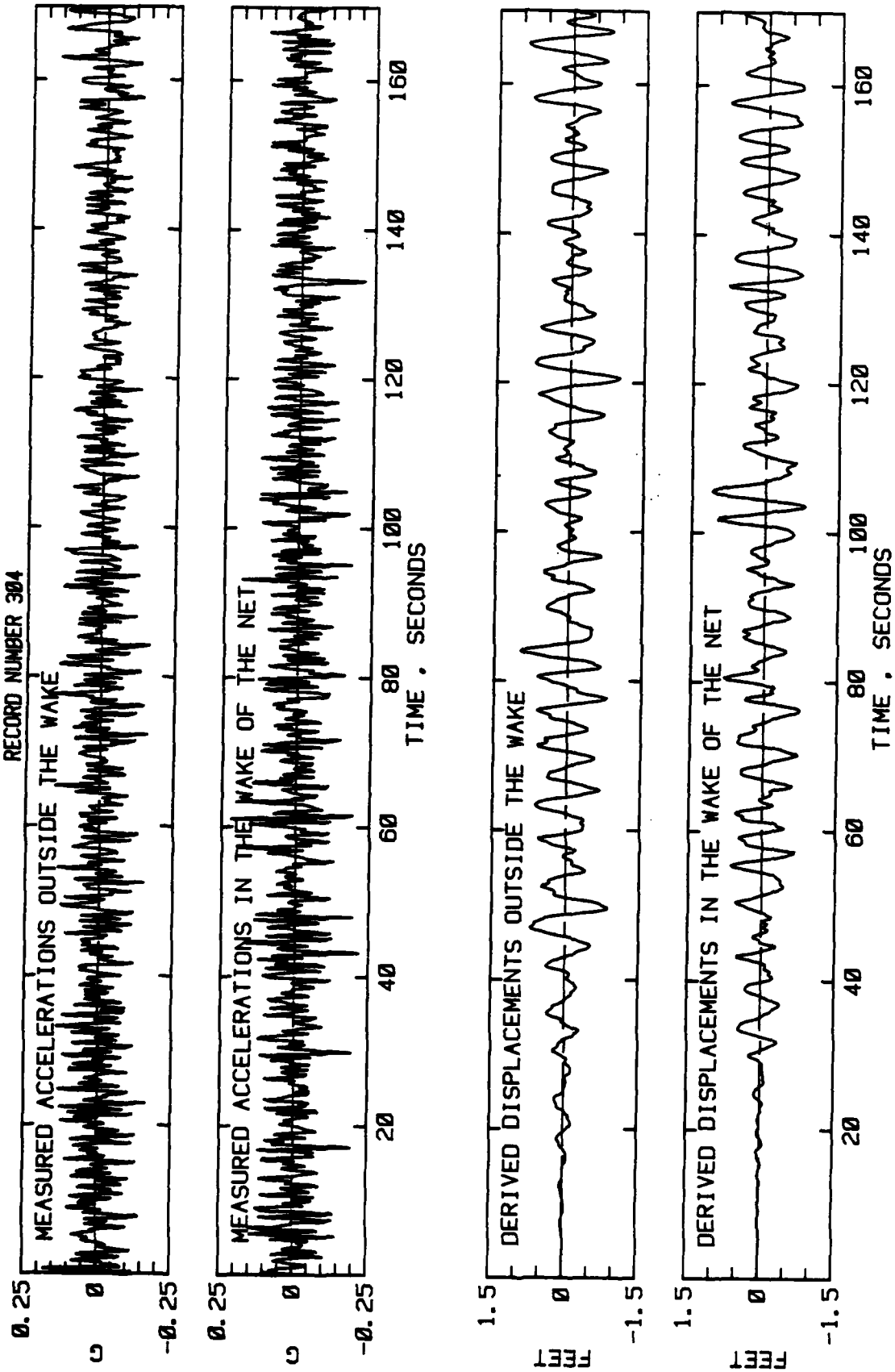
RECORD NUMBER 304
MEASURED ACCELERATIONS OUTSIDE THE WAKE
MEASURED ACCELERATIONS IN THE WAKE OF THE NET
DERIVED DISPLACEMENTS OUTSIDE THE WAKE
DERIVED DISPLACEMENTS IN THE WAKE OF THE NET
G
FEET
TIME . SECONDS
0.25
0
-0.25
1.5
-1.5
20
40
60
80
100
120
140
160

FIGURE 37 A.

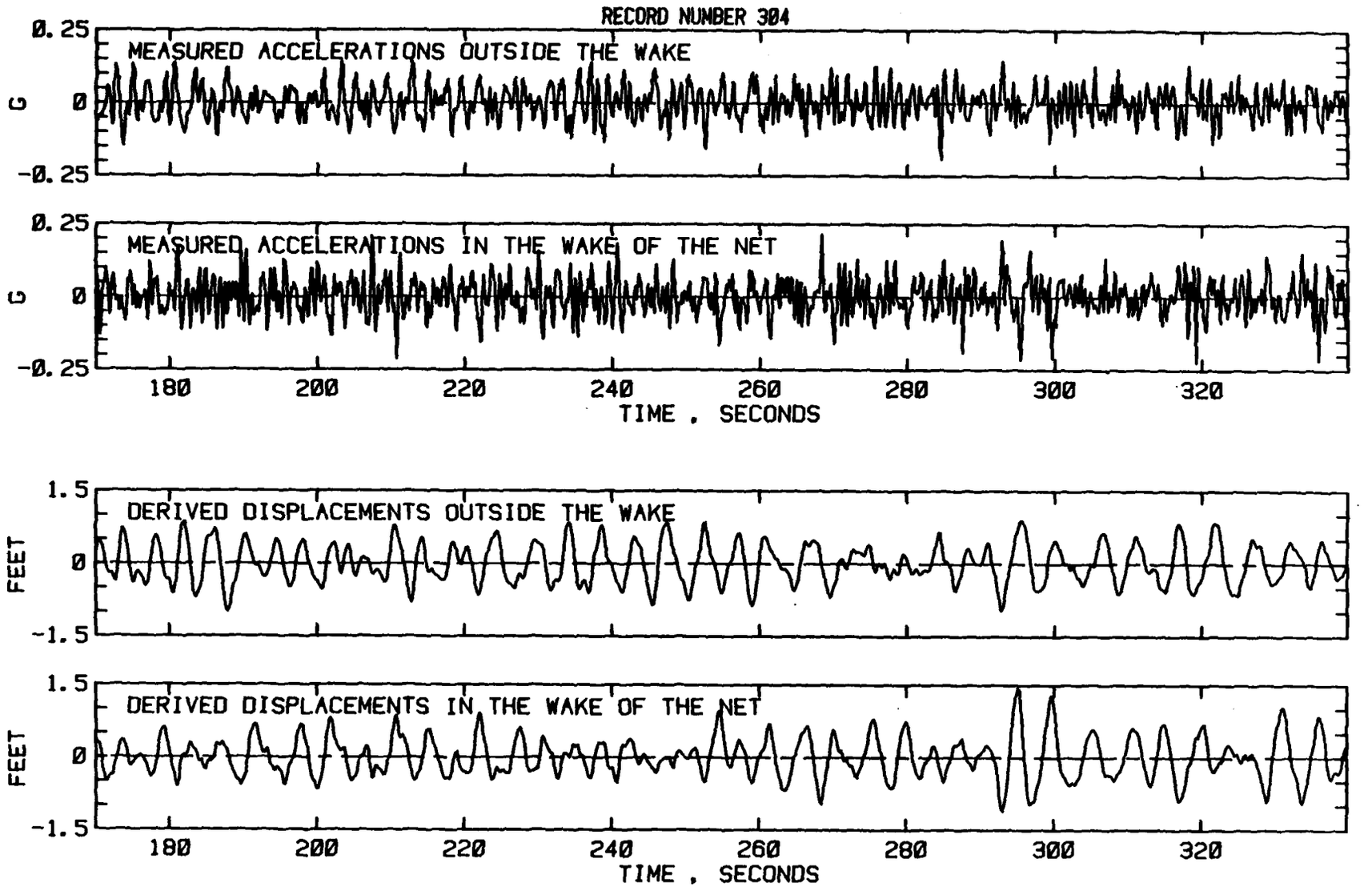

FIGURE 37 B.

R-2302

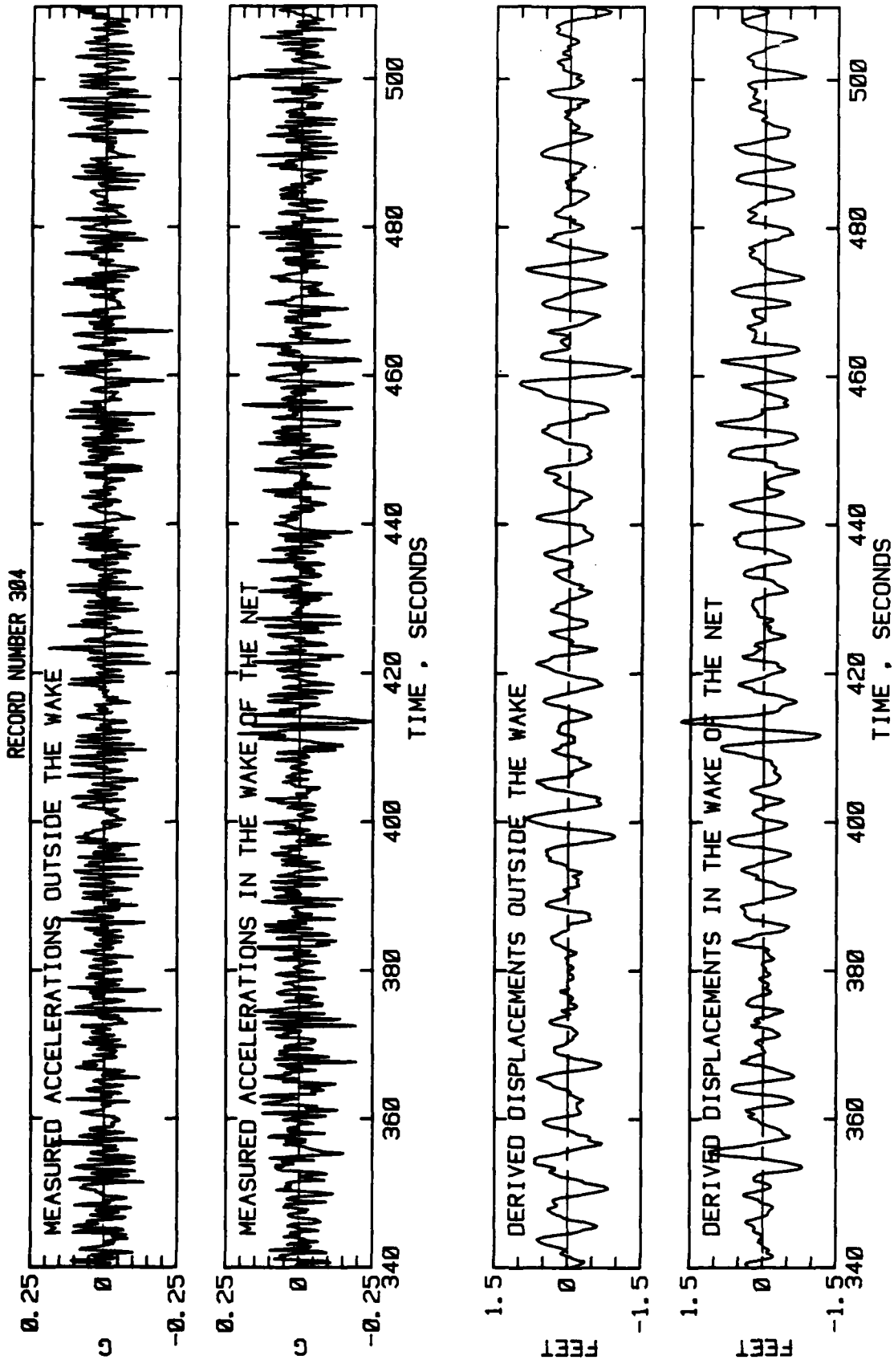
RECORD NUMBER 304
MEASURED ACCELERATIONS OUTSIDE THE WAKE
MEASURED ACCELERATIONS IN THE WAKE OF THE NET
DERIVED DISPLACEMENTS OUTSIDE THE WAKE
DERIVED DISPLACEMENTS IN THE WAKE OF THE NET
G
FEET
TIME . SECONDS
0.25
0
-0.25
1.5
-1.5
340
360
380
400
420
440
460
480
500

FIGURE 37 C.

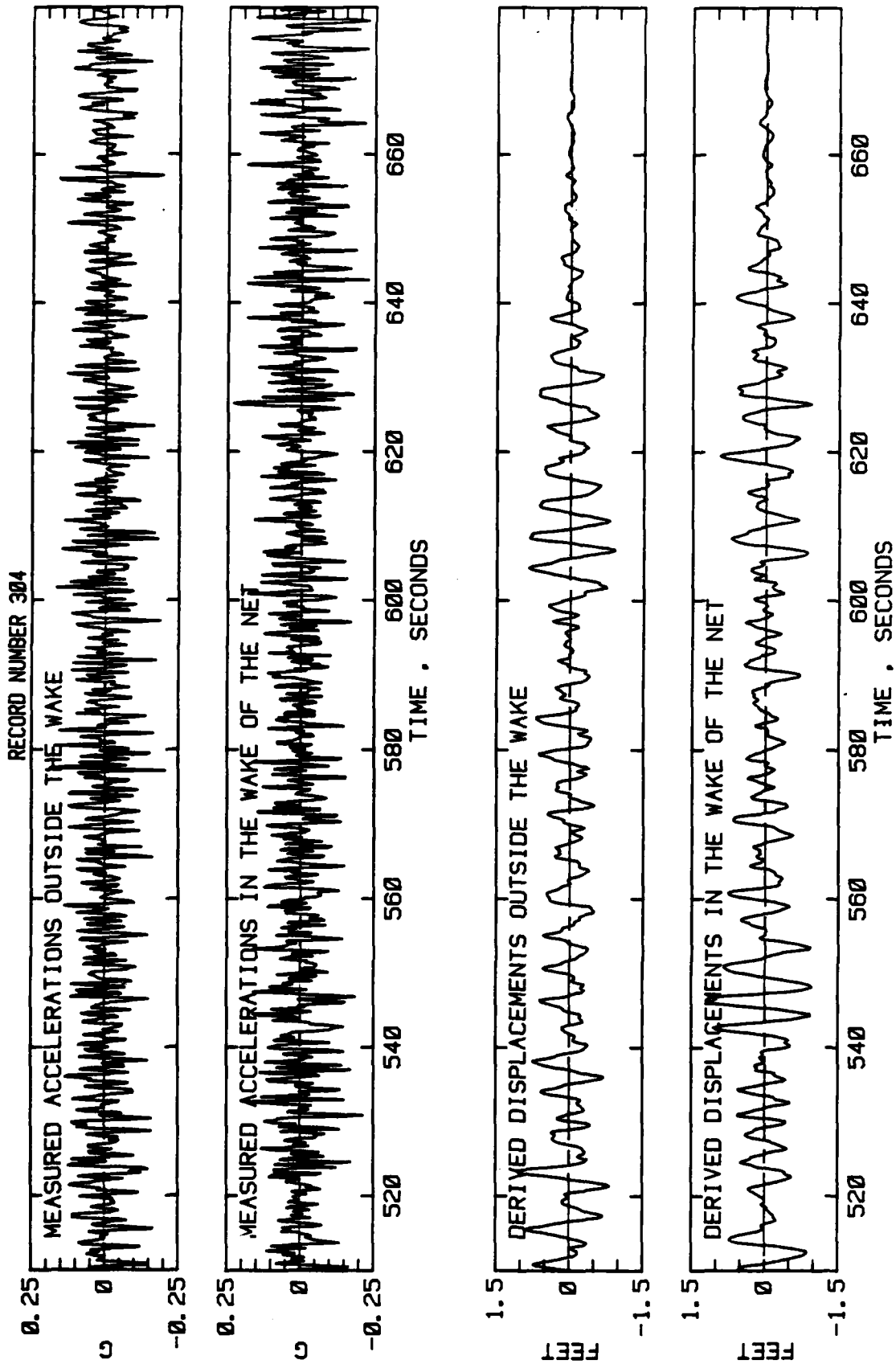
RECORD NUMBER 304
MEASURED ACCELERATIONS OUTSIDE THE WAKE
G
0.25
0
-0.25
MEASURED ACCELERATIONS IN THE WAKE OF THE NET
G
0.25
0
-0.25
520
540
560
580
600
620
640
660
TIME . SECONDS
DERIVED DISPLACEMENTS OUTSIDE THE WAKE
FEET
1.5
0
-1.5
DERIVED DISPLACEMENTS IN THE WAKE OF THE NET
FEET
1.5
0
-1.5
520
540
560
580
600
620
640
660
TIME . SECONDS

FIGURE 37 D.

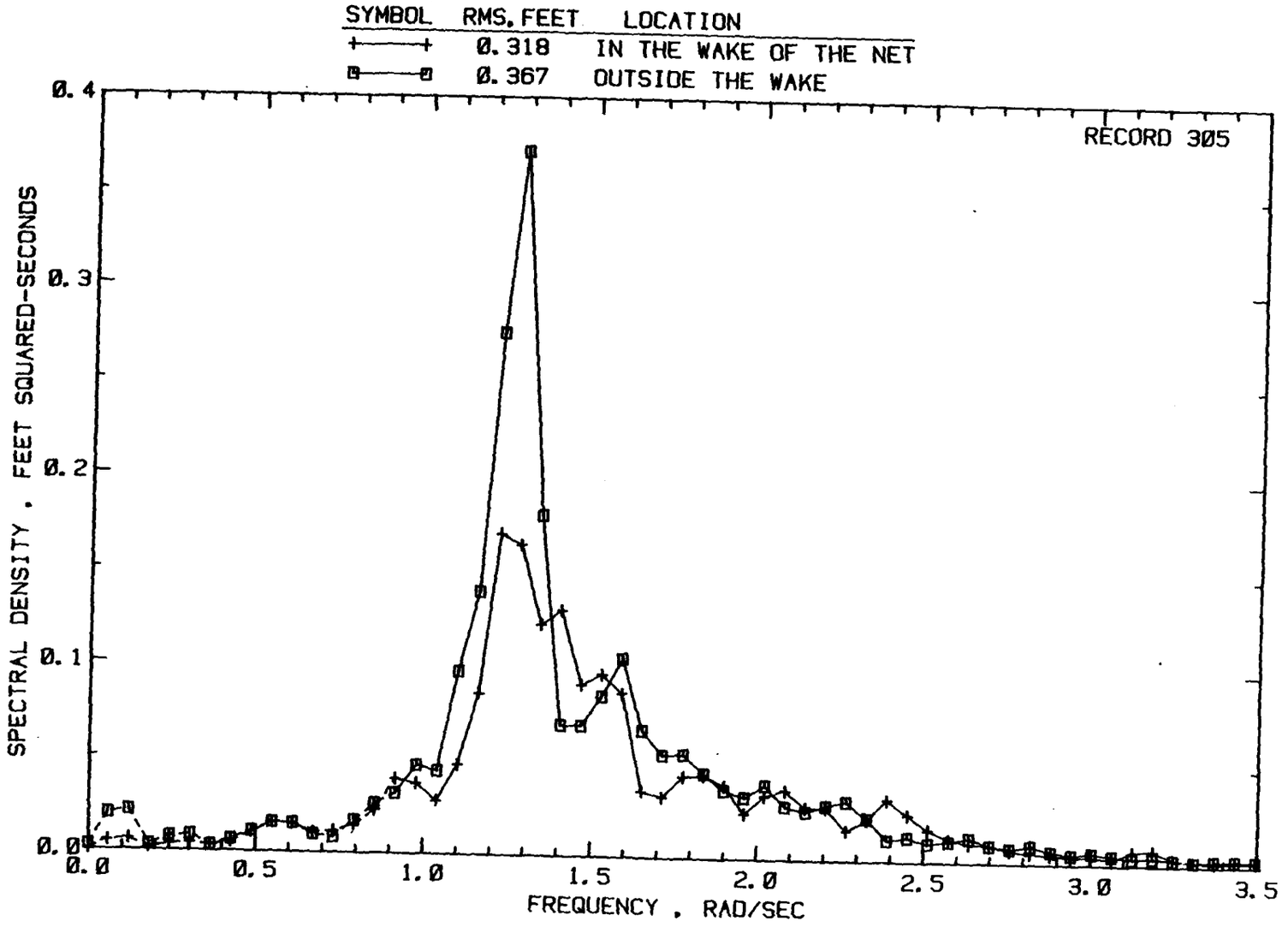
SYMBOL RMS, FEET LOCATION
Ø.318 IN THE WAKE OF THE NET
Ø.367 OUTSIDE THE WAKE
RECORD 305
SPECTRAL DENSITY , FEET SQUARED-SECONDS
Ø.4
Ø.3
Ø.2
Ø.1
Ø.Ø
0.0
0.5
1.0
1.5
2.0
2.5
3.0
3.5
FREQUENCY , RAD/SEC

FIGURE 38.

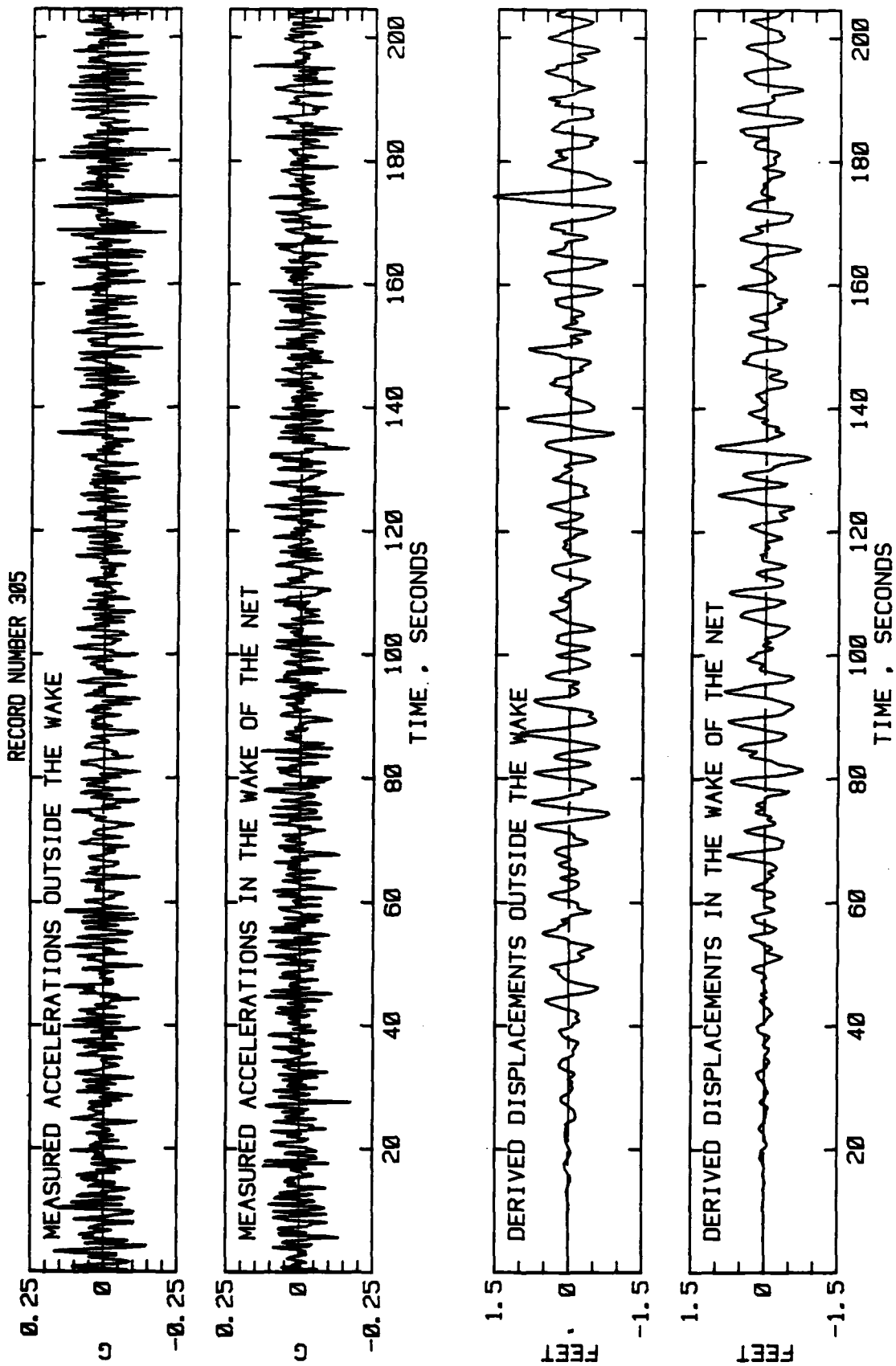
RECORD NUMBER 305
MEASURED ACCELERATIONS OUTSIDE THE WAKE
MEASURED ACCELERATIONS IN THE WAKE OF THE NET
DERIVED DISPLACEMENTS OUTSIDE THE WAKE
DERIVED DISPLACEMENTS IN THE WAKE OF THE NET
G
FEET
TIME , SECONDS
0.25
0
-0.25
1.5
-1.5
20
40
60
80
100
120
140
160
180
200

FIGURE 39A.

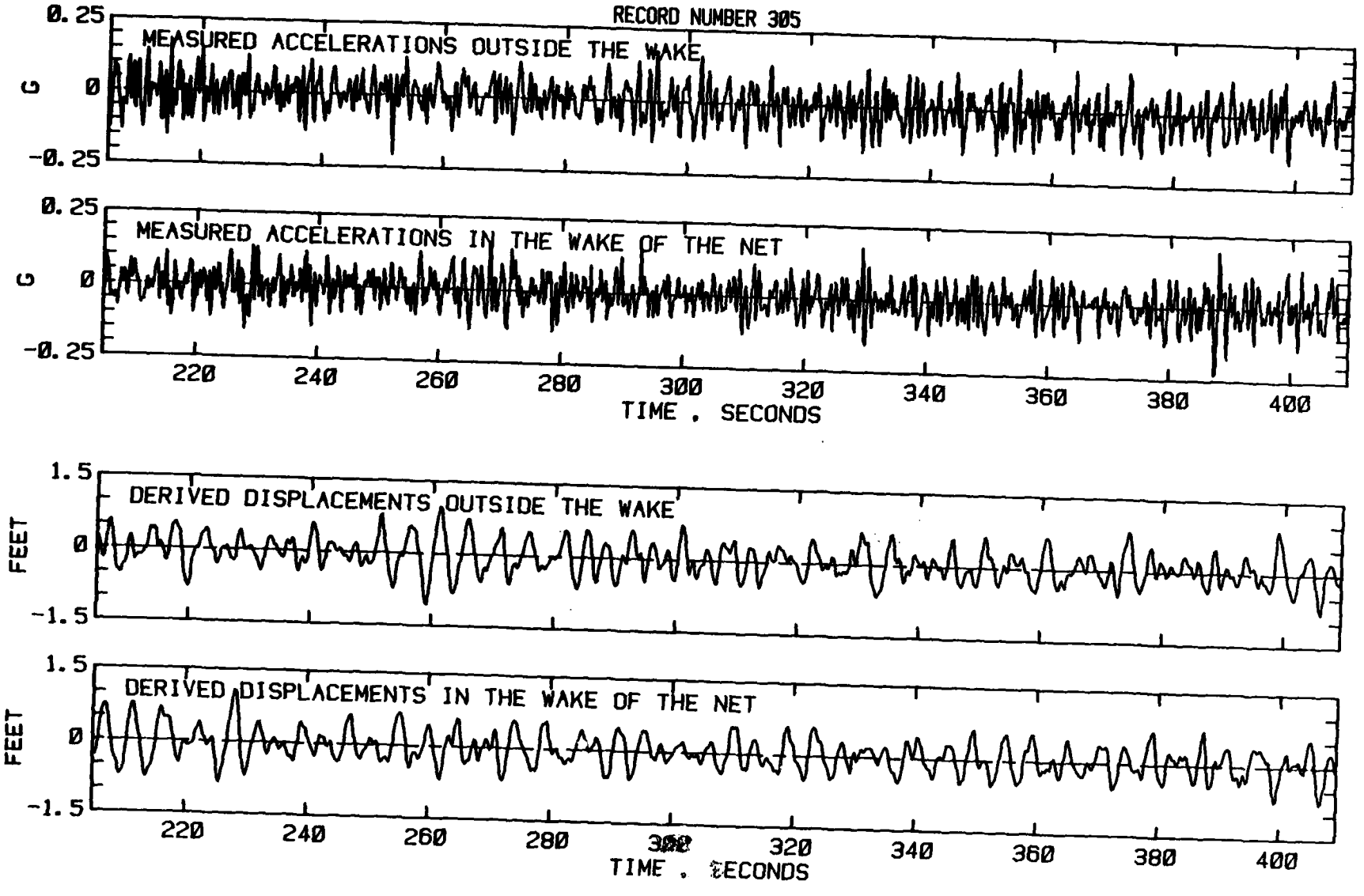
RECORD NUMBER 305
MEASURED ACCELERATIONS OUTSIDE THE WAKE
MEASURED ACCELERATIONS IN THE WAKE OF THE NET
G
0.25
0
-0.25
220
240
260
280
300
320
340
360
380
400
TIME . SECONDS
DERIVED DISPLACEMENTS OUTSIDE THE WAKE
DERIVED DISPLACEMENTS IN THE WAKE OF THE NET
FEET
1.5
0
-1.5

FIGURE 39 B.

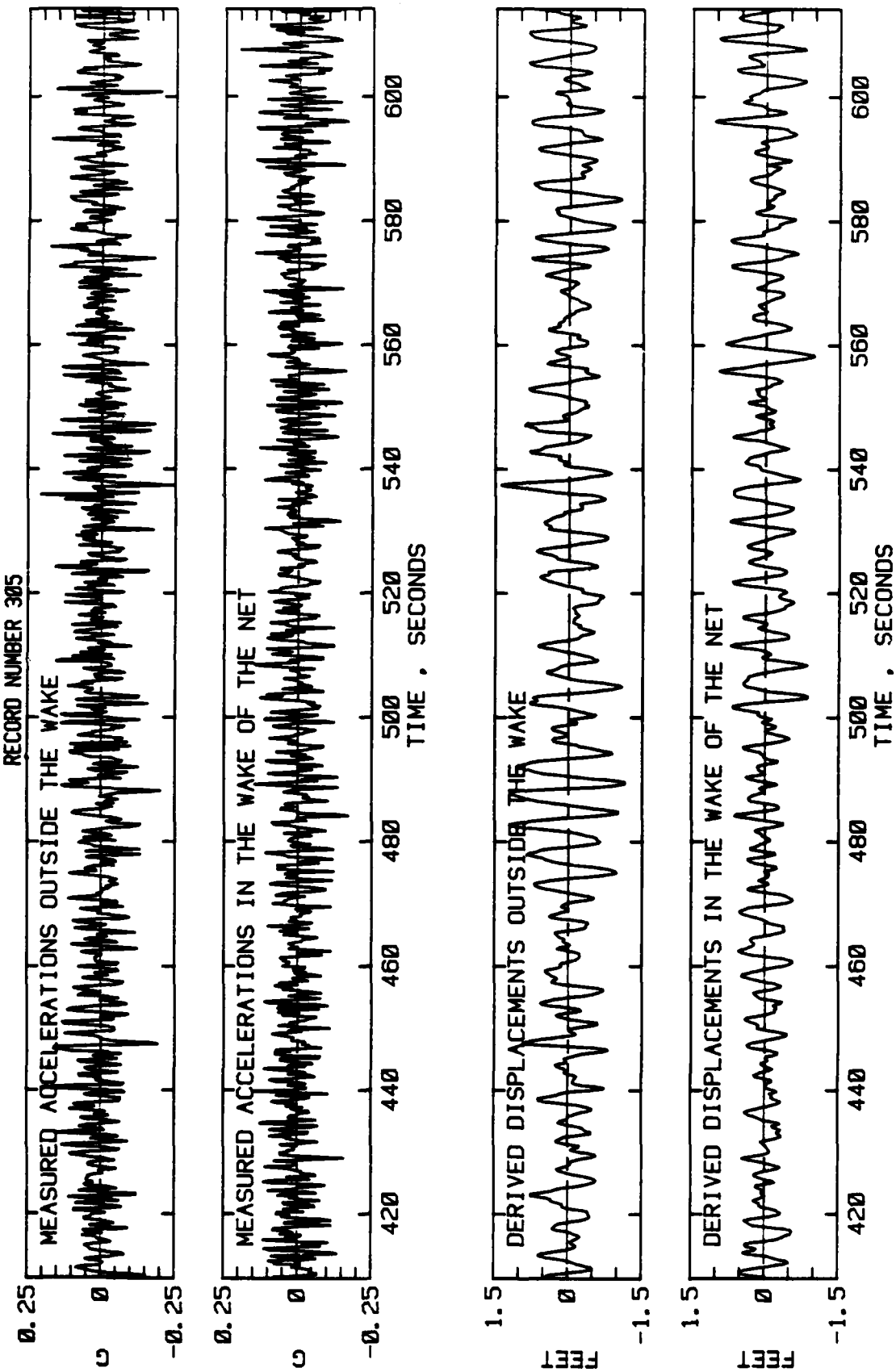
RECORD NUMBER 305
MEASURED ACCELERATIONS OUTSIDE THE WAKE
MEASURED ACCELERATIONS IN THE WAKE OF THE NET
DERIVED DISPLACEMENTS OUTSIDE THE WAKE
DERIVED DISPLACEMENTS IN THE WAKE OF THE NET
G
FEET
TIME , SECONDS
0.25
0
-0.25
1.5
-1.5
420
440
460
480
500
520
540
560
580
600

FIGURE 39 C.

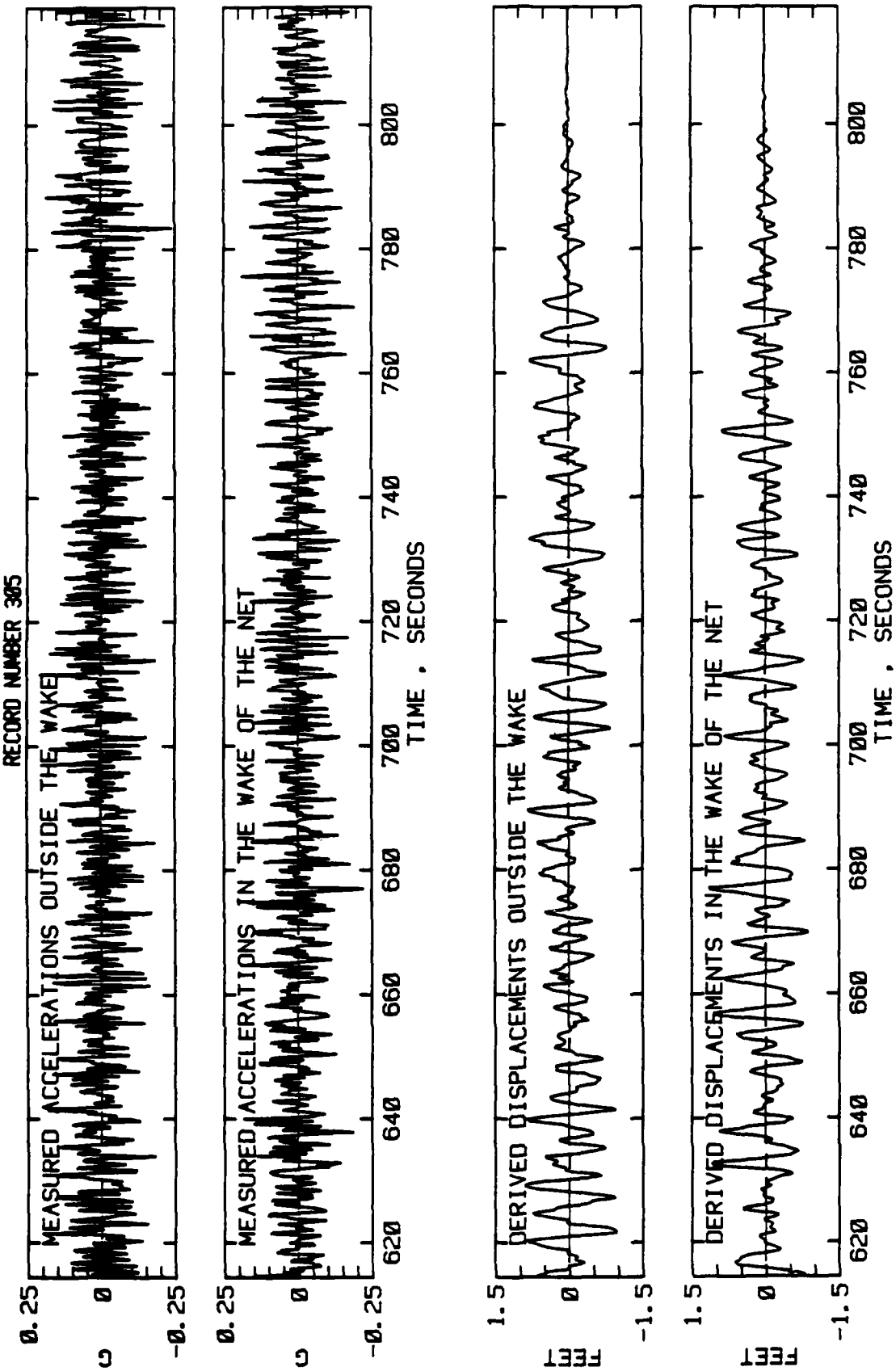
RECORD NUMBER 305
MEASURED ACCELERATIONS OUTSIDE THE WAKE
MEASURED ACCELERATIONS IN THE WAKE OF THE NET
DERIVED DISPLACEMENTS OUTSIDE THE WAKE
DERIVED DISPLACEMENTS IN THE WAKE OF THE NET
G
FEET
TIME , SECONDS
0.25
0
-0.25
1.5
-1.5
620
640
660
680
700
720
740
760
780
800

FIGURE 39 D

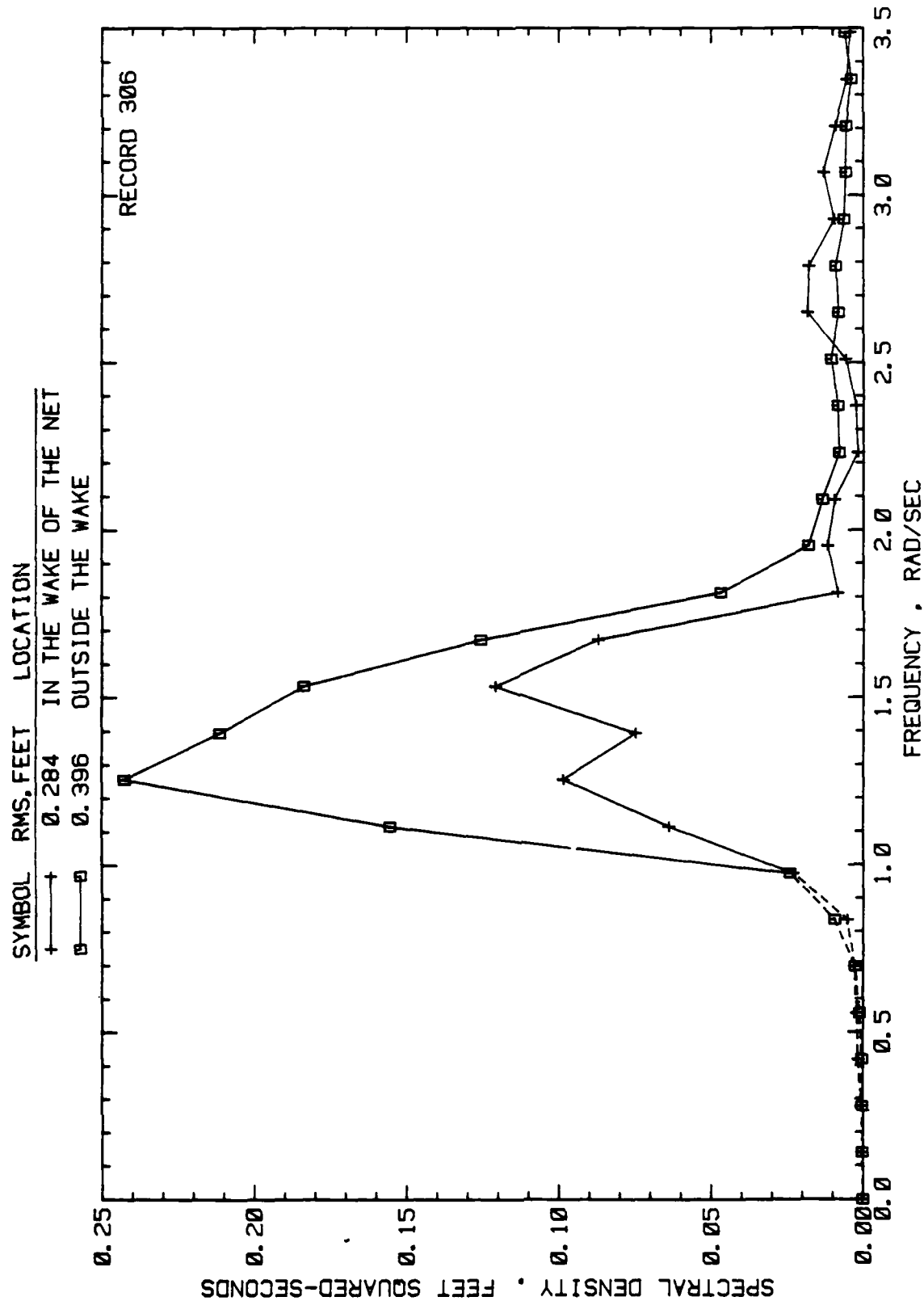
RECORD 306
SYMBOL RMS, FEET LOCATION
0.284 IN THE WAKE OF THE NET
0.396 OUTSIDE THE WAKE
SPECTRAL DENSITY , FEET SQUARED-SECONDS
FREQUENCY , RAD/SEC
0.25
0.20
0.15
0.10
0.05
0.00
0.0
0.5
1.0
1.5
2.0
2.5
3.0
3.5

FIGURE 40.

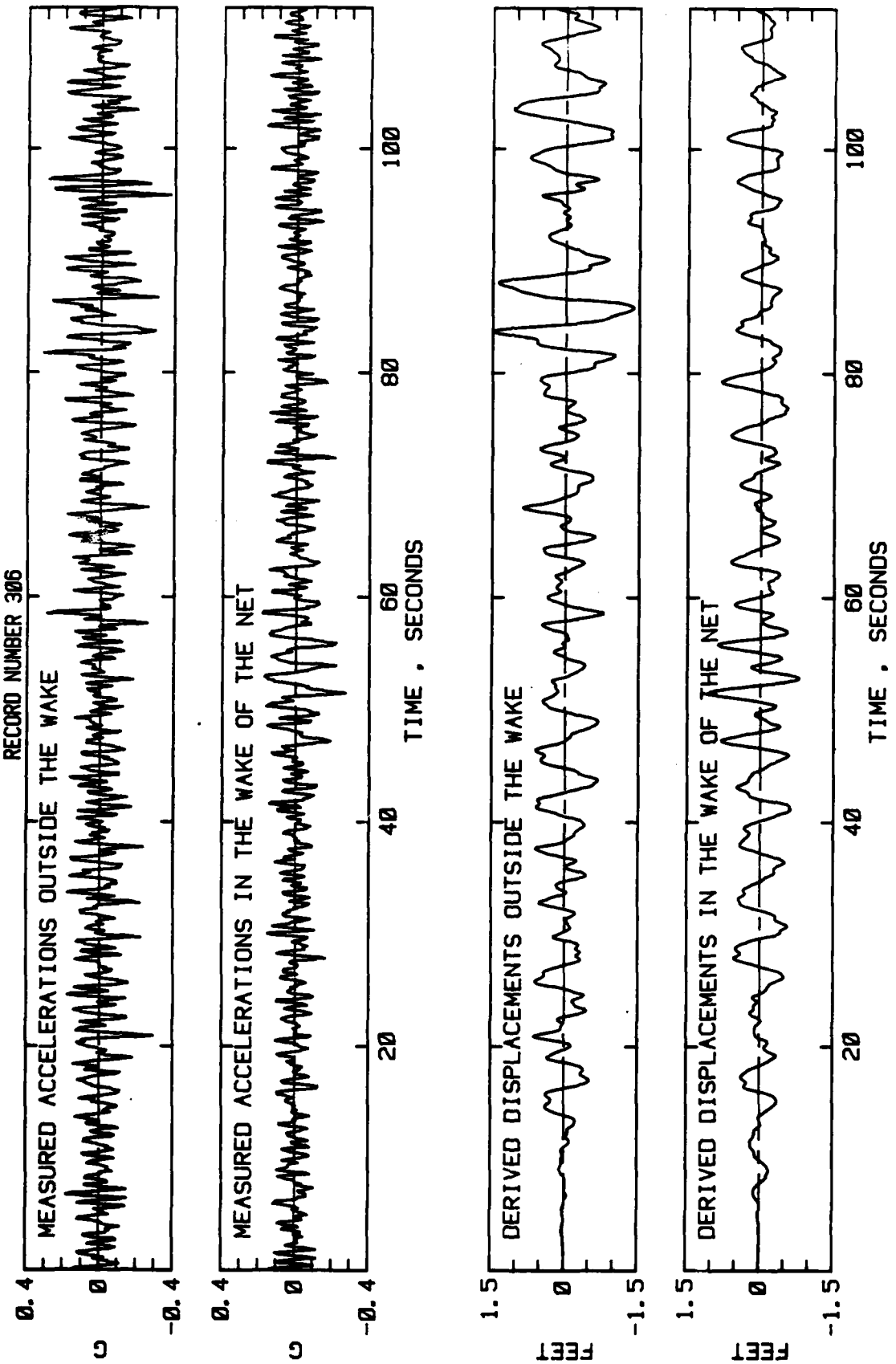
RECORD NUMBER 306
MEASURED ACCELERATIONS OUTSIDE THE WAKE
MEASURED ACCELERATIONS IN THE WAKE OF THE NET
DERIVED DISPLACEMENTS OUTSIDE THE WAKE
DERIVED DISPLACEMENTS IN THE WAKE OF THE NET
G
FEET
TIME . SECONDS
0.4
0
-0.4
1.5
-1.5
20
40
60
80
100

FIGURE 41 A.

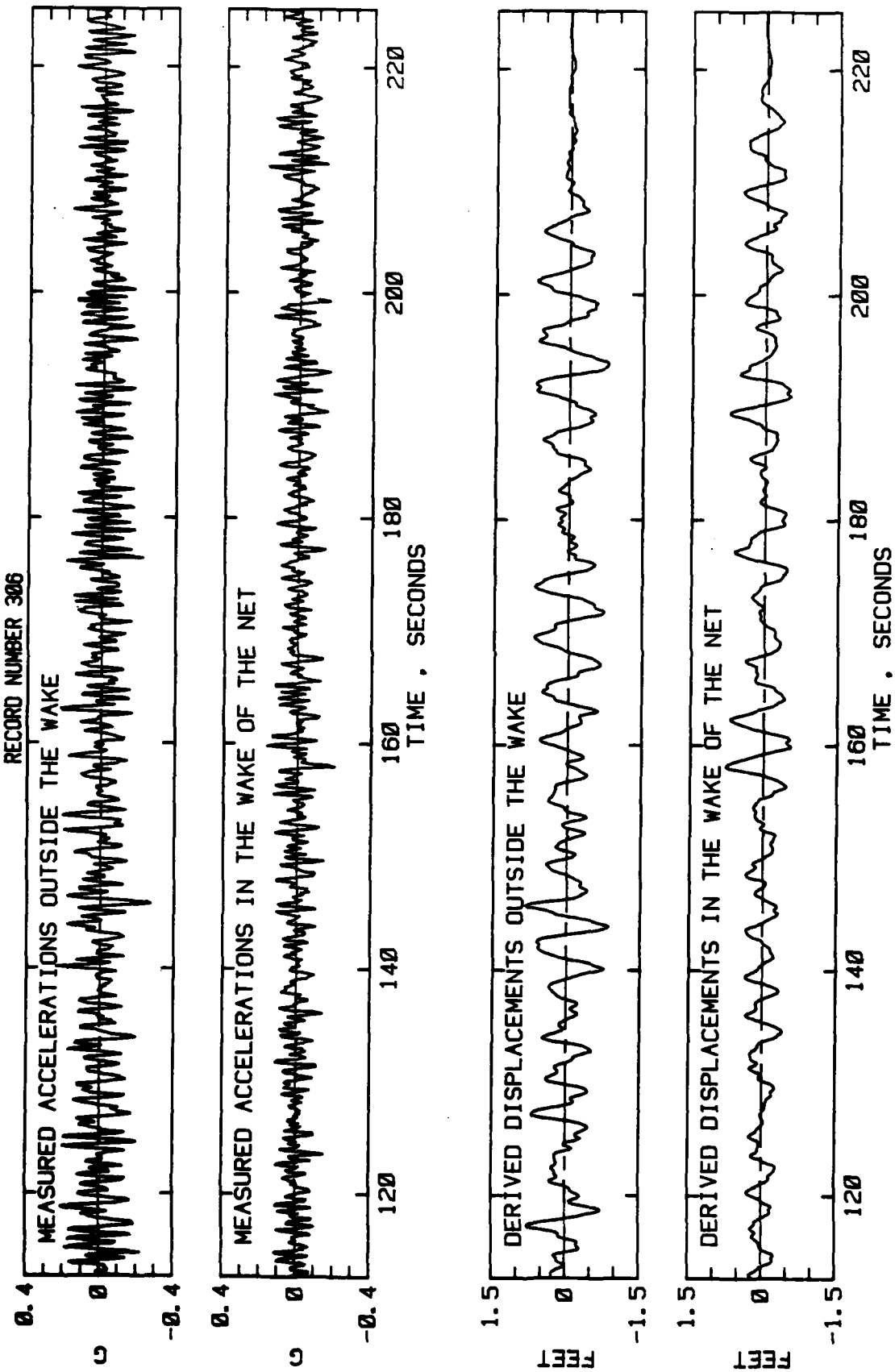
RECORD NUMBER 306
MEASURED ACCELERATIONS OUTSIDE THE WAKE
MEASURED ACCELERATIONS IN THE WAKE OF THE NET
DERIVED DISPLACEMENTS OUTSIDE THE WAKE
DERIVED DISPLACEMENTS IN THE WAKE OF THE NET
G
FEET
TIME . SECONDS
0.4
0
-0.4
1.5
-1.5
120
140
160
180
200
220

FIGURE 41 B.

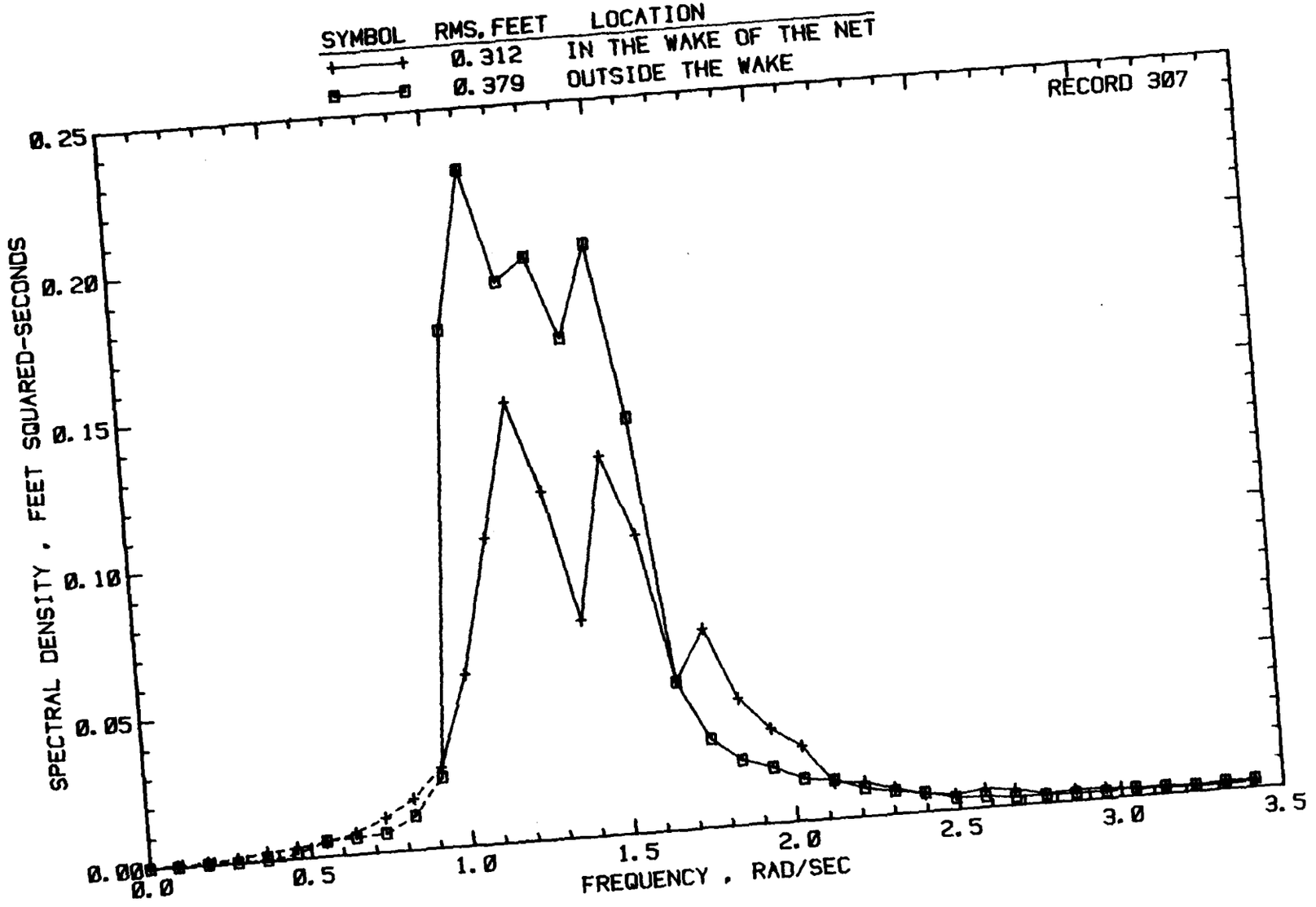
SYMBOL RMS, FEET LOCATION
0.312 IN THE WAKE OF THE NET
0.379 OUTSIDE THE WAKE
RECORD 307
SPECTRAL DENSITY , FEET SQUARED-SECONDS
0.25
0.20
0.15
0.10
0.05
0.00
0.0
0.5
1.0
1.5
2.0
2.5
3.0
3.5
FREQUENCY , RAD/SEC

FIGURE 42.

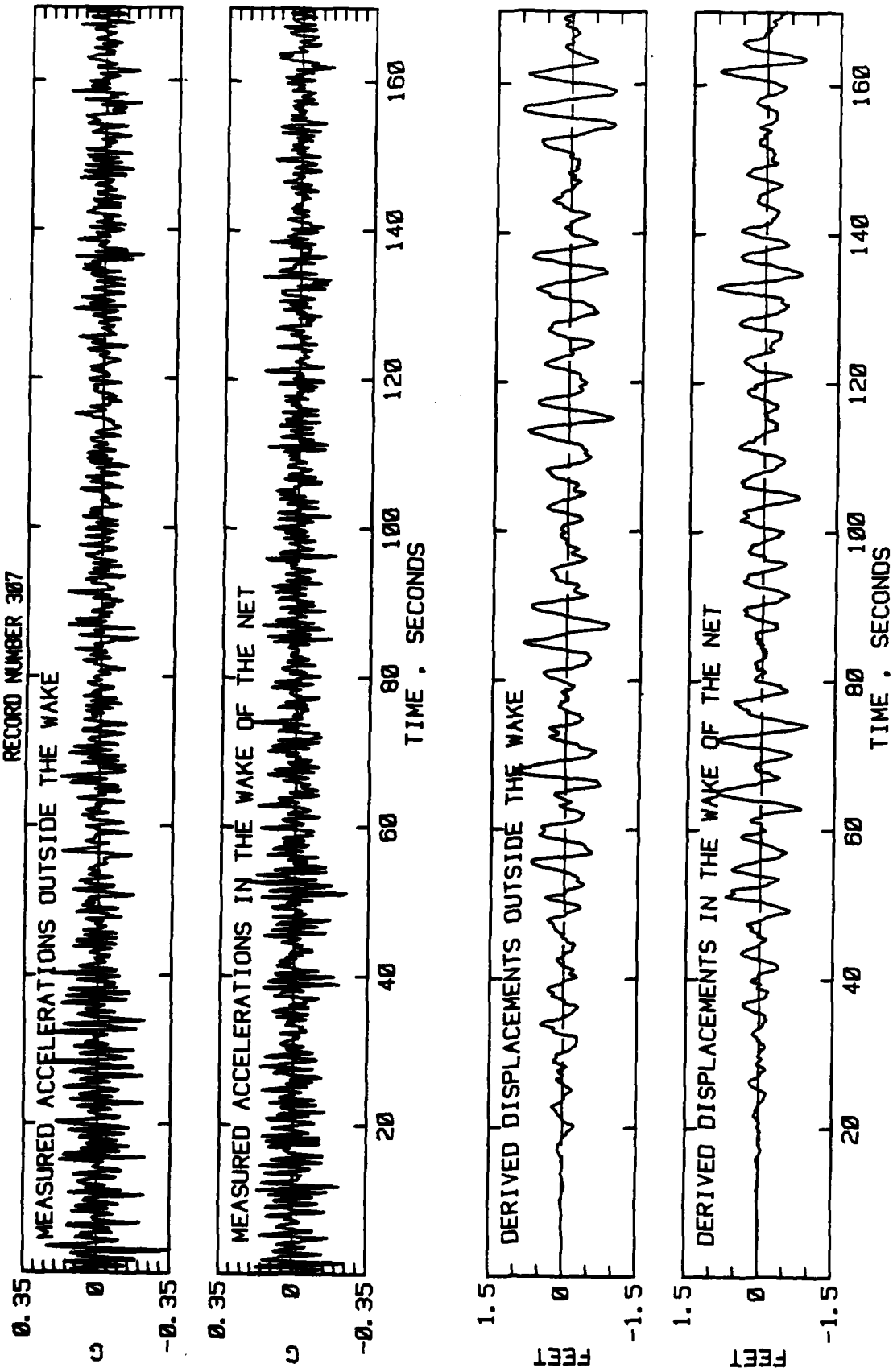
RECORD NUMBER 307
MEASURED ACCELERATIONS OUTSIDE THE WAKE
MEASURED ACCELERATIONS IN THE WAKE OF THE NET
DERIVED DISPLACEMENTS OUTSIDE THE WAKE
DERIVED DISPLACEMENTS IN THE WAKE OF THE NET
G
FEET
TIME, SECONDS
0.35
0
-0.35
1.5
-1.5
20
40
60
80
100
120
140
160

FIGURE 43 A.

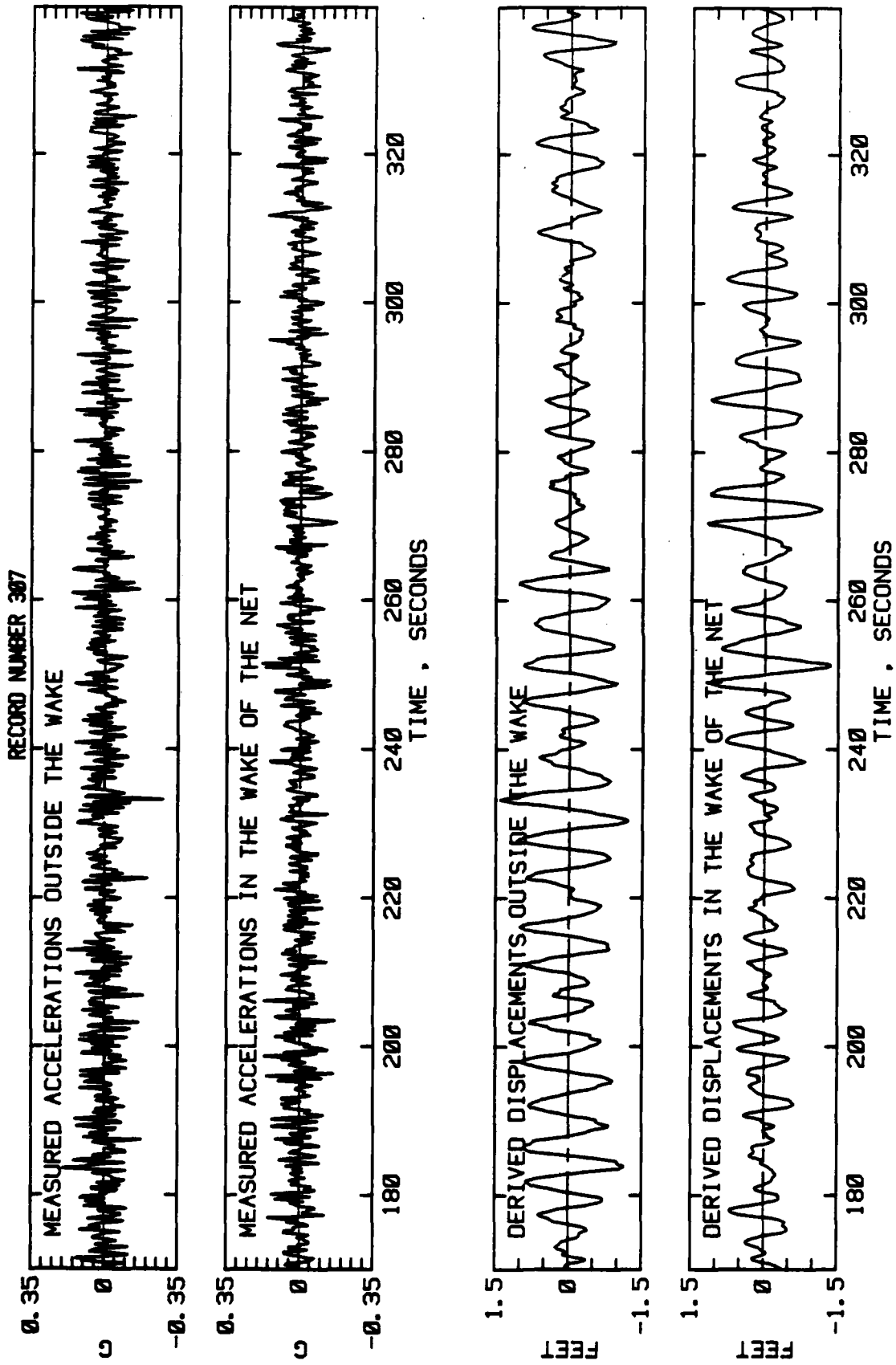
RECORD NUMBER 307
MEASURED ACCELERATIONS OUTSIDE THE WAKE
MEASURED ACCELERATIONS IN THE WAKE OF THE NET
DERIVED DISPLACEMENTS OUTSIDE THE WAKE
DERIVED DISPLACEMENTS IN THE WAKE OF THE NET
G
FEET
TIME . SECONDS
0.35
0
-0.35
1.5
-1.5
180
200
220
240
260
280
300
320

FIGURE 43 B.

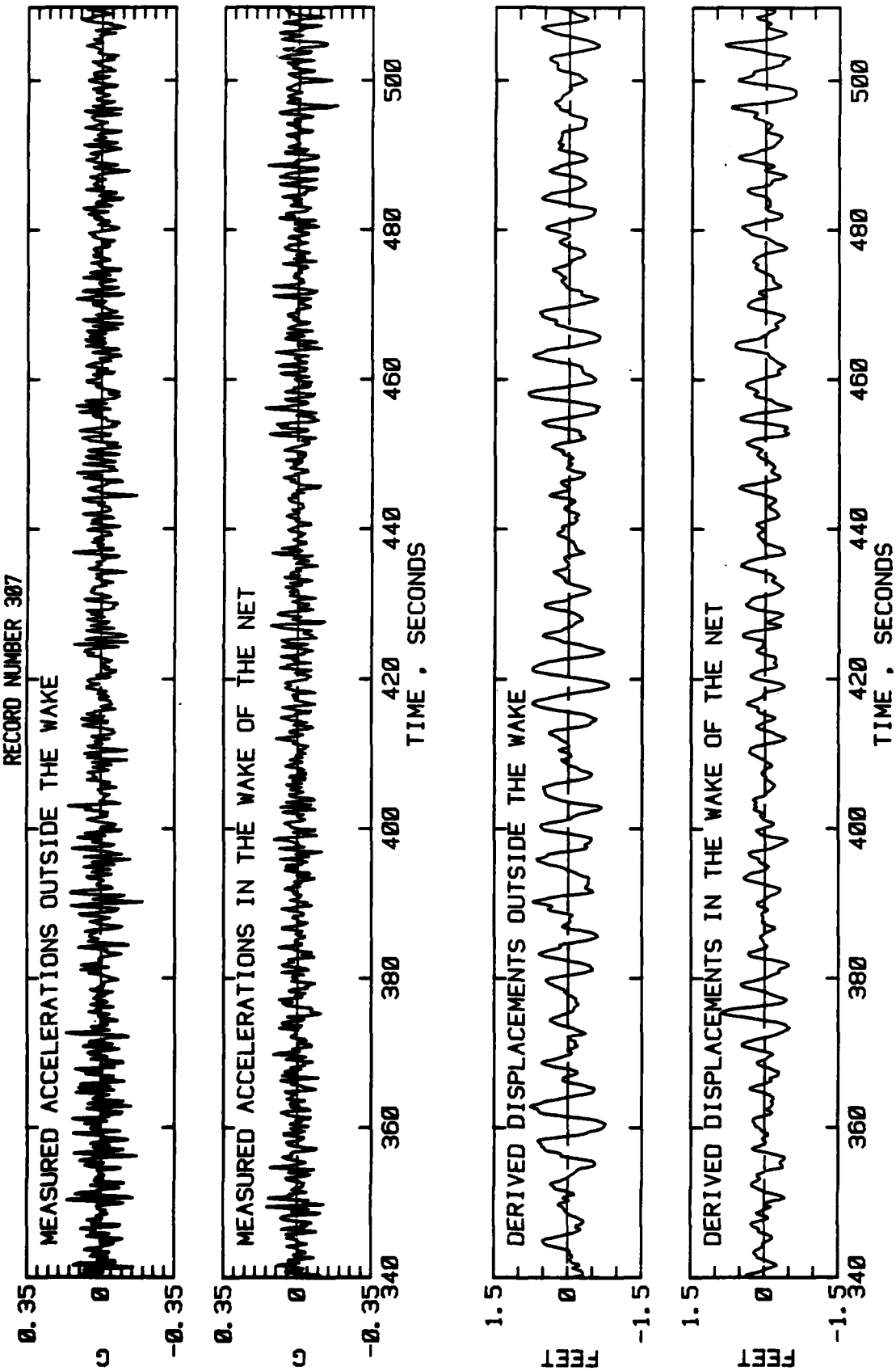
RECORD NUMBER 307
MEASURED ACCELERATIONS OUTSIDE THE WAKE
MEASURED ACCELERATIONS IN THE WAKE OF THE NET
DERIVED DISPLACEMENTS OUTSIDE THE WAKE
DERIVED DISPLACEMENTS IN THE WAKE OF THE NET
G
FEET
TIME , SECONDS
0.35
0
-0.35
1.5
-1.5
340
360
380
400
420
440
460
480
500

FIGURE 43 C.

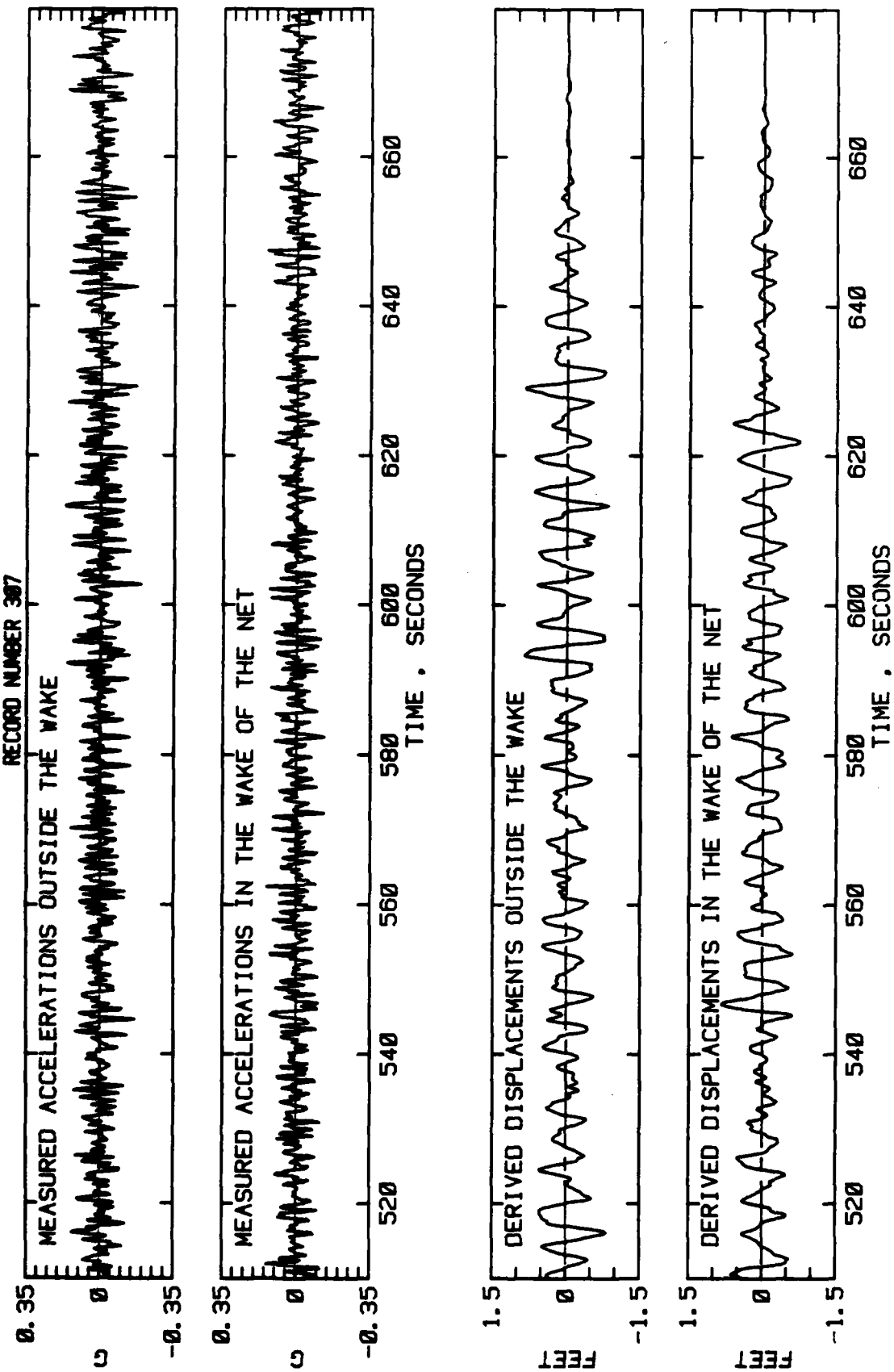
RECORD NUMBER 307
MEASURED ACCELERATIONS OUTSIDE THE WAKE
MEASURED ACCELERATIONS IN THE WAKE OF THE NET
DERIVED DISPLACEMENTS OUTSIDE THE WAKE
DERIVED DISPLACEMENTS IN THE WAKE OF THE NET
G
FEET
TIME . SECONDS
0.35
0
-0.35
1.5
-1.5
520
540
560
580
600
620
640
660

FIGURE 43 D.

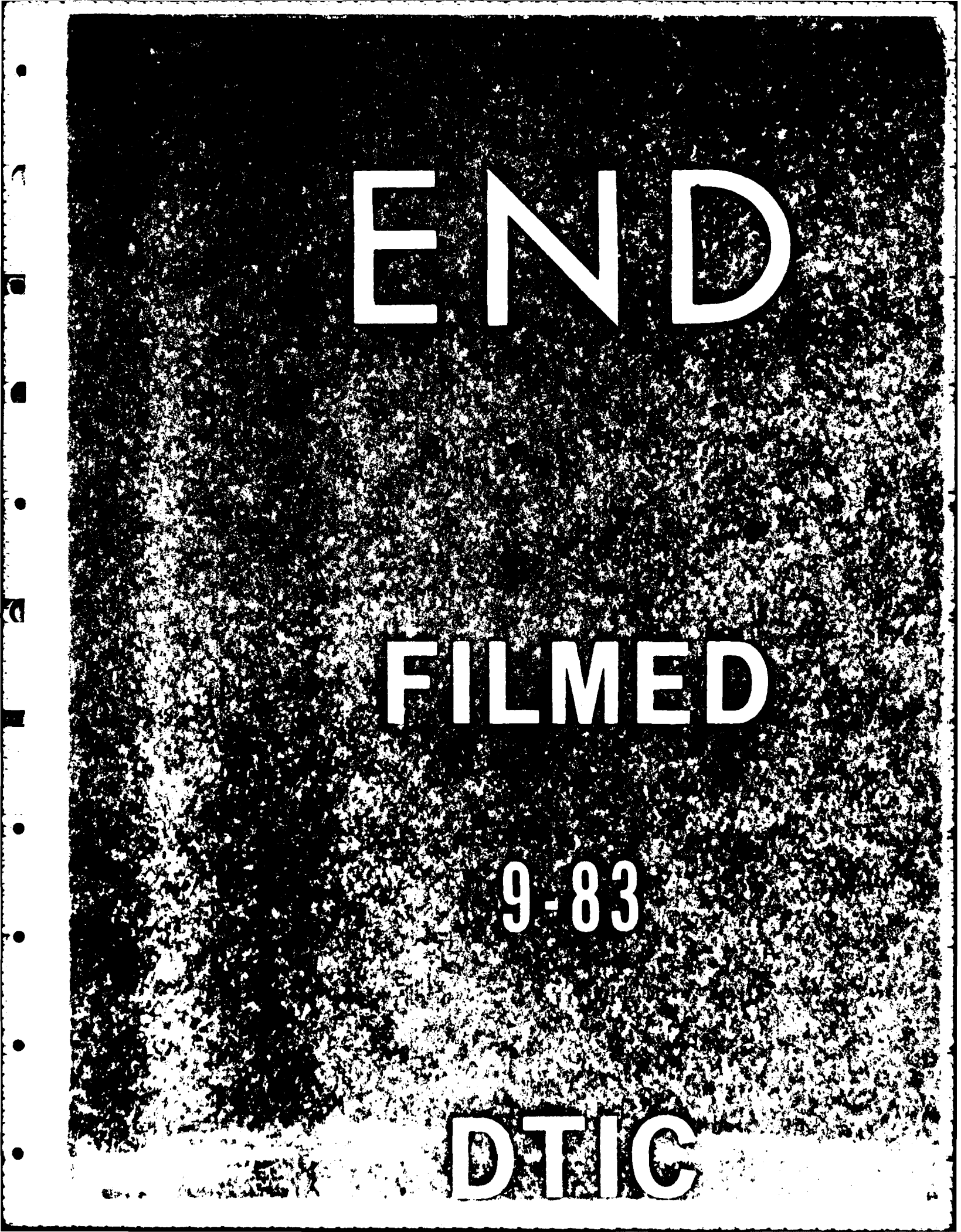
END
FILMED
9-83
DTIC